MASTERARBEIT | MASTER'S THESIS

Titel | Title

Synthesis of siderophores and their biological evaluation

verfasst von | submitted by

Lisa Christiane Jobst B.Sc.

angestrebter akademischer Grad | in partial fulfilment of the requirements for the degree of

Master of Science (MSc)

Wien | Vienna, 2025

Studienkennzahl lt. Studienblatt | Degree programme code as it appears on the student record sheet:	UA 066 862
Studienrichtung lt. Studienblatt | Degree programme as it appears on the student record sheet:	Masterstudium Chemie
Betreut von | Supervisor:	Univ.-Prof. Dr. Thomas Böttcher

Acknowledgements

First, I would like to thank Dr. Felix Anderl for his exceptional guidance and support throughout my master's thesis.
I would like to extend my thanks to Prof. Dr. Thomas Böttcher for giving me the opportunity to conduct my master's thesis in his lab. My appreciation goes out to the entire lab team for their valuable advice, support and kindness.
Additionally, I want to thank the NMR Centre and the Mass Spectrometry Centre at the Faculty of Chemistry, as well as the NMR Centre at the Faculty of Life Sciences, for their reliable and efficient work.
I am especially grateful to my friends for their unwavering support throughout my studies. Lastly, I would like to thank my family for their constant encouragement during this journey.

Abstract

Bacteria require iron to support their metabolism and maintain normal cellular functions. However, in biologically relevant aerobic environments, iron has very low bioavailability due to the formation of insoluble iron(III) hydroxides and other species. Bacteria address this issue by producing chelating ligands known as siderophores. These compounds can be isolated from microorganisms, but usually in small quantities, insufficient for further studies. Therefore, chemical synthesis is required to obtain larger amounts. Agrochelin A, which was first isolated from the marine organism *Agrobacterium sp.* in 1999, shows structural similarities to other siderophores such as aerugine, pyochelin, and yersiniabactin. This raises the question of whether structural resemblance also implies functional similarity. This master's thesis describes the progress towards the chemical synthesis of the siderophore agrochelin, starting from 2-bromo-6-methoxy-benzoic acid and D- and L-cysteine. The synthesis follows a convergent strategy involving two main building blocks that were subsequently combined in a key coupling reaction.

The essential steps included the amide formation between 2-methoxy-6-pentylbenzoyl chloride and *S*-PMB-protected cysteine methyl ester, followed by cyclization to form a thiazoline ring. The Weinreb amide is formed, which, upon reduction, yields the corresponding aldehyde. The second building block was synthesized from Boc-protected (*R*)-thiazolidine-4-carboxylic acid and 2-(trimethylsilyl)ethyl isobutyrate, using LDA as base.

While the synthesis of both building blocks was successful, the final coupling step did not proceed as expected under the initial reaction conditions. This unexpected outcome led to a detailed exploration and discussion of various conditions under which this key reaction was attempted. Unfortunately, only traces of the target molecule could be detected by HRMS.

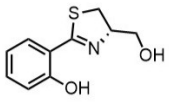

aerugine

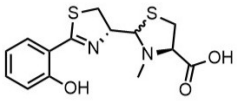

pyochelin

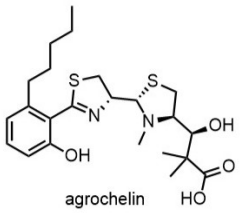

agrochelin

Zusammenfassung

Bakterien benötigen Eisen, um ihren Stoffwechsel aufrechtzuerhalten und normale Zellfunktionen zu gewährleisten. In aeroben Umgebungen mit biologischer Relevanz ist Eisen jedoch aufgrund der Bildung von Eisen(III)-hydroxiden und anderen unlöslichen Spezies nur in geringen Mengen bioverfügbar. Bakterien lösen dieses Problem, indem sie chelatbildende Liganden produzieren, die man Siderophore nennt. Diese Verbindungen können einerseits direkt aus Mikroorganismen isoliert werden, was jedoch meist nur in geringen Mengen realisierbar ist. Andererseits ist eine chemische Synthese möglich, um größere Mengen zu erhalten. 1999 wurde erstmals Agrochelin A aus dem Meeresorganismus *Agrobacterium sp.* isoliert und, es weist strukturelle Ähnlichkeiten mit anderen Siderophoren wie Aerugin, Pyochelin und Yersiniabactin auf. Dies wirft die Frage auf, ob strukturelle Ähnlichkeit auch funktionelle Ähnlichkeit impliziert.

Diese Masterarbeit beschreibt die Fortschritte bei der chemischen Synthese des Siderophors Agrochelin ausgehend von 2-Brom-6-methoxy-benzoesäure und *D*- und *L*-Cystein. Die Synthese folgt einer konvergenten Strategie mit zwei Hauptbausteinen, die anschließend in einer Schlüsselkupplungsreaktion kombiniert wurden.

Die wichtigsten Schritte umfassten die Amidbildung zwischen 2-Methoxy-6-pentylbenzoylchlorid und *S*-PMB-geschütztem Cysteinmethylester, gefolgt von einer Cyclisierung zur Bildung eines Thiazolinrings. Es wird das Weinreb-Amid hergestellt, das bei Reduktion den entsprechenden Aldehyd ergibt. Der zweite Baustein wurde aus Boc-geschütztem (*R*)-Thiazolidin-4-carbonsäure und 2-(Trimethylsilyl) ethylisobutyrat unter Verwendung von LDA als Base synthetisiert. Es war möglich, beide Bausteine unter Verwendung geeigneter Schutzgruppenstrategien erfolgreich zu synthetisieren. Der abschließende Kupplungsschritt verlief jedoch unter den ursprünglichen Reaktionsbedingungen nicht wie erwartet. Auch unter unterschiedlichen Reaktionsbedingungen konnte das Produkt der Kombinationsreaktion nur in Spuren synthetisiert werden. Diese Reaktionsbedingungen werden vorgestellt und diskutiert.

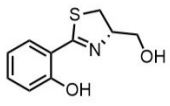

aerugine

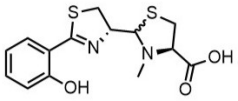

pyochelin

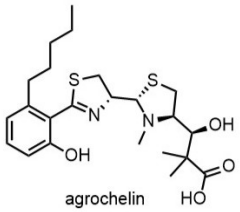

agrochelin

List of abbreviations

$LiAlH_4$ lithium aluminium hydride

AcOH acetic acid

Boc *tert*-butoxycarboxylic

BSR basal slowing response

CDI carbonyldiimidazole

COSY two-dimensional correlation spectroscopy

CV column volumes

DA dopaminergic

DAT dopamine transporter

DCM dichloromethane

DMSO dimethyl sulfoxide

EC_{50} half maximal effective concentration

EE ethoxyethyl

Fur ferric iron uptake regulation protein

HMBC heterobinuclear multibound correlation

HPLC High-performance liquid chromatography

HRFABMS high-resolution fast atomic bombardment mass spectrometry

HSQC heteronuclear single quantum coherece

KOAc potassium acetate

LDA lithium diisopropylamide

MPTP 1-methyl-4-phenyl-1,2,3,6-tetrahydropyridine

MS mass spectrometry

NMR nuclear magnetic resonance

NOE nuclear overhauser effect

NOESY nuclear overhauser effect spectroscopy

NRPSs non-ribosomal peptide synthetases

octenol 1-octen-3-ol

PCP peptide carrier protein

PD Parkinson's disease

PMB *p*-methoxybenzyl

PyBroP bromo-tris-pyrrolidino-phosphonium hexafluorophosphate

sp. species

TBAF tetra-*n*-butylammonium fluoride

TBDPS *tert*-butyldiphenylsilyl

TBDPS-Cl *tert*-butyl(chloro)diphenylsilane

THF tetrahydrofuran

TOCSY total correlation spectroscopy

VOC volatile organic metabolite

Table of Contents

1 Agrochelin A

1.1 Isolation

The target molecule agrochelin A (**1**, figure 1) was first isolated from the Gram-negative marine bacterium of the genus *Agrobacterium* species (sp.) in 1999.[1] Further studies on the strain ALET-304 led to the re-isolation of the compound. It was obtained from the marine tunicate *Ecteinascidia turbinata* off Formentera Island in Spain.[2] The bacterial cells were extracted with $CHCl_3$ – MeOH, washed with hexane, and the residue was extracted with $CHCl_3$. The organic layer was purified on silica gel chromatography, medium-pressure liquid chromatography, and C18 reversed phase High-performance liquid chromatography (HPLC), affording pure agrochelin A.[1]

1.2 Structural Investigation

The molecular formula for agrochelin was determined to be $C_{23}H_{34}N_2O_4S_2$ using high-resolution fast atomic bombardment mass spectrometry (HRFABMS).[1,2] NMR-based structural elucidation of agrochelin was performed by Riguera *et al.* and the proposed structure is shown in figure 1.

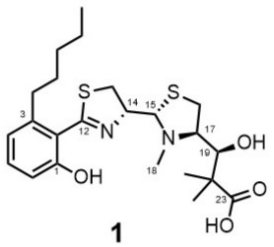

1

Figure 1: Proposed structure of agrochelin/isolated from *Agrobacterium* sp., the stereochemistry was elucidated by NOE experiments of it Zn^{2+} complex.[1]

To further study the stereochemistry, an attempt was made to form crystals for X-ray structural analysis, but this was unsuccessful. Since Zn^{2+} is chelated by agrochelin, it was possible to carry out nuclear overhauser effect spectroscopy (NOESY) nuclear magnetic resonance (NMR) experiments. A strong nuclear overhauser effect (NOE) was observed between the protons H-14 and H-15 and H-17 and the N-Me (C-18) group, but no signal was visible between H-15 and H-17. Consequently, C-14 has an *R* and C-15 has an *S* configuration.[1]

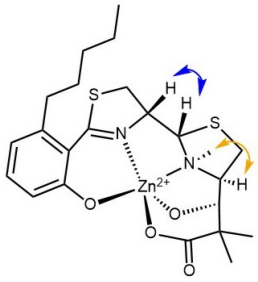

Figure 2: Agrochelin chelating Zn^{2+}. NOE between H-14 and H-15 in blue, NOE between N-Me (C-18) and H-17 in orange.[1]

The structure of agrochelin is very similar to other siderophores such as yersiniabactin (isolated from *Yersinia strains*), micacocidins (isolated from *Pseudomonas sp.*) and pyochelin I/II (isolated from *Pseudomonas aeruginosa*)(figure 3).[2] All mentioned siderophores consist of a thiazolidine, a thiazoline, and a phenol moiety. Agrochelin and massiliachelin only differ in the absolute configuration at C-15 position. The configuration at this position in agrochelin is *S*. In contrast to agrochelin, the epimer massiliachelin displays an *R* configuration at that position.[3] Pyochelin lacks the secondary alcohol and the two methyl groups, but yersiniabactin and micacocidin have an additional thiazoline subunit. However, yersiniabactin and pyochelin have been researched much more intensively than agrochelin. Structural similarities to these siderophores suggested that the same functional properties may apply to agrochelin.[1]
Siderophores, including those containing thiazoline rings, are typically synthesised by non-ribosomal peptide synthetases (NRPSs). Since agrochelin contains one thiazoline and one thiazolidine, the involvement of this modular enzyme system is very likely.
The core steps of NRPS synthesis involve three domains for peptide bond formation, which are explained in more detail in the section on siderophores.[4,5]

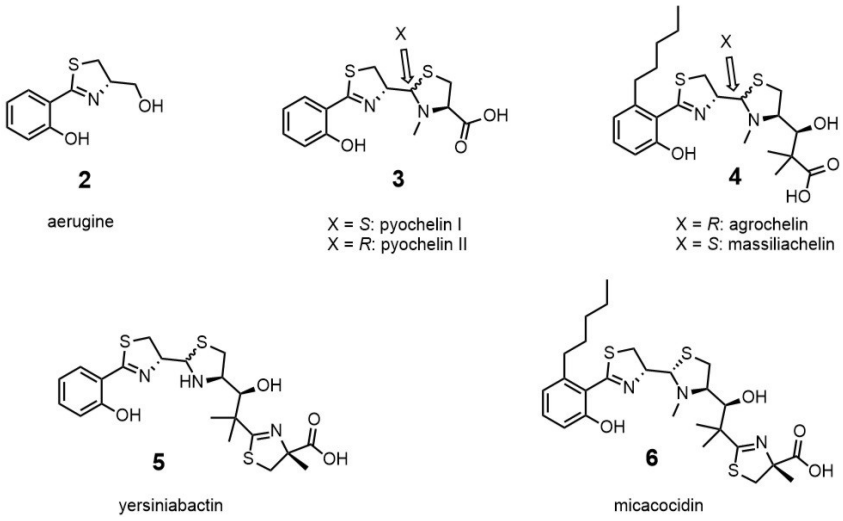

Figure 3: Comparison of various siderophores with similar structural characteristics.

1.3 Biological Investigation

Structurally, agrochelin A is capable of forming complexes with Zn^{2+} ions, which may contribute to its bioactivity. Considering the formation of the complex, it can be assumed that oxygen and nitrogen serve as donor atoms, as is already known for other siderophores. A potential coordination site is the carboxylate group, where one oxygen atom of the carboxylic acid acts as an electron donor. The *N*-methyl group may also participate in metal coordination. Thus, it is conceivable that iron could coordinate to agrochelin at up to five distinct sites.[1]
So far, little information is available regarding the biological activity of agrochelin. In initial studies following its isolation, agrochelin was found to exhibit significant *in vitro* cytotoxicity, with half maximal inhibitory concentration values ranging from 0.1 to 0.4 μM against mouse (P-388) and human tumor cell lines A-549 (lung carcinoma), HT-29 (colon carcinoma), and MEL-28 (melanoma). The molecular mechanism underlying the cytotoxic effects of agrochelin remains unknown and requires further study.[1,2]

2 Neurodegenerative Diseases

First studies indicate a correlation between natural metabolites and the development of Parkinson's disease (PD).[6] Since PD is characterized by a loss of dopaminergic (DA) neurons, experiments were conducted on the influence factors for the degeneration of these cells. Preliminary results with siderophore, like aerugine, indicate an influence. Therefore, a structural-functional correlation with other siderophores remains to be proven.[7]
The number of people affected by PD has steadily increased over the past decades. Approximately 0.1% to 0.2% of the global population is affected. The incidence of PD increases with age, with rates among those over 60 years reaching 1% of the population. This also makes age one of the most significant risk factors for developing Parkinson's disease (figure 4).[8]
At the molecular level, PD is caused by dysfunction in cellular processes, leading to a long-term loss of DA neurons. This can be triggered by protein disruption and aggregation, mitochondrial function disruption, oxidative stress, and iron dysregulation. In addition, dopamine itself may contribute to dysregulation of dopamine metabolism. These factors can lead to decreased dopamine production and release in the brain. As a result, neuronal transmission functions less effectively, movements are no longer performed smoothly, and a widespread symptom of PD, tremor, occurs.[9]

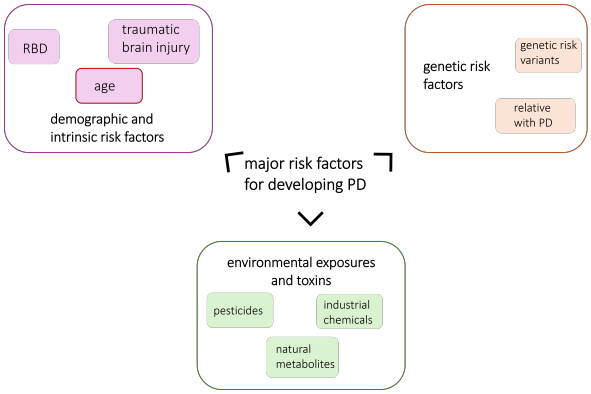

Figure 4: The major risk factors for developing PD, Traumatic Brain Injury (TBI), Idiopathic REM sleep behaviour disorder (RBD).[7–9]

Seven distinct mutations in the leucine-rich repeat kinase 2 gene have been identified and are directly linked to PD development.[9] Six other genes are also directly linked to the onset of PD. The risk of developing PD is at least twice as high if a relative has PD or tremors. However, only 5% of cases are linked to monogenetic inheritance and involve genetic mutations, in contrast, 95% of Parkinson's disease cases remain unexplained and can not be traced back to any genetic origin.[8] Therefore, it remains important to identify other risk factors. Epidemiological studies have shown that pesticides and industrial chemicals can be linked to PD. The pesticides 1-methyl-4-phenyl-1,2,3,6-tetrahydropyridine (MPTP), paraquat, and rotenone have been shown to cause dopaminergic toxicity in animal models. Furthermore, industrial chemicals such as trichloroethylene can also be linked to PD. Thus, the high incidence can be attributed to environmental pollution with these chemicals. At the cellular level, these chemicals can generate reactive oxygen species and oxidative stress, which contribute to dopaminergic neuron toxicity.[9,10] However, since Parkinson's disease was likely already prevalent before the introduction of artificial pesticides, it can be concluded that natural compounds may have an influence.[6,10,11] To fully understand the development of PD, substances that were in contact with humans before the use of pesticides and industrial chemicals must be investigated. One group that has received little attention until now are natural metabolites, like 1-octen-3-ol (octenol). Octenol is a volatile organic metabolite (VOC) of molds found in natural and human-made environments. Experiments were conducted to investigate the effects of exposure. The focus here lied on examining its neurotoxicity and mechanism of action, in particular the disruption of dopamine home-

ostasis. The results of the *in vivo* studys in *Drosophila melanogaster* show that exposure of wild-type flies to 0.5 ppm octenol significantly shortened their survival time and led to motor defects. Exposure for 24 hours led to a significant loss of dopaminergic neurons in almost all subgroups of the fly brain. Similar effects on dopaminergic neurons can be demonstrated in *in vitro* experiments. In human embryonic kidney cells expressing the dopamine transporter (DAT), octenol significantly inhibited dopamine uptake. At 10 ppm, uptake was reduced by 95% after 2 hours. These findings suggest that natural compounds may influence PD development.[11]
To further assess the relation on PD and natural metabolites, aerugine was tested for its neurotoxicity. Aerugin is a siderophore isolated from the bacteria *S. venezuelae*.[12] The half maximal effective concentration (EC_{50}) value for aerugine is 3-4 μM for human dopaminergic neurons differentiated from LUHMES cells. Aerugine shows strong specificity and selective for dopaminergic neurons, as it was less toxic to other neurons with EC_{50} of 10-20 μM and non-toxic <100 μM for common human cell lines. Aerugine (20 μM) had no cytotoxic or bacteriostatic effects on Gram-positive or Gram-negative bacteria, underscoring its specificity for DA neurons. Neurotoxicity was completely prevented by several iron chelators, suggesting an iron-dependent cell death pathway, possibly ferroptosis. The worm *C. elegans* was used for *in vivo* testing. Dopaminergic neurons were labeled with green fluorescent protein and a concentration-dependent degeneration was observed. In this experiment, the behaviour of the worms after contact with aerugine was observed using the basal slowing response (BSR) behavioural test. This test serves as a proxy for the worms' dopaminergic system's functionality. Aerugine led to a concentration-dependent reduction of the BSR. The observation showed that the function of the dopaminergic neuron system was disrupted by aerugine.[7]
Aerugine was initially isolated from the soil bacterium *S. venezuelae*,[7] although exposure to soil microorganisms by humans plays a rather minor role in the uptake of metabolites.[6] Nevertheless, the relevance lies in the biosynthetic gene cluster of aerugine, not in the isolation of the compound. This biosynthesis cluster is widespread among many bacteria, which are also found in the intestinal microbiome or as human pathogens. These include genera such as *Pseudomonas sp., E. coli, Yersinia sp.* and *Salmonella sp.*. For *P. aeruginosa*, aerugine was described by Wuest *et al.* as a by-product of pyochelin biosynthesis.[13] Since *P. aeruginosa* occurs as a pathogen in humans, especially in cystic fibrosis patients, in the lungs.[14] Therefore, it can be assumed that aerugine could also be a side product of the siderophore biosyntheses in humans . The biosynthesis cluster for pyochelin in *P. aeruginosa* belongs to the family of watasemycin-pyochelin-yersiniabactin families, which also includes the biosynthesis cluster for aerugine. Thus, hypothetically, aerugine can also be produced in the gut microbiome as a shunt product.[7,13]

As previously mentioned, there is limited knowledge regarding the biosynthesis of agrochelin. Nevertheless, due to its structural resemblance to yersiniabactin and aerugine, it is plausible to assume that the biosynthesis process is similar. Yersiniabactin biosynthesis utilizes the same precursor as both pyochelin and aerugine.[7] Therefore, it is reasonable to hypothesize, as with aerugine, that agrochelin could be a byproduct of yersiniabactin synthesis. Should this hypothesis prove accurate, it would be necessary to investigate the neurotoxic potential of agrochelin. Initial studies have shown toxicity to human cells in tumor models, highlighting the need for further research specifically targeting DA neurons.[1,2]

3 Siderophores

Siderophores are chelating ligands produced by microorganisms, fungi, and plants to bind ferric iron (Fe^{3+}). Iron plays an essential role in the coordination and activation of oxygen, as well as in the redox chemistry of electron transport and various metabolic processes within cells.[4]
In biologically relevant aerobic environments, ferric iron (Fe^{3+}) exhibits low bioavailability because it readily forms insoluble hydroxides such as ferrihydroxide ($Fe(OH)_3$).[15] The solubility product (K_{sp}) of $Fe(OH)_3$ is approximately 10^{-39} M resulting in a free iron concentration of about 10^{-18} M in water. Due to this extremely low solubility, microorganisms have evolved mechanisms to overcome iron limitation by synthesizing these high-affinity chelating ligands that solubilize and transport iron into cells.[4,16] Siderophores can be classified according to the chemical nature of their iron-binding groups. The main classes include catecholates, hydroxamates, phenolates, carboxylates, and mixed types, the latter combining two or more of these binding motifs within a single molecule. The Fe^{3+} is coordinated by six donor atoms, often being oxygen or nitrogen atoms.[4]

Siderophores are produced within the bacterial cell through the NRPS. These NRPSs link amino acids through a thioester intermediate. Core steps in NRPS synthesis involve three domains for peptide bond formation: the adenylation domain, attachment to the peptide carrier protein (PCP) domain, and the condensation domain. Additionally, auxiliary domains catalyze steps such as epimerization, methylation, cyclization, reduction, and oxidation, which can also be involved in the process.[4,15] The genes encoding the NRPS system are regulated through the ferric iron uptake regulation protein (Fur). When Fur is bound to iron(II), sufficient iron is available in the cell, allowing Fur-protein to bind to a DNA regulatory sequence, which leads to the repression of the transcription of the biosynthetic gene cluster. Another possible mechanism for regulating siderophore biosynthesis is the quorum-sensing system. The precise details of how quorum sensing controls siderophore production are not yet fully understood. In general, quorum sensing regulates the production of metabolites in a cell-density-dependent manner. Bacteria respond to signaling molecules, and when the concentration of these molecules exceeds a certain threshold at high cell density, siderophore production can be initiated.[4,15,16] Once produced, the siderophore needs to be exported into the extracellular environment, where it can function in iron chelation.

4 Aim

Understanding the causes of Parkinson's disease is the first step toward preventing future cases. Several factors are already known, including age, genetic predisposition, and exposure to pesticides and industrial chemicals. Recently, new potential causes have been proposed, such as exposure to natural metabolites produced by fungi or bacteria. The death of dopaminergic neurons is induced by the natural metabolites 1-octen-3-ol and aerugine. Given the structural similarity between agrochelin and aerugine, it remains to be determined whether agrochelin plays an essential role in dopaminergic neurodegeneration. Therefore, this study aimed to synthesise agrochelin and evaluate its effects on dopaminergic neurons. The synthesis was influenced by studies on other siderophores with similar structures, using them as benchmarks. The complete synthesis of yersiniabactin and micacocidin has been reported. This master's thesis outlines a partial synthesis pathway towards agrochelin.

5 Retrosynthetic Analysis

5.1 Major Disconnections

The synthesis of agrochelin was carried out using a discontinuous and convergent approach, employing two key building blocks to achieve higher yields and expedite the synthetic process. Building blocks A and B, both ultimately leading to the final product **1**, were coupled *via* a reaction involving aldehyde, thiol, and amide functional groups.
The synthesis of agrochelin was inspired by and partially adapted from the syntheses of micacocidin and yersiniabactin.[17] The synthesis of micacocidin was published in 1999 by Ino and Murabayashi.[18] Since agrochelin contains analogous subunits and functional groups, this established synthesis served as a guiding framework for the design of the current synthetic strategy. Agrochelin features a thiazolidine and a thiazoline ring, both of which can be readily constructed from commercially available cysteine. These rings not only provide a convenient entry point for synthetic elaboration but, by using D- or L-cysteine, also inherently incorporate the required stereochemical information into the molecule.

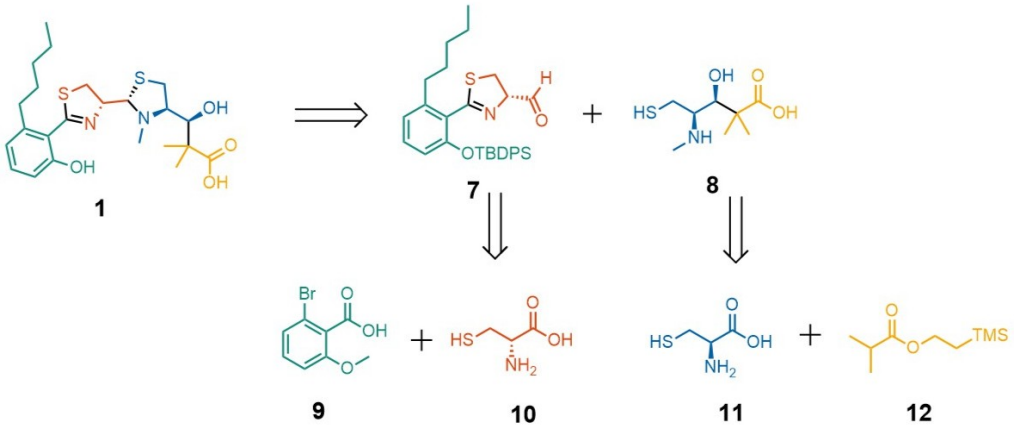

Figure 5: Retrosynthesis of agrochelin.

5.2 Building block A

The thiazoline ring was traced back to D-cysteine, while the aromatic ring motif was derived from 2-bromo-6-methoxybenzoic acid. Bromine attached to the aromatic ring was viewed as a feasible starting material for a cross-coupling reaction with an alkyl chain, allowing the introduction of a pentyl chain adjacent to the carboxylic acid. It was thought that upon activation of a carboxylic acid, an amid bond formation could be conducted with an amine.

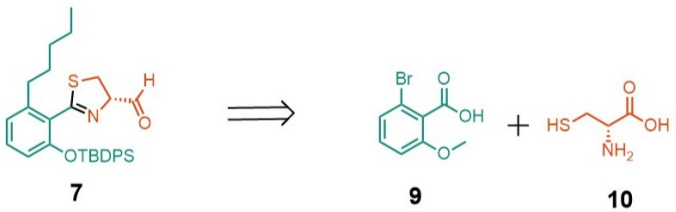

Figure 6: Retrosynthesis of building block A.

5.3 Building block B

The stereochemistry of the chiral center originating from L-cysteine should be retained throughout the entire reaction sequence. Deprotonation at a *sec*-propyl site can be stabilized through enolate formation. The resulting carbanion is capable of creating a new C-C bond with the carbonyl carbon. To prevent reactions at the carboxylic acid site, various protecting groups should be evaluated.

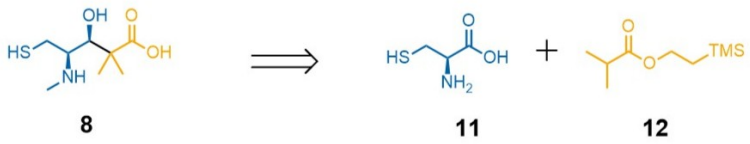

Figure 7: Retrosynthesis for building block B.

6 Synthetic Work

6.1 Building block A

The synthesis of building block A begins with the preparation of the *n*-pentlyzinc (II) bromide **14** (figure 8). Using a Negishi coupling, a new C–C single bond is formed, with Pd(dppf)Cl_2 employed as the catalyst. This coupling reaction formed acid **15**.[19]
During the reaction, not all of the 2-bromo-6-methoxybenzoic acid (**9**) was consumed, indicating that more than three equivalents of *n*-pentlyzinc (II) bromide are necessary. One equivalent of **14** is required to neutralise the acid, two equivalents are used with respect to the catalyst (0.01 equiv.), and one equivalent is necessary for product formation, resulting in a total usage exceeding two equivalents. Increasing the amount of the organozinc reagent may allow the reaction to achieve a higher yield than the observed 72%. It should also be noted that the formation of compound **14** was assumed to proceed in quantitative yield, which was not experimentally verified.

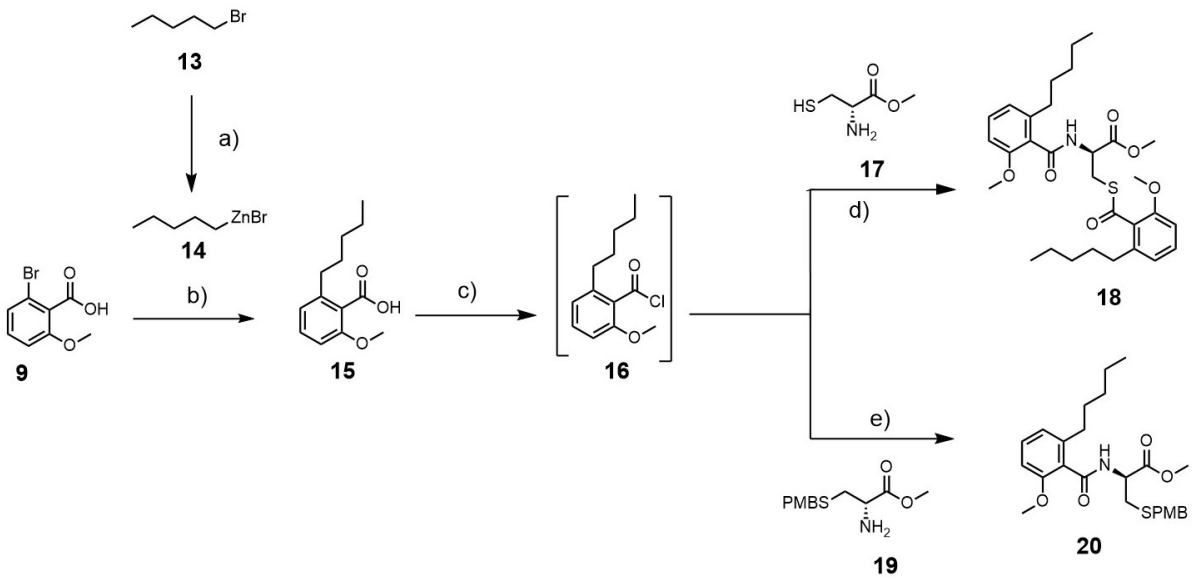

Figure 8: Synthesis of **20**. Conditions a) Zn, dimethylformamide, iodine, 70 °C for 48 h b) 2-brom-6-methoxybezoic acid, Pd(dppf)Cl_2 (2 mol%), 60 °C for 72 h, 72% c) thionyl chloride, (cat.) dimethylformamide, 1,2-dichloroethane, 80 °C for 1.5 h d) dichloromethane, D-cystein-OMe (**17**), triethylamine, (cat.) 4-dimethylaminopyridine, 0 °C (30 min) $\rightarrow$ romm temperature for 18 h, 43%, e) 2-methxy-6-pentylbenzoyl chlorid, dichloromethane, PMB-D-cystein-OMe (**19**), pyridine romm temperature for 1 h, 43%,

Cysteine serves as the starting material for the thiazoline formation. To ensure the correct stereochemistry, *D*-cysteine was used. Thus, the chiral centre is introduced at the very beginning of the synthesis and should be preserved throughout the whole synthesis. The carboxylic acid group is esterified to prevent reactivity at this position and D-cystein-OMe (**17**) is formed.[20] Amide **17** is formed from the acid **15** and the esterified cysteine **17**. Therefore, the carbonyl group was activated by conversion to the corresponding acid chloride using thionyl chloride, since chloride serves as a better leaving group compared to the hydroxide anion.[21] Additionally, pyridine further activates the carbonyl through the formation of an acylpyridinium chloride intermediate. This activation facilitates the nucleophilic attack of the amine **17** on the carbonyl carbon, leading to the formation of the amide bond.[22]
A side reaction was detectable by NMR, as the signals of the aromatic and phenyl protons appeared in a 2:1 ratio relative to the methyl group of the ester. A possible explanation for this is that the reac-

tion was carried out in dichloromethane, in which **16** is readily soluble. However, **17** is highly polar, resulting in a suspension with only small amounts dissolving. After amide formation, the product became fully soluble in dichloromethane, but because of the excess acid chloride, the thiol group also acted as a nucleophile and reacted with a second **16**, forming **18**. To prevent reactivity at the thiol, **17** was subsequently protected with a *p*-methoxybenzyl (PMB) group to compound **19**.[23] When the reaction was repeated under these conditions, no nucleophilic attack of the thiol on the acid chloride was observed and instead amine **20** was formed.[23]

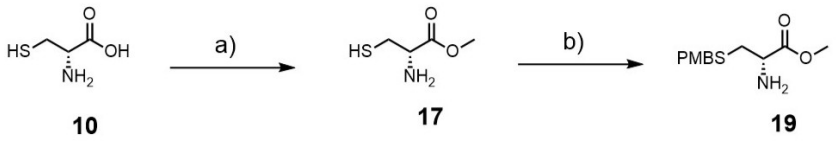

10 **17** **19**

Figure 9: Synthesis of PMB-Cys-OMe **19**. Conditions a) acetyl chlorid, methanol, *D*-cysteine, reflux for 21 h, 71% b) *p*-methoxybenzyl chloride, dichloromethane, trifluoroacetic acid, 0 °C for 2 h, RT for 16 h, 48%.

Phosphorus pentachloride was used to convert the amide (**20)** into a thiazoline ring.[22] As illustrated in the proposed mechanism (figure 10), the electron pair of the carbonyl oxygen can attack the phosphorus atom, resulting in the cleavage of one chloride ion. The lone pair on nitrogen can subsequently shift to form a double bond between nitrogen and the carbonyl carbon, forming an imine (**21**). It is now possible for the oxygen atom to donate an electron pair to phosphorus, forming a P = O bond (**22**). A chloride ion can abstract the amide proton, releasing hydrogen chloride. The thiol can subsequently attack the amide carbon atom nucleophilically, leading to the elimination of $OPCl_3$ and **23**. Since the thiol bears an electron-donating substituent, electron density can be delocalized into the ring system, and the electron pair on the sulfur atom forms a new bond while a previously eliminated chloride ion can attack the PMB^+ cation to generate PMB – Cl. Thus, the thiazoline ring is formed, and the protecting group is cleaved simultaneously.

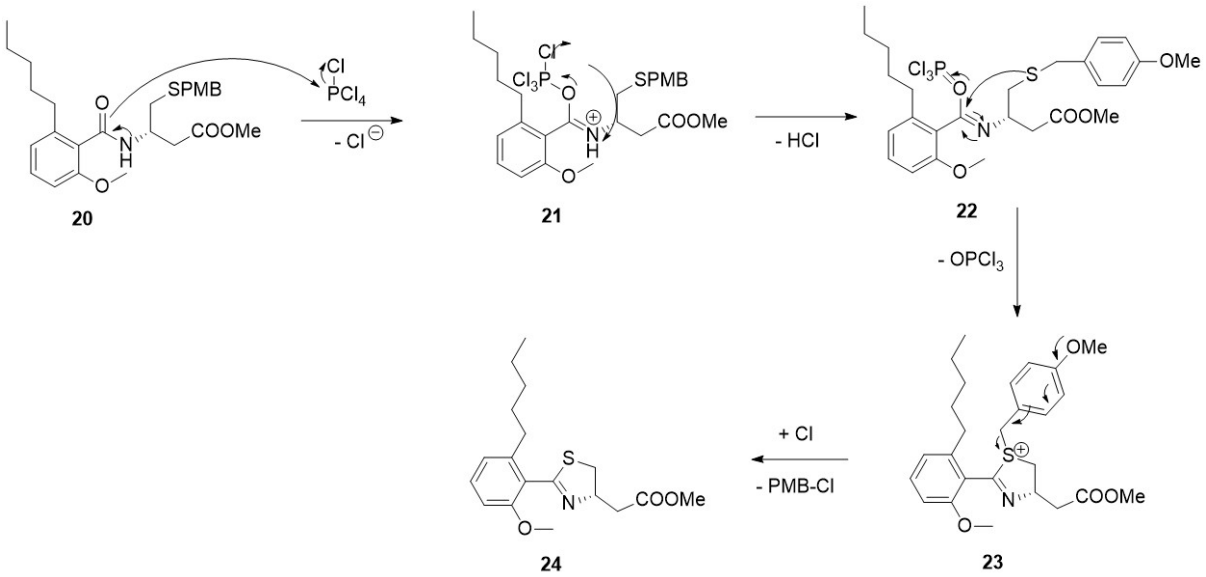

Figure 10: Possible mechanism of thiazoline ring formation from the amide (**20**) using phosphorus pentachloride.

The methylether and ester of **24** were cleaved using boron tribromide.[22] Boron tribromide acts as a Lewis acid due to an empty p-orbital and thus serves as an electrophile. The lone pairs of the methoxy oxygen **24** can attack boron tribromide nucleophilically. A bromide ion is then cleaved, attacking the methyl group to produce methyl bromide and remove the methoxy substituent. Upon aqueous work-up, the phenol is obtained. A similar mechanism applies to ester cleavage. At -80 °C, mostly the phenol is formed, whereas upon warming to room temperature, the corresponding carboxylic acid is obtained **25**.
In the next step, the Weinreb amide **26** was prepared. The formation of an amide bond between a carboxylic acid and an amine can be efficiently achieved using the coupling reagent bromo-tris-pyrrolidino-phosphonium hexafluorophosphate (PyBroP) in the presence of a base such as triethylamine. Initially, triethylamine deprotonates the carboxylic acid, generating the corresponding carboxylate anion. This deprotonation is favored due to the pK_A difference between triethylamine ($\sim$10.8) and the carboxylic acid ($\sim$4.8).[24] The resulting carboxylate then attacks the electrophilic phosphorus atom of the coupling reagent, forming an activated intermediate with a good leaving group. Subsequently, the amine nucleophilically attacks the carbonyl carbon of the activated intermediate. The O=P leaving group is displaced, yielding the desired Weinreb amide **26**.

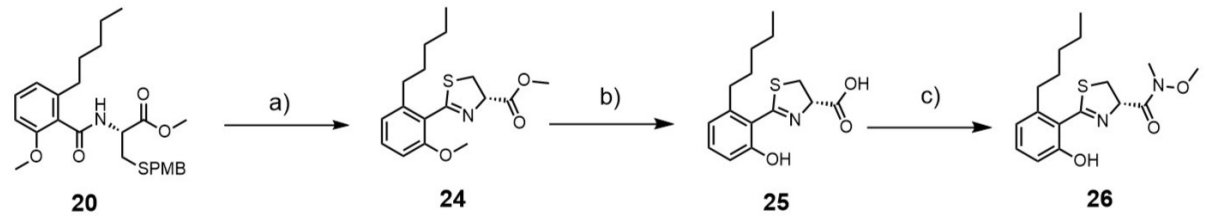

Figure 11: Synthesis of **26**. Conditions a) phosphorus pentachloride, dichloromethane, 85% b) boron tribromide, dichloromethane, -80 °C→RT for 5 h, 94% c) *N,O*-dimethylhydroxylamine hydrochloride, PyBroP, triethylamine, dichloromethane, RT over night, 42%

To form the aldehyde (**27**) the Weinreb amid (**26**) is reduced by lithium aluminum hydride.[25] During

reduction with $LiAlH_4$, the Weinreb amide is not reduced to the corresponding primary alcohol, but selectively to the aldehyde. This selectivity arises because the Weinreb amide can stabilize with a five-membered cyclic intermediate through coordination of the lithium cation to the carbonyl oxygen. Additionally, the oxygen atom of the *N*-methoxy group coordinates to the same lithium ion. This chelation strongly stabilizes the intermediate and prevents a second hydride transfer from lithium aluminium hydride ($LiAlH_4$). Upon aqueous work-up, the intermediate collapses to give the corresponding aldehyde **27**. Although the resulting aldehyde is unstable, it can be used directly in the subsequent step without purification.[26]
However, only very low yields were observed by ^{1}H-NMR. This low conversion may be attributed to the deprotonation of the phenolic group by $LiAlH_4$. This side reaction can be effectively prevented by introducing a protecting group, forming an *tert*-butyldiphenylsilyl (TBDPS) protected Weinreb amid **28**.[17] Upon repeating the reduction under the same conditions, the yield of the aldehyde **7** increased to 50%.

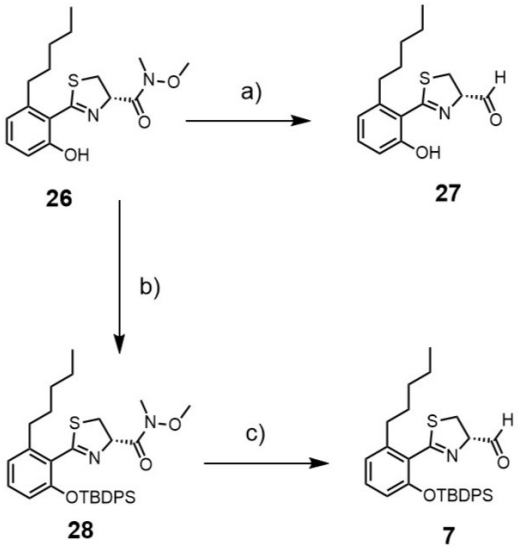

Figure 12: Synthesis of **7**. Conditions a) lithium aluminum hydride, tetrahydrofuran, 0 °C 30 min, b) *tert*-Butyl(chloro)diphenylsilane, imidazole, dimethylformamide, RT for 16 h, 84% c) lithium aluminum hydride, tetrahydrofuran, 0 °C 40 min, 50%

6.2 Building block B

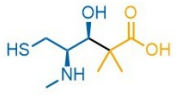

8

Figure 13: Building block B. Colors indicate the starting material.

6.2.1 Methyl ester approach

For the synthesis of building block B, L-cysteine was used as the starting material. Cysteine underwent cyclisation with formaldehyde to form a thiazolidine ring (**29**), thereby protecting the two reactive groups, the thiol and amine, to prevent side reactions in the subsequent step.[27] During this step, the latent *N*-methyl group is introduced, remaining protected within the thiazolidine ring and becoming exposed after ring cleavage in later steps. The amine group was protected by a *tert*-butoxycarboxylic (Boc) group, resulting in **30**.[28] During the formation of **31**, the carbonyl acid proved to be an ineffective electrophile, and the hydroxyl group was unsuitable as a leaving group. Therefore, **30** was treated with carbonyldiimidazole (CDI) to form an acylimidazole intermediate, which acted as a sufficient leaving group. The formation of lithium diisopropylamide (LDA) involved the reaction of *n*-butyllithium with diisopropylamine, which was subsequently employed to deprotonate methyl isobutyrate at the *sec*-propyl site. This position is resonance-stabilised, by Li-enolate. After the prepared acylimidazole intermediate was added, the carbanion attacked the carbonyl group, resulting in the formation of a new C-C bond and the displacement of imidazole as an effective leaving group, thereby producing compound **31**.[29]

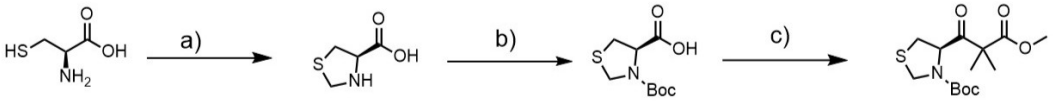

11 29 30 31

Figure 14: Synthesis of **31**. Conditions a) formaldehyde, water, RT for 15 h, then pyridine, 92% b) Boc_2O, pyridine, RT for 96 h, 55% c) carbonyldiimidazole, tetrahydrofuran, 0 °C for 30 min, RT for 1 then *n*-butyllithium, diisopropylamine, methylisobutyrate, -78 °C, 50%.

Ketone **31** was reduced with sodium borohydride to the secondary alcohol **32** with an *S* configuration. In the reduction of a chiral ketone to a secondary alcohol, typically two diastereomers can be formed, depending on the face of nucleophilic attack.[29]

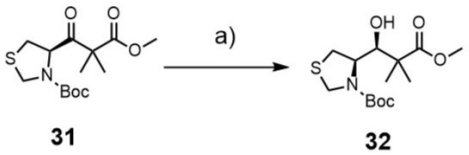

Figure 15: Synthesis of **32**. Conditions a) Sodium borohydride, methanol, 0 °C for 20 min, 76%.

According to the Felkin–Anh model, the nucleophile, in this case the borohydride, attacks as illustrated in the Newman projection figure 16. The amine protected with the Boc group sterically hinders si-face attack, forcing the hydride to attack from the re-face, giving only one diastereomer as product.[29]

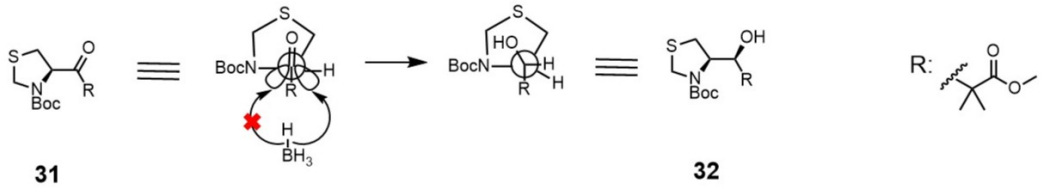

Figure 16: Newman projection of the Felkin-Ahn model and nucleophilic attack of the bohrhydride at the ketone **31** to form secondary alcohol **32**.

To facilitate the combination reaction of the two building blocks, the thiazolidine ring **32** needs to be cleaved between the amine and thiol groups. This will expose the reactive sides for subsequent combination with the aldehyde **7**. The thiazolidine ring can be opened using Birch reduction. This reaction successfully opened the ring, but it also reduced the ester to a primary alcohol **33** and triggered intramolecular ring formation. Therefore, it is essential to cleave the ester **32** before performing the Birch reduction.

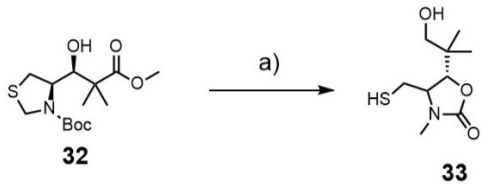

Figure 17: Synthesis of **33**. Conditions a) sodium, liquid ammonia, –50 °C . Main product from Birch reduction of **32**.

Various methods were tested for cleaving the ester. The first method used lithium hydroxide, which

successfully cleaved the ester to form a carboxylic acid, but also involved an intramolecular ring formation. Since, the lithium hydroxide is a strong base ($pK_A \sim 14$) it was able to deprotonated the secondary alcohol ($pK_A \sim 16$).[24] The oxygen could then nucleophilically attack the carbonyl of the Boc protecting group, forming a cycle and a *tert*-butoxide leaving group. It was not possible to recover the molecule to its original form or to cleave the cyclic intermediate in alkaline conditions.[30]

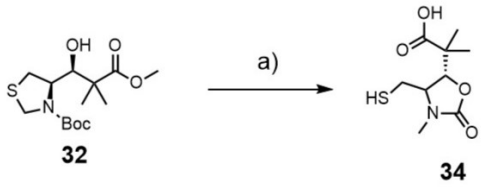

Figure 18: Synthesis of **34**. Conditions a) lithium hydroxide, methanol, tetrahydrofuran. Main product from the ester cleaved with LiOH.

The cleavage of the ester in an enzymatic reaction was tested using pig liver esterase in a phosphate buffer. It was expected that the enzyme would be more specific, cleaving the ester without forming side products, but even after 46 h, no product formation was detectable.[31]
Ester cleavage was tested by protecting the secondary alcohol with an ethoxyethyl (EE) group. Ester **32** was cleaved in alkaline conditions using sodium hydroxide and methanol. During the acidic work-up, the EE-protecting group was deliberately cleaved, yielding compound **35**.[32] This reaction was an improvement over the previous failed experiments, but the entire 3-step sequence took up to 4 days and proved difficult to reproduce. Therefore, a 2-(trimethylsilyl)ethyl ester, which is susceptible to either fluoride or acid-mediated cleavage, was employed.

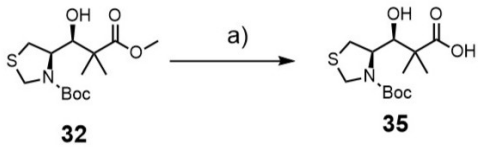

Figure 19: Synthesis of **35**. Conditions a) pyridinium *p*-toluenesulfonate, ethyl vinyl ether, dichloromethane, RT for 2 d, evaporating, aqueous sodium hydroxide solution, tetrahydrofuran, methanol, RT for 3 d, then 60 °C for 26 h, 72%.

6.2.2 2-(trimethylsilyl)ethyl ester

This compound was selected due to its distinct protecting group compared to the methyl group in **32**, anticipating that the cleavage would proceed more efficiently. The ester (**12**) was synthesized by reacting isobutyryl chloride with 2-(trimethylsilyl)ethanol. The alcohol attacks the carbonyl carbon, while the chloride acts as an effective leaving group. Pyridine deprotonates the intermediate, yielding compound **12**.[33]

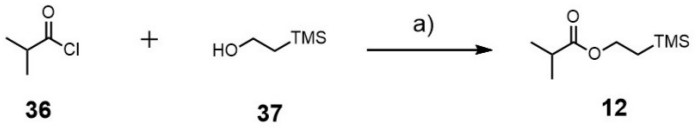

Figure 20: Synthesis of **12**. Conditions a) isobutyryl chloride, 2-(trimethylsilyl)ethanol, dichloromethane, pyridine, RT for 3 h, 95%

The next step is analogous to that performed with the methyl ester. Compound **31** is treated with CDI, forming the acylimidazole intermediate. LDA deprotonates **12**, and the resulting carbanion attacks the carbonyl group of the intermediate, yielding **38**. The reduction with sodium borohydride proceeds in the same manner and results in **39** with *S*-configuration at the newly formed stereocenter.[29]

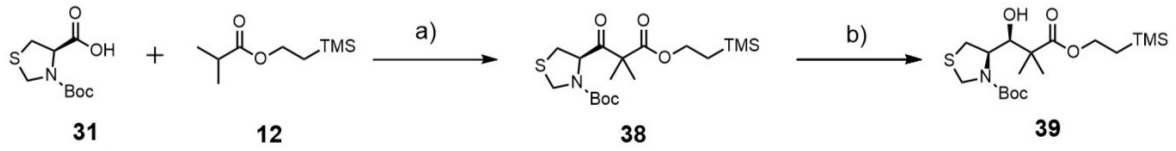

Figure 21: Synthesis of **39**. Conditions a) carbonyldiimidazole, tetrahydrofuran, 0 °C for 30 min, RT for 1 h, then *n*-butyllithium, diisopropylamine, tetrahydrofuran, -78 °C, 69% b) sodium borohydride, 0 °C for 15 min, 95%

In the final step, the amine was deprotected, and the thiazolidine ring was opened using a Birch reduction, resulting in the formation of an *N*-methyl group and a thiol group. To prevent disulfide formation, an attempt was made to protect the thiol with a trityl group. However, no formation of the protected thiol was observed. Therefore, to minimise reactivity and unwanted side reactions in the following steps, intermediates containing the free thiol group were used directly in the subsequent reaction and kept under oxygen-free conditions to suppress the formation of disulfide side products. It was not clear which order would be preferred with the Boc deprotection and the Birch reduction. When the sequence involved first opening the thiazolidine **39** *via* Birch reduction, followed by Boc deprotection, a ring-forming reaction **40** was observed. It was presumed that during Birch reduction, the secondary alcohol is deprotonated and can subsequently attack the carbonyl of the Boc group, leading to intramolecular ring closure. Therefore, the reaction sequence was modified. Boc deprotection and simultaneous cleaving of the ester was performed first with trifluoroacetic acid, which proceeded smoothly and afforded **41**.[34,35] The subsequent Birch reduction then proceeded without any observable side reactions or ring formation, yielding **8**. Since the thiol and amine groups are now unprotected, the next step was carried out immediately to minimize side reactions at these reactive sites.

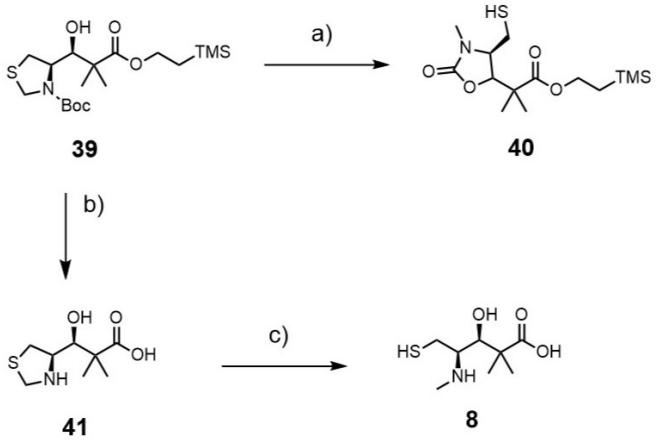

Figure 22: Synthesis of **8**. Conditions a) sodium, tetrahydrofuran, liquid ammonia, –50 °C b) trifluoroacetic acid, dichloromethane, 0 °C for 5 h b) sodium, tetrahydrofuran, liquid ammonia, -50 °C

In summary, the final building blocks could be synthesized. Building block A results in the aldehyde **7**, which is very unstable. Building block B resulted in the molecule **8** being very unstable due to a thiol group that can form a disulfide bond and an amine group. The next step is the combination reaction of those two molecules before the final reaction, the deprotection of the phenol has to be performed to complete agochelin **1**.

6.3 Connecting the building blocks

For the connection of the building blocks, different approaches with different reaction conditions were tested, as shown in Table 1. The initial attempts followed the same synthetic approaches used for the combination reaction of the natural products yersiniabactin and micacocidin.[17,18,22]

Table 1: Reaction conditions that were tested for the combination reaction of the final product building block A and building block B.

reaction	educts (theoretical amount)	solvents	reagent	reaction conditions	result
A	**7** (0.05 mmol), **8** (0.1 mmol)	DCM (2 mL), MeOH (0.6 mL), D_2O (1 mL)	KOAc (50 mg, 0.5 mmol, 5 equiv.)	RT for 48 h	not detected
B	**7** (0.1 mmol), **8** (0.1 mmol)	dry DCM (3 mL), dry MeOH (1 mL)	KOAc (50 mg, 0.5 mmol, 5 equiv.)	RT for 16 h	n. d.
C	**7** (0.01 mmol), **8** (0.1 mmol)	MeOH (3 mL), dry THF (3 mL), H_2O (10 mL)	KOAc (0.5 g, 5 mmol, 50 equiv.)	RT for 16 h	n. d.
D	**7**(0.1 mmol), **8** (0.1 mmol)	degassed THF (1.5 mL), degassed H_2O (1.3 mL)	KOAc (0.5 g, 5 mmol, 50 equiv.)	RT for 96 h	n. d.
E	**7** (0.1 mmol), **8** (0.1 mmol)	degassed THF (1.5 mL), degassed H_2O (1.5 mL), degassed DMSO (1.5 mL)	KOAc (0.5 g, 5 mmol, 50 equiv.)	RT for 16 h	n. d.
F	**7** (0.1 mmol), **8** (0.1 mmol)	degassed DMSO (1.5 mL)	dry pyridin (81 μL, 1 mmol, 10 equiv.)	RT for 16 h	traces observed *via* MS
G	**7** (0.2 mmol), **8** (0.2 mmol)	degassed DMSO (3.5 mL)	dry pyridin (0.16 mL, 2 mmol, 10 equiv.)	RT for 16 h	traces observed *via* MS

For the combination reaction, the final product from the building block syntheses were used. For building block A, the aldehyde **8**, for building block B, two different compounds were tested. In most cases, the combination reaction was conducted in the same flask as the Birch reduction, leaving sodium and ammonium salts from the quenching of elemental sodium. As the product is a colourless salt, it was difficult to differentiate from the remaining salts in the flask.
Both key building blocks are unstable due to unprotected reactive groups such as the thiol, amine, and aldehyde groups. Therefore, the reactions needed to be carried out under a nitrogen atmosphere and conducted immediately.
In the first approach **A**, the same reaction conditions were used as those reported by Ino *et al.* in 1999 for the synthesis of micacocidin.[22] Unlike the original synthesis, our approach included the addition of water. In contrast, reaction **B** was performed under strictly anhydrous conditions to ensure complete consistency with the reported synthesis. Both reactions were diluted with ethyl acetate and washed with aqueous saturated NH_4Cl and NaCl solutions. The organic layer was dried over sodium sulfate and concentrated under reduced pressure. The residues showed no product formation in ei-

ther NMR or MS analysis. It was hypothesised that incomplete solvent mixing prevented the reactants from interacting. Thus, the more polar organic solvent tetrahydrofuran (THF) was used instead of dichloromethane (DCM) in step **C**. The KOAc salt was dissolved in water and then added to the reaction as a solution to ensure complete dissolution. After the addition of all reactants, the pH of the reaction mix was checked and found to be pH $\sim$ 8, since the proposed mechanism requires slightly alkaline conditions. The work up was the same as for **A** and **B** and in the MS analysis only the ion [M + H^+] 514.2240 m/z and the associated iron [M + H^+ + Na] 536.2059 m/z were detectable. This could be assigned to an oxidised aldehyde (figure 23 and no other side reaction or fragment form building block B could be detected.

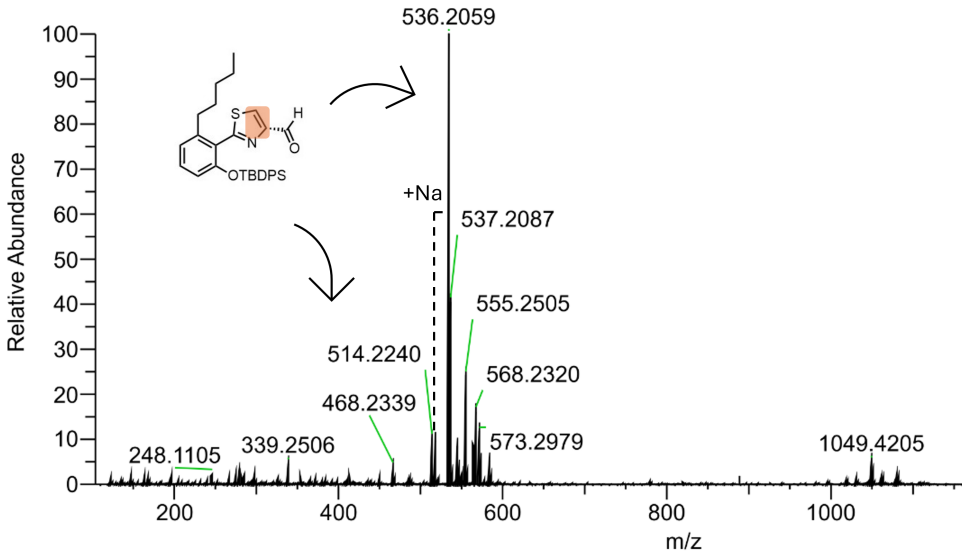

Figure 23: electrospray ionization-MS in positive mode for reaction **C**. Main product is the oxidized building block A.

Since the oxidised species was the only detectable compound, it was assumed that oxygen was the oxidising reagent in this reaction. Therefore, reactions under oxygen-free conditions were tested. The reaction was performed under a nitrogen atmosphere, and to ensure complete oxygen exclusion, the solvents were degassed. Since THF and water were propsed to be miscible, methanol was not used. According to Ino *et al.*, dichloromethane, as the sole solvent, also yielded the desired product.[29] In **D** solvents, tetrahydrofuran and water were degassed before they were used. Additionally, the workup was changed to an aqueous and acidic workup, by diluting the reaction mix to pH $\sim$ 4 with citric acid. The assumption was that the reaction is carried out in alkaline conditions, therefore, the carbolic acid is deprotonated ($pK_A \sim 4.8$).[24] When the pH is lowered to acidic conditions, the carboxylic acid should be protonated and become more soluble in organic solvents than in water, resulting in a higher yield. The now acidic reaction mixture was extracted with ethyl acetate, the organic layer was washed with aqueous saturated NH_4Cl and NaCl, dried over sodium sulfate, and concentrated under reduced pressure. Further purification on flash chromatography (petrol ether : ethyl acetate + 1% acetic acid (AcOH), 2 : 1 (3 column volumes (CV)), dichloromethane : methanol + 1%, 9 : 1 (2.5 CV)) yielded two main fractions. The first eluting fraction is the main side product, the oxidised aldehyde with a thiazol ring instead of a thiazolin ring, already detected in reaction **C** (figure 23). The later eluting fraction was characterised with NMR and MS and could be identified as a derivative of the desired product with an oxidised thiazolin ring to a thiazol [M+H^+] m/z 703.4974.

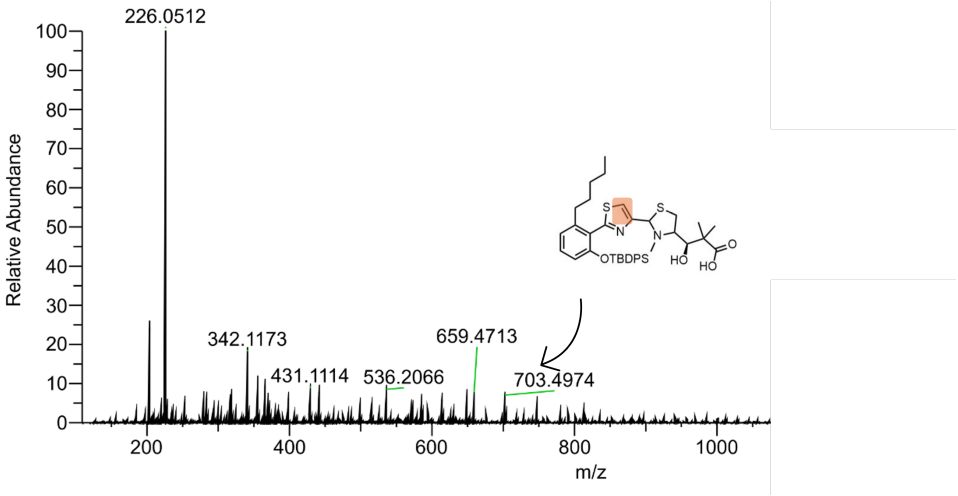

Figure 24: Mass spectrum in positive mode for reaction **D**.

It was now confirmed that the combination reaction was feasible, although the oxidation of the thiazolin ring likely occurred prior to the cyclisation. The main objective was to minimise the oxidation reaction and to find a more suitable solvent.
In reaction **E**, after the addition of tetrahydrofuran and water, a phase separation was observable. Degassed dimethyl sulfoxide (DMSO), being miscible with organic solvents and water, was added. Although phase separation persisted, increased mixing between the two phases was visually observed. The same acidic and aqueous workup as for **D** was performed, but no product was detectable by MS or NMR. Since building blocks A and B both dissolved in DMSO, degassed DMSO was used as the solvent in reaction **F**. potassium acetate (KOAc) probably does not dissolve in DMSO, therefore, pyridine was used as a base. The pH was checked to be approximately 8, the same as in the previous reaction. In the workup of **F**, the reaction mixture was diluted to pH $\sim$ 4 with citric acid, and aqueous saturated NaCl solution was added. The reaction mixture was extracted with ethyl acetate, dried over sodium sulfate, and concentrated under reduced pressure. MS analysis of the residue showed the first time a formation of the target molecule $[M + H^+]$ 705.311 m/z figure 25. The oxidised target molecule is detectable with $[M+H^+]$ m/z 703.4974. The aldehyde side product is detectable, and additionally, the reduction product of the aldehyde (**8**). Since the reaction was the first to show formation of the target molecule, albeit at low yield, it was repeated with twice the amount of starting material to obtain sufficient material for purification.

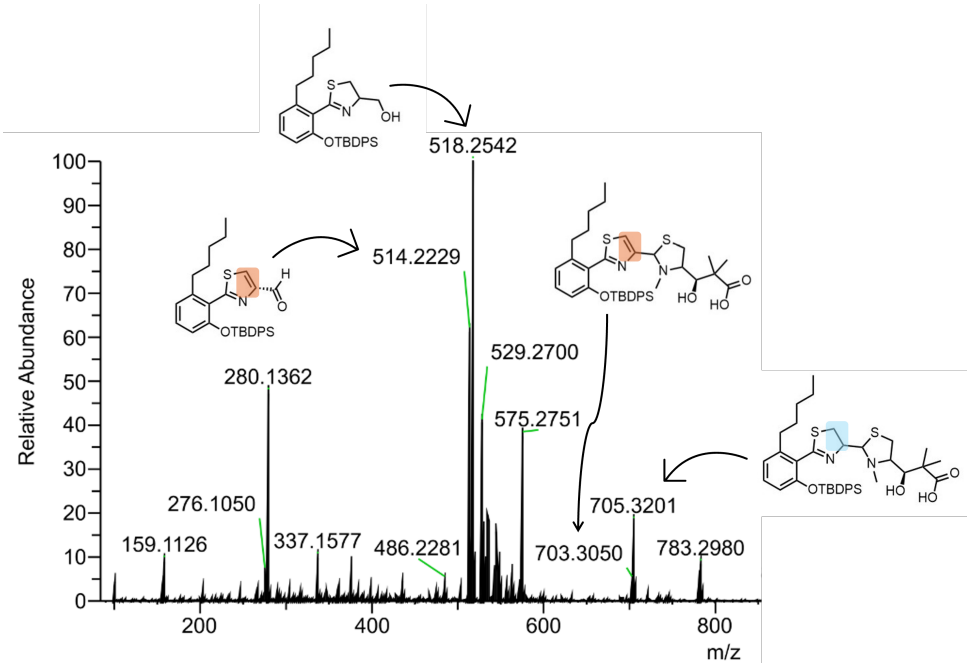

Figure 25: Mass spectrum in positive mode for reaction **F**.

Reaction **G** was conducted exactly as reaction **F**. It was therefore assumed that the reaction yielded the same product, and the crude product was directly treated with tetra-*n*-butylammonium fluoride (TBAF) (1.0 M in THF, 0.20 mL, 0.20 mmol, 1.0 equiv.) at 0 °C. The reaction mixture was allowed to reach RT and was stirred for 1 h. The reaction mixture was diluted with ethyl acetate and washed with aqueous 5% $KHSO_4$ solution and aqueous saturated NaCl solution. The organic layer was dried over sodium sulfate and concentrated under reduced pressure to yield a yellow oil (0,14 g). The mass spectrum (figure 26) of the deprotection reaction showed minimal amounts of agrochelin.

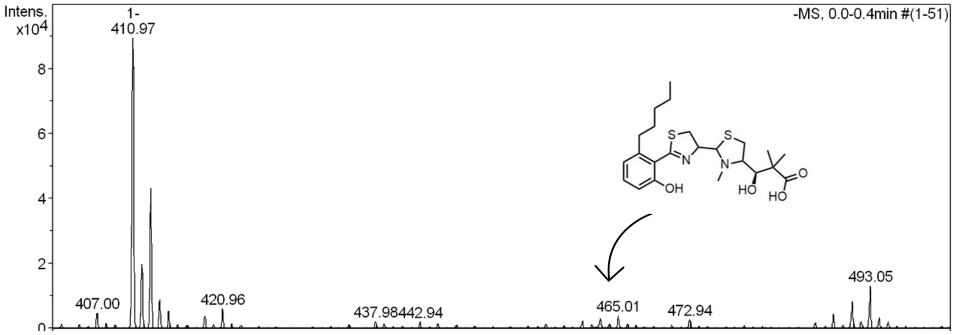

Figure 26: Mass spectrum of negative mode for reaction **G** after deprotection step.

Agrochelin needs to be purified on an HPLC system, therefore, different methods were tested on an analytical HPLC system. Using analytical HPLC with a ReproSil 100 C18 column, optimal peak separation was achieved with a gradient of 20% to 100% methanol in water over 45 min. Therefore, this method was used to perform a preparative HPLC separation with the **G** crude product. All fractions needed to be tested with mass analysis to identify the fraction with the target molecule. The fraction marked in orange showed traces of the target molecule.

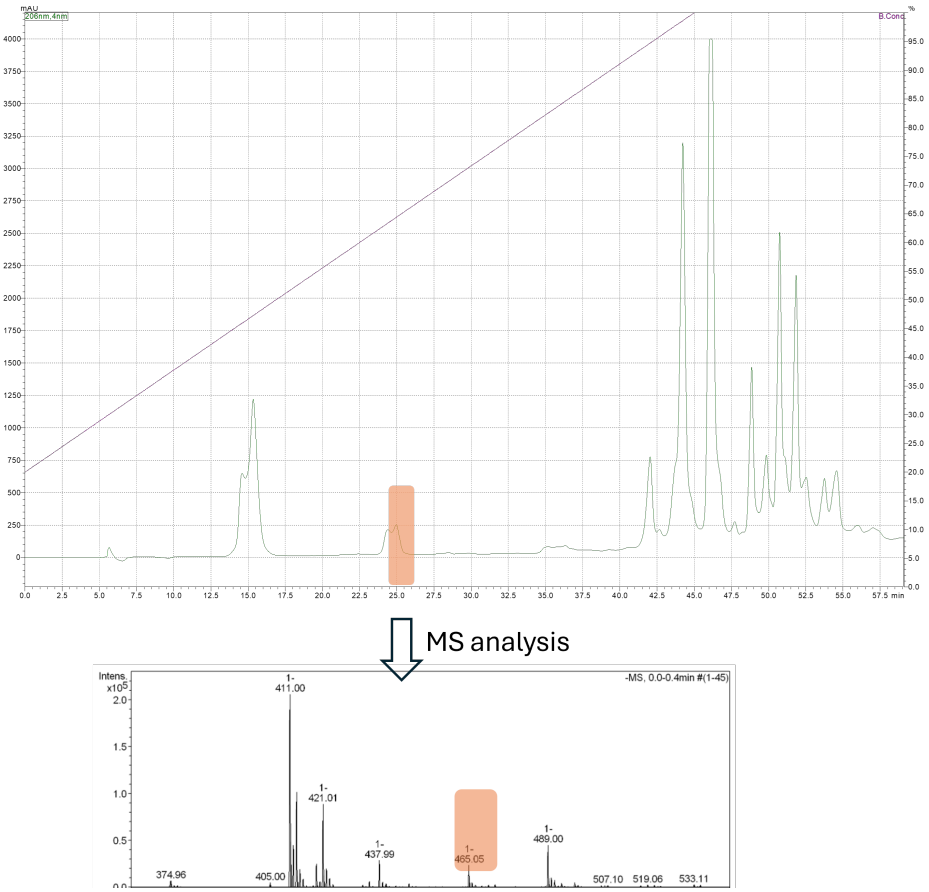

Figure 27: Chromatogram for crude product of deprotection reaction of **G**. The fraction in orange contained the target molecule.

The mass spectrum (figure 27) shows the target compound at very low yield, along with various side products and impurities. The HPLC method is therefore insufficient for purifying agrochelin. Although the solubility issues improved with the use of DMSO, the key challenge remained identifying a solvent capable of dissolving both building blocks. The highly non-polar building block A, containing a pentyl chain, a non-polar protecting group, and an aromatic structure, and the highly polar building block B, bearing a carboxylic acid, a secondary alcohol, a thiol, and an amine group, have difficulty dissolving in the same solvent. Since various solvents had already been tested, with DMSO giving the best results, a modification of the building blocks was considered. To increase the overall hydrophobicity, the secondary alcohol of building block B was protected with a nonpolar TBS group.[29] The protecting group was chosen due to its ability to be cleaved concurrently with the TBDPS group in a single TBAF-mediated step.

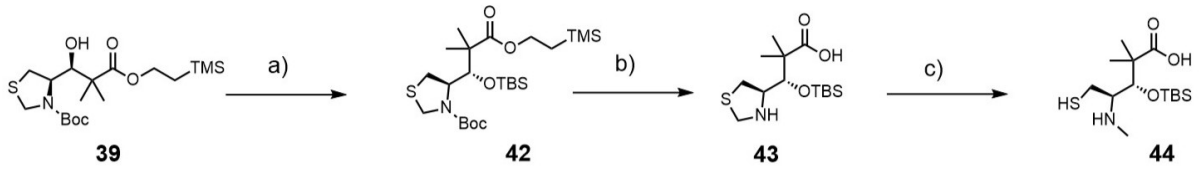

Figure 28: Synthesis of **44**. Conditions a) *tert*-butyldimethylsilyl trifluormethansulfonate, dry lutidine, dry dichloromethane, 0 °C for 15 min. b) trifluoroacetic acid, dichloromethane, 0 °C for 5 h c) sodium, tetrahydrofuran, liquid ammonia, –50 °C

For the reaction using the TBS-protected building block B, DMSO was used as solvent, as previous experiments had shown it to be suitable. It was also assumed that thiazolin formations can occur in buffered media. Therefore, pyridine and acetic acid were added in a ratio of 2:1 in reaction **H**. After the reaction, DMSO was removed from the mixture by distillation. Mass spectrometry analysis of the residue did not show formation of the desired product. To further investigate whether the reaction proceeds under basic or acidic conditions, since both have been reported in the literature,[36,37] reaction **J** was performed under acidic conditions with acetic acid, and reaction **I** was carried out under alkaline conditions. Both reactions were heated to 80 °C, as temperature variation had not been studied previously.[37,38] Neither reaction showed formation of the desired product.

Table 2: Reaction conditions that were tested for the combination reaction of the final product building block A and building block B.

reaction	educts (theoretical amount)	solvents	reagent	reaction conditions	result
H	**7** (0.25 mmol), **44** (0.32 mmol)	degassed DMSO (4.0 mL)	dry pyridin (0.26 mL, 3.2 mmol, 10 equiv.), AcOH (91 μL, 1.6 mmol, 5.0 equiv.)	RT for 16 h	n. d.
I	**7** (0.27 mmol), (**44** (0.25 mmol)	degassed *n*-butanol (3 mL)	pyridine (4.0 mL, 50 mmol)	80 °C for 20 h, RT for 72 h	n. d.
J	**7** (0.27 mmol), **44** (0.25 mmol)	degassed *n*-butanol (3 mL)	AcOH (0.15 mL, 2.5 mmol, 10 equiv.)	80 °C for 20 h, RT for 72 h	n. d.

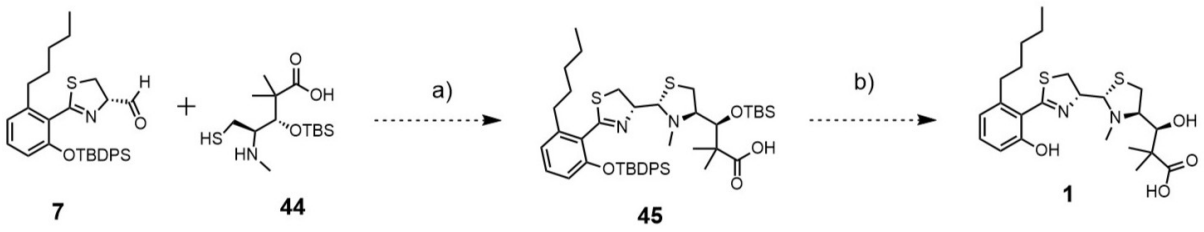

Figure 29: Proposed synthesis of **1**. Conditions a) tested conditions are shown in table 1 and 2 b) TBAF, tetrahydrofuran, 0 °C → RT, 16 h

6.4 Conclusion

For both building blocks A and B, stable precursors to the unstable intermediates could be prepared. At several stages, undesired reactivity can be prevented by using protecting groups, allowing the synthesis to proceed in a controlled manner. The use of readily available chiral molecules, such as D- and L-cysteine, laid the foundation for the introduction of three out of four chiral centres in the final molecule.
Building block A was synthesised by a Negishi coupling of a *n*-pentlyzinc (II) bromide with 2-bromo-6-methoxybenzoic acid, followed by an amid formation with an *S*-PMB protected D-cysteinmethyl ester and the thiazolin ring closure. It was determined that a thiol protection was necessary to prevent reactivity. The ester and the methoxy group were cleaved by boron tribromide, and subsequently a Weinreb amide was formed. The reduction to the aldehyde was feasible in good yield by TBDPS-protection of the phenol. For building block B, L-cysteine was cyclized to a thiazolidine and Boc-protected at the amine positions. *Via* a carbanion, a coupling to 2-(trimethylsilyl)ethyl ester was possible. The ester cleavage and Boc deprotection could be performed in a single step, followed by birch reduction, hence preventing an intramolecular ring formation.
It was possible to shorten the previously reported synthesis for micacocidin, through Negishi coupling instead of Wittig reaction followed by hydrogenation. Furthermore, combining the ester cleavage with the Boc deprotection shortens the procedure.[22]
Despite evaluating ten different reaction conditions for coupling the two building blocks, the target compound could not be obtained in a sufficient amount for HPLC purification. A range of temperatures, pH values, and solvents were tested to determine the optimal conditions for agrochelin formation. Among these parameters, the solvent had the strongest effect on fragment coupling, while variations in pH or reaction temperature did not lead to improved yields. The final step, the deprotection of the phenol was successfully achieved, although only on a very small scale.

6.5 Outlook

To further improve the reaction conditions for fragment coupling, it might be helpful to remove the salts formed during the quenching step after the Birch reduction. This could be achieved by performing a HPLC preparative purification. Consequently, it would allow better visual control in the subsequent combination step, making it easier to determine whether both building blocks are fully soluble in the chosen solvent. Up to this point, the educts in the penultimate step have remained impure, as purification is hindered by their instability and high reactivity. By purifying both educts, fewer side reactions could occur, thereby increasing the currently low yield.

7 Experimental Section

7.1 General

Chemical Reagents and Solvents:
Analytical thin-layer chromatography was performed on silica gel 60-F plates from *Sigma-Aldrich*. Flash chromatography was performed using 40 - 63 μm silica gel from *VWR*. Yields refer to chromatographically and spectroscopically pure materials, unless otherwise stated. All other reagents were used as supplied by *Sigma-Aldrich*, *TCI*, *Merck*, *BLD Pharm* and *Thermo Scientific*. All reactions were carried out in heat-gun-dried glassware under nitrogen atmosphere unless otherwise stated.

HPLC:
Analytical HPLC was performed on an *Shimadzu* (manual injector, DGU-20A, LC-20AT, CBM-20A, SPD-M20A) system. The used column was *Dr. Maisch* ReproSil 100 C18 (250 x 4.6 mm, 5 μm). As solvents, a gradient of water/methanol 0.1% formic acid was used with a flow rate of 1 mL/min.
Preparative HPLC was performed on an *Shimadzu* (manual injector, SCL-40, DGU-405, LC-20AR, SPD-M40) with a *Dr. Maisch* ReproSil 100 C18 column (250 x 20 mm, 10 μm). As solvents, a gradient water/methanol with 0.1% formic acid was used with a flow rate of 10 mL/min. Samples were collected in rinsed test tubes.

NMR Analysis:
^{1}H NMR and ^{13}C NMR spectra were either recorded at room temperature on a *Bruker* Avance III operating at 400 MHz for proton nuclei or by the NMR center of the faculty of chemistry at room temperature on a *Bruker* Avance III operating at 600 MHz for proton nuclei. ^{1}H chemical shifts are reported in ppm relative to chloroform (δ H = 7.26) and dimethyl sulfoxide-d6 (δ H = 2.50). ^{13}C chemical shifts are reported in ppm relatively to chloroform (δ C = 77.16) and dimethyl sulfoxide-d6 (δ C = 39.52). The software used for data processing and signal assignment was *MestReNova* Version 14.3.0. The following abbreviations were used: s = singlet, d = doublet, t = triplet, m = multiplet; coupling constants are given in Hertz. two-dimensional correlation spectroscopy (COSY), total correlation spectroscopy (TOCSY), nuclear overhauser effect spectroscopy (NOESY), heterobinuclear multibound correlation (HMBC) and heteronuclear single quantum coherece (HSQC) experiments were used. The sample was measured in NMR tubes (*Wilmad* 507-PP-8)

High resolution mass spectrometry (MS) Analysis:
High-resolution ESI mass spectra were performed by the Mass Spectrometry Center of the faculty of chemistry on an ESI/MALDI-Qq-TOF with dual-TIMS analyzer.

7.2 Synthesis of building block A

Pentylzinc(II) bromide (14)[19]
Zinc dust (7.8 g, 0.12 mol, 1.2 equiv.) was heated in a Schlenk tube to 70 °C under high vacuum for 30 min. The zinc dust was cooled to room temperature. Dimethylformamide (100 mL) and 10 crystals of iodine were added and the resulting mixture was stirred until the yellow color faded. *n*-Pentylbromide (12 mL, 0.10 mol) was added and the resulting reaction mixture was heated to 70 °C for 2 days. The reaction mix was cooled to room temperature, and the zinc dust was allowed to settle. The yellow supernatant was directly used in the next step.

2-Methoxy-6-pentyl benzoic acid (15)[19]

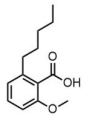

2-Bromo-6-methoxybezoic acid (4.6 g, 20 mmol) was added in several portions to pentylzinc bromide (**14**) (in dimethylformamide, 60 mL, ≤ 60 mmol, 3 equiv.). $Pd(dppf)Cl_2$ (0.2 g, 0.2 mmol, 0.01 equiv.) was added and the solution was heated to 60 °C for 3 days, resulting in a color change from black to yellow to brown. The reaction mixture was diluted with hydrochloric acid (1 M, 300 mL) and subsequently extracted with diethyl ether (3 x 250 mL). The combined organic layers were dried over sodium sulfate and concentrated under reduced pressure. The residue was purified by flash chromatography (dichloromethane : methanol, 95 : 5 + 1% acetic acid) to yield the product **15** (3.2 g, 14 mmol, 72%) as a brown liquid.
The product was identified in accordance with literature data.[19]

2-Methxy-6-pentylbenzoyl chlorid (16)[21]

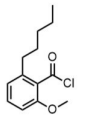

Thionyl chloride (0.66 mL, 9.1 mmol, 1.1 equiv.) and dimethylformamide (2 drops) were added to a stirred solution of **15** (8.3 mmol, 1.8 g) in 1,2-dichloroethane (12 mL). The resulting solution was heated to 80 °C. The reaction progress could be observed with a toluene-filled bubbler. No more sulfur dioxide evolution indicated completion after 30 min and the reaction mixture was stirred for another hour. The reaction mixture was concentrated under reduced pressure and the crude product was used directly in the next step.
The product was identified in accordance with literature data.[21]

Methyl *N*-(2-methoxy-6-pentylbenzoyl)-*S*-(4-methoxybenzyl)-L-cysteinate (20)[22]

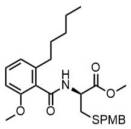

2-Methxy-6-pentylbenzoyl chlorid (**16**) (≤ 8.3 mmol) dissolved in dry dichloromethane (5 mL) was added dropwise to a stirred solution of PMB-*D*-cystein-OMe (**19**) (2.3 g, 9.1 mmol, 1.1 equiv.) in dry dichloromethane (11 mL) and dry pyridine (1.8 mL, 23 mmol, 2.7 equiv.) at 0 °C. The mixture was allowed to reach room temperature and was further stirred for 1 h. The resulting mixture was concentrated under reduced pressure, and the remaining residue was dissolved in ethyl acetate (100 mL). The organic layer was washed with aqueous saturated NH_4Cl solution (80 mL), aqueous saturated $NaHCO_3$ solution (80 mL) and aqueous saturated NaCl solution (80 mL). The organic layer was dried over sodium sulfate and concentrated under reduced pressure. The residue was purified by flash chromatography (petrol ether : ethyl acetate, 3 : 2) to yield the product **20** (1.7 g, 3.6 mmol, 43%) as a yellow liquid.
The product was identified in accordance with literature data.[22]

Methyl (*S*)-2-(2-methoxy-6-pentylphenyl)-4,5-dihydrothiazole-4-carboxylate (24)[22]

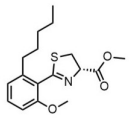

Phosphorus pentachloride (1.5 g, 7.4 mmol, 2.1 equiv.) was added in portions to a stirred solution of **20** (1.7 g, 3.5 mmol) in dichloromethane (7.7 mL) at 0 °C. After 1 h, the mixture was diluted with ethyl acetate (100 mL) and washed with aqueous saturated $NaHCO_3$ solution (80 mL) and aqueous saturated NaCl solution (80 mL). The organic layer was dried over sodium sulfate and concentrated under reduced pressure. The residue was purified by flash chromatography (petrol ether : ethyl acetate, 4 : 1) to yield the product **24** (0.97 g, 3.0 mmol, 85%) as a yellow liquid.
The product was identified in accordance with literature data.[22]

(*S*)-2-(2-Hydroxy-6-pentylphenyl)-4,5-dihydrothiazole-4-carboxylic acid (25)[22]

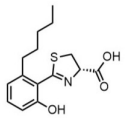

Boron tribromide (1.0 M in dichloromethane, 6.3 mL, 6.3 mmol, 2.1 equiv.) was added to a stirred solution of **24** (0.97 g, 3.0 mmol) in dry dichloromethane (7 mL) at -80 °C. After 15 min at the same conditions, the yellow solution was allowed to reach room temperature. After 5 h, ice cubes were added and the mixture was diluted with ethyl acetate (100 mL). The mixture was washed with aqueous saturated NaCl solution (2 x 80 mL). The organic layer was dried over sodium sulfate and concentrated under reduced pressure to yield **25** (0.82 g, 2.9 mmol, 94%) as a yellow, viscous liquid.
The product was identified in accordance with literature data.[22]

(*S*)-2-(2-Hydroxy-6-pentylphenyl)-*N*-methoxy-*N*-methyl-4,5-dihydrothiazole-4-carboxamide (26)[22]

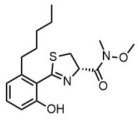

N,O-dimethylhydroxylamine hydrochloride (0.33 g, 3.4 mmol, 1.2 equiv.), PyBroP (1.5 g, 3.1 mmol, 1.1 equiv.) and dry triethylamine (1.0 mL, 7.1 mmol, 2.5 equiv.) were added to a stirred solution of **25** (0.84 g, 2.9 mmol) in dry dichloromethane (10 mL) at 0 °C. The mixture was allowed to reach room temperature overnight. After 14 h, the mixture was diluted with ethyl acetate (100 mL) and washed with aqueous saturated 5% $KHSO_4$ solution (80 mL), aqueous saturated $NaHCO_3$ solution (80 mL) and aqueous saturated NaCl solution (80 mL). The organic layer was concentrated under reduced pressure. The residue was purified by flash chromatography (petrol ether : ethyl acetate, 3 : 1→1 : 1) to yield the product **26** (0.42 g, 1.2 mmol, 42%) as a colorless liquid.
The product was identified in accordance with literature data.[22]

(*S*)-2-(2-((*tert*-Butyldiphenylsilyl)oxy)-6-pentylphenyl)-*N*-methoxy-*N*-methyl-4,5-dihydrothiazole-4-carboxamide (28)[17]

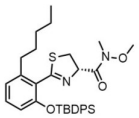

tert-butyl(chloro)diphenylsilane (TBDPS-Cl) (0.62 mL, 2.4 mmol, 2.1 equiv.) and imidazole (0.33 g, 4.9 mmol, 4.3 equiv.) were added to a stirred solution of **26** (0.38 g, 1.1 mmol) in dry dimethylformamide (9 mL) at 0 °C. The mixture was allowed to reach room temperature overnight and was then diluted with ethyl acetate (100 mL) and washed with aqueous saturated NaCl solution (3 x 100 mL). The organic layer was dried over sodium sulfate and concentrated under reduced pressure. The residue was purified by flash chromatography (petrol ether : ethyl acetate, 9 : 1→3 : 1) to yield the product **28** (0.57 g, 0.96 mmol, 84%) as a colorless liquid.
The product was identified in accordance with literature data.[17]

(*S*)-2-(2-((*tert*-Butyldiphenylsilyl)oxy)-6-pentylphenyl)-4,5-dihydrothiazole-4-carbaldehyde (7)[17,25]

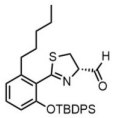

Lithium aluminum hydride (1 M in THF, 0.064 mL, 0.064 mmol, 1.2 equiv.) was added slowly to a stirred solution of **28** (30 mg, 0.050 mmol) in dry tetrahydrofuran (1.5 mL) at 0 °C. After 40 min at the same conditions, the mixture was diluted with ethyl acetate (10 mL) and poured into an aqueous saturated NH_4Cl solution (10 mL). The layers were separated and the aqueous layer was extracted with ethyl acetate (10 mL). The combined organic layers were dried over sodium sulfate and concentrated under reduced pressure to yield **7** (13 mg) 50% pure as judged by ^{1}H-NMR as a yellow viscous liquid.
The product was identified in accordance with literature data.[17,25]

Methyl-D-cysteinate (17)[20]

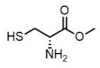

Acetyl chloride (18 mL, 0.25 mol, 10 equiv.) was added dropwise to methanol (0.25 L) at 0 °C and was stirred for 15 min. D-cysteine (3.0 g, 25 mmol) was added to the stirring solution and heated to reflux. After 21 h, the mixture was cooled to room temperature and the solvent was removed under reduced pressure to yield **17** (2.4 g, 18 mmol, 71%) as a white solid.
The product was identified in accordance with literature data.[20]

Methyl *S*-(4-methoxybenzyl)-D-cysteinate (19)[23]

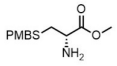

p-Methoxybenzyl chlorid (2.5 mL, 18 mmol, 1.0 equiv.) in dichloromethane (30 mL) was added drop wise over 2 h to a stirred solution of **17** (2.4 g, 18 mmol) in dichloromethane (30 mL) and trifluoroacetic acid (5.0 mL, 64 mmol) at 0 °C. The mixture was allowed to reach room temperature overnight. The mixture was concentrated under reduced pressure and the residue was taken up in ethyl acetate (100 mL). The organics layer was washed with aqueous saturated $NaHCO_3$ solution (3 x 50 mL) and aqueous saturated NaCl solution (2 x 50 mL). The organic layer was dried over sodium sulfate and concentrated under reduced pressure to yield **19** (2.2 g, 8.6 mmol, 48%) as a white solid.
The product was identified in accordance with literature data.[23]

7.3 Synthesis of building block B

(*R*)-Thiazolidine-4-carboxylic acid (29)[27]

Formaldehyde (37% in water, 10 mL, 0.12 mol) was added to a stirred solution of L-cysteine hydrochloride monohydrate (18 g, 0.10 mol) in water (40 mL). After 15 h, pyridine (10 mL) and ethanol (40 mL) were added and crystals formed. After 50 min, the precipitate was filtered and washed with ethanol (2 x 50 mL) and diethyl ether (2 x 50 mL). The crystals were dried at high vacuum and yielded **29** (12. g, 92 mmol, 92%) as white crystals.

^{1}H NMR (600 MHz, DMSO) δ = 4.21 (d, J = 8.9 Hz, 1H), 4.03 (d, J = 9.0 Hz, 1H), 3.83 (t, J = 6.8 Hz, 1H), 3.07 (dd, J = 10.1, 7.1 Hz, 1H), 2.81 (dd, J = 10.1, 6.6 Hz, 1H).
^{13}C NMR (151 MHz, DMSO) δ = 172.5, 65.0, 54.0, 36.1
HR-MS: ESI+: m/z calculated for $C_4H_6O_2NS$ [M^-]: 132.0124, found: 132.0125

(*R*)-3-(*tert*-Butoxycarbonyl)thiazolidine-4-carboxylic acid (30)[28]

Di-*tert*-butyl dicarbonate (8.7 mL, 40 mmol, 1.2 equiv.) was added to to stirred solution of **29** (4.4 g, 33 mmol) in dry pyridine (33 mL) at 0 °C. The gray suspension was allowed to reach room temperature, and the evolving carbon dioxide was vented through a toluene-filled bubbler. After 4 days, toluene (30 mL) was added to the yellow solution, and the resulting mixture was extracted with ice-cooled aqueous saturated NaOH solution (2 M, 3 x 60 mL). The combined aqueous layers were washed with toluene (3 x 100 mL) and petrol ether (100 mL). The aqueous layer was brought to pH 3 by addition of citric acid and was extracted with dichloromethane (3 x 250 mL). The combined organic layers were dried over sodium sulfate and concentrated under reduced pressure. The residue was purified by flash chromatography (dichloromethane : methanol, 95 : 5 + 2% acetic acid) to yield **30** (4.2 g, 18 mmol, 55%) as white solid.

^{1}H NMR (600 MHz, $CDCl_3$) δ = 5.01 – 4.21 (m, 3H), 3.33 (d, J = 7.2 Hz, 2H), 1.48 (s, 9H).
^{13}C NMR (151 MHz, $CDCl_3$) δ = 61.6, 49.0, 32.7, 28.4
Due to insufficient measuring time, no quaternary carbons are visible in ^{13}C NMR.
HR-MS: ESI+: m/z calculated for $C_9H_{15}O_4NSNa$ [M+Na^+]: 256.0619, found: 256.0614

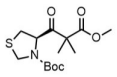

***tert*-Butyl (*R*)-4-(3-methoxy-2,2-dimethyl-3-oxopropanoyl)thiazolidine-3-carboxylate (31)[29]**

Carbonyldiimidazole (2.5 g, 15 mmol, 1.0 equiv.) was added in portions to a stirred solution of **30** (3.5 g, 15 mmol) in dry tetrahydrofuran (17 mL) at 0 °C. The mixture was held at 0 °C for 30 min and at room temperature for 1 h. The yellow solution was diluted with ethyl acetate (15 mL) and washed with water (15 mL) and aqueous saturated NaCl solution (2 x 15 mL). The organic layer was dried over sodium sulfate and concentrated under reduced pressure.

n-butyllithium (2.5 M in hexan, 12 mL, 30 mmol, 2.0 equiv.) was added slowly to a stirred solution of diisopropylamine (4.2 mL, 30 mmol, 2.0 equiv.) in dry tetrahydrofuran (60 mL) at -78 °C. After 30 min at the same conditions, methyl isobutyrate (3.6 mL, 32 mmol, 2.1 equiv.) was added. After another 30 min, the activated **30** in dry tetrahydrofuran (40 mL) was added. After 25 min, aqueous citric acid (10%, 60 mL) was added and allowed to reach room temperature. The mixture was extracted with ethyl acetate (3 x 50 mL). The combined organic layers were washed with water (40 mL) and aqueous saturated NaCl solution (2 x 40 mL). The organic layer was dried over sodium sulfate and concentrated under reduced pressure. The residue was purified by flash chromatography (petrol ether : ethyl acetate, 5 : 1) to yield the product **31** (2.4 g, 7.5 mmol, 50%) as a colorless viscous liquid.

^{1}H NMR (600 MHz, $CDCl_3$) δ = 5.19 (s, 1H), 4.69 (s, 1H), 4.38 (d, J = 9.1 Hz, 1H), 3.74 (s, 3H), 3.21 (s, 1H), 3.08 (s, 1H), 1.51 (s, 3H), 1.45 (s, 9H), 1.44 (s, 3H).
^{13}C NMR (151 MHz, $CDCl_3$) δ = 63.4, 55.7, 52.77, 49.7, 33.4, 28.4, 23.0, 22.7.
Due to insufficient measuring time, no quaternary carbons are visible in ^{13}C NMR.
HR-MS: ESI+: m/z calculated for $C_{14}H_{23}O_5NSNa$ [M+Na$^+$]: 340.1195 , found: 340.1189.

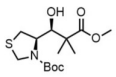

***tert*-Butyl (*R*)-4-((*S*)-1-hydroxy-3-methoxy-2,2-dimethyl-3-oxopropyl)thiazolidine-3-carboxylate (32)[29]**

Sodium borohydride (0.14 g, 3.8 mmol, 1.0 equiv.) was added to a stirred solution of **31** (1.2 g, 3.8 mmol) in methanol (6 mL) at 0 °C. After 20 min, at the same temperature, the mixture was diluted with ice-cooled aqueous saturated NH_4Cl solution (30 mL) and was extracted with ethyl acetate (3 x 40 mL). The combined organic layers were dried over sodium sulfate and concentrated under reduced pressure. The residue was purified by flash chromatography (petrol ether : ethyl acetate, 4 : 1) to yield the product **32** (0.90 g, 2.9 mmol, 76%) as white crystalline solid.

^{1}H NMR (600 MHz, $CDCl_3$) δ = 4.75 (d, J = 4.1 Hz, 1H), 4.63 – 4.57 (m, 1H), 4.19 (d, J = 9.5 Hz, 1H), 3.70 (s, 3H), 3.65 (d, J = 5.8 Hz, 1H), 3.12 (dd, J = 11.2, 7.3 Hz, 1H), 2.85 (dd, J = 11.2, 3.4 Hz, 1H), 1.48 (s, 9H), 1.32 (s, 3H), 1.30 (s, 3H).
^{13}C NMR (151 MHz, $CDCl_3$) δ = 177.9, 82.0, 79.5, 60.2, 52.2, 49.9, 46.6, 34.9, 28.4, 21.9, 21.2.
Due to insufficient measuring time, no quaternary carbons are visible in ^{13}C NMR.
HR-MS: ESI+: m/z calculated for $C_{14}H_{2505}NSNa$ [M+Na$^+$]: 342.1351 , found: 342.13.

(*S*)-3-((*R*)-3-(*tert*-Butoxycarbonyl)thiazolidin-4-yl)-3-hydroxy-2,2-dimethylpropanoic acid (35)[32]

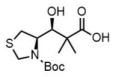

Pyridinium *p*-toluenesulfonate (0.10 g, 0.40 mmol, 2.4 equiv.) was added to a stirred solution of **32** (0.53 g, 0.17 mmol) in ethyl vinyl ether (8.0 mL, 83 mmol) and dichloromethane (16 mL). After 2 days, the clear solution was concentrated under reduced pressure. Aqueous sodium hydroxide solution (5 M, 7.2 mL, 37 mmol, 20 equiv.) was added to a stirred solution of **26** in tetrahydrofuran (15 mL) and methanol (10 mL). The mixture was stirred at room temperature for 3 days and then, at 60 °C for 1 day. The mixture was cooled to room temperature and diluted with aqueous hydrogen chloride solution (10%) till pH $\sim$ 1 was reached. The mixture was stirred for another 10 min, and then was saturated with solid sodium chloride and extracted with ethyl acetate (3 x 100 mL). The combined organic layers were dried over sodium sulfate and concentrated under reduced pressure. The residue was purified by flash chromatography (petrol ether : ethyl acetate, 4 : 1$\rightarrow$1 : 1) to yield the product **35** (0.38 g, 1.2 mmol, 72%) as colorlessness viscous liquid.

^{1}H NMR (400 MHz, $CDCl_3$) δ = 4.80 (s, 1H), 4.70 – 4.61 (m, 1H), 4.22 (d, J = 9.3 Hz, 1H), 3.71 (d, J = 5.7 Hz, 1H), 3.17 (dd, J = 11.3, 7.0 Hz, 1H), 2.90 (dd, J = 11.3, 3.0 Hz, 1H), 1.48 (s, 9H), 1.35 (s, 3H), 1.34 (s, 3H).
^{13}C NMR (151 MHz, $CDCl_3$) δ = 181.4, 79.0, 59.9, 49.0, 34.9, 28.2, 24.1, 21.4.
Due to insufficient measuring time, no quaternary carbons are visible in ^{13}C NMR.
HR-MS: ESI+: m/z calculated for $C_{13}H_{23}O_5NSNa$ [M+Na$^+$]: 329.1195, found: 328.1189.

(*3S,4R*)-3-Hydroxy-5-mercapto-2,2-dimethyl-4-(methylamino)pentanoic acid (8)[34]

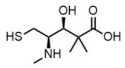

Triethylsilane (50 μL, 0.30 mmol, 3.0 equiv.) was added to a stirred solution of **35** (31 mg, 0.10 mmol,) in dry 1,4-dioxan (1.0 mL) and in hydrogen chloride solution in 1,4-dioxan (2.0 mL, 8.0 mmol, 4.0 M). After 3 h, the solvents were removed at high vacuum.

Sodium pieces (pre-washed with methanol) were added alternately with Boc deprotected compound **35** (dissolved in dry tetrahydrofuran,1.5 mL) to liquid ammonia (1.5 mL) at –50 °C. Upon the addition of sodium, the solution turned dark blue. Addition of **35** in dry tetrahydofuran discharged the blue color, which necessitated the further addition of sodium pieces. This alternating addition was continued until all of **35** had been introduced. After the final addition, the mixture was maintained for 5 min with a persistent dark blue color. Solid ammonium chloride was then added, and the mixture was allowed to warm to room temperature, during which the ammonia was evaporated through a toluene-filled bubbler. The remaining solvent was removed under high vacuum, and the crude residue was used directly in the subsequent step without further purification.

2-(trimethylsilyl)ethyl isobutyrate (12)[33]

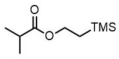

Isobutyryl chloride (2.4 mL, 22 mmol, 1.1 equiv.) was added dropwise to a stirred solution of 2-(trimethylsilyl)ethanol (3.0 mL, 20 mmol) in dry dichloromethane (50 mL) and dry pyridine (1.8 mL, 22 mmol, 1.1 equiv.) at 0 °C. The mixture was allowed to reach room temperature and was stirred for 3 h. The mixture was diluted with water (200 mL) and extracted with dichloromethane (3 x 150 mL). The combined organic layers were dried over sodium sulfate and concentrated under reduced pressure. The residue was purified by flash chromatography (petrol ether : ethyl acetate, 9 : 1) to yield the product **12** (3.6 g, 19 mmol, 95%) as a colorless, viscous liquid.
The product was identified in accordance with literature data.[33]

***tert*-Butyl (*R*)-4-(2,2-dimethyl-3-oxo-3-(2-(trimethylsilyl)ethoxy)propanoyl)-thiazolidine-3-carboxylate (38)[29]**

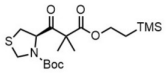

Carbonyldiimidazole (1.5 g, 9.0 mmol, 1.0 eqiv.) was added in portions to a stirred solution of **30** (2.1 g, 9.0 mmol) in dry tetrahydrofuran (10 mL) at 0 °C. The mixture was held at 0 °C for 30 min and at room temperture for 1 h. The solution was diluted with ethyl acetate (30 mL) and washed with aqueous saturated NaCl solution (2 x 20 mL). The organic layer was dried over sodium sulfate and concentrated under reduced pressure.
n-Butyllithium (2.5 M in hexan, 7.2 mL, 18 mmol, 2.0 equiv.) was added slowly to a stirred solution of diisopropylamine (2.5 mL, 18 mmol, 2 equiv.) at -78 °C. After 30 min at the same conditions, **12** (3.6 g, 19 mmol, 2.1 equiv.) in dry tetrahydrofuran (10 mL) was added. After another 30 min, the activated **30** in dry tetrahydrofuran (10 mL) was added. After 30 min, aqueous citric acid (10%, 100 mL) was added and the resulting mixture was allowed to reach room temperature. The mixture was extracted with ethyl acetate (3 x 100 mL). The combined organic layers were washed with aqueous saturated NaCl solution (2 x 100 mL). The organic layer was dried over sodium sulfate and concentrated under reduced pressure. The residue was purified by flash chromatography (petrol ether : ethyl acetate, 3 : 1) to yield the product **38** (2.5 g, 6.2 mmol, 69%) as a color less viscous liquid.

^{1}H NMR (600 MHz, $CDCl_3$) δ = 5.20 (s, 1H), 4.74 (s, 1H), 4.39 (d, J = 9.0 Hz, 1H), 4.21 (m, 2H), 3.23 (s, 1H), 3.08 (s, 1H), 1.51 (s, 3H), 1.45 (s, 9H), 1.42 (s, 3H), 1.04 – 0.97 (m, 2H), 0.05 (s, 9H).
^{13}C NMR (151 MHz, $CDCl_3$) δ = 178.8, 173.4, 153.2, 81.3, 64.2, 63.3, 55.2, 49.7, 33.5, 28.5, 24.5, 22.9, 17.4, -1.4.
HR-MS: ESI+: m/z calculated for $C_{18}H_{33}O_5NSSiNa$ [M+Na$^+$]: 426.1746, found: 426.1741.

***tert*-Butyl (*R*)-4-((*S*)-1-hydroxy-2,2-dimethyl-3-oxo-3-(2-(trimethylsilyl)ethoxy)propyl)thiazolidine-3-carboxylate (39)[29]**

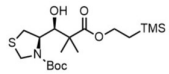

Sodium borohydride (7.0 mg, 0.19 mmol, 1.0 equiv.) was added to a stirred solution of **38** (78 mg, 0.19 mmol) in methanol (6.0 mL) at 0 °C. After 15 min at the same temperature, the mixture was diluted with ice-cooled aqueous saturated NH_4Cl solution (30 mL) and was extracted with ethyl acetate (3 x 40 mL). The combined organic layers were dried over sodium sulfate and concentrated under reduced pressure. The residue was purified by flash chromatography (petrol ether : ethyl acetate, 8 : 1) to yield the product **39** (72 mg, 0.18 mmol, 95%) as white crystaline solid.

^{1}H NMR (600 MHz, $CDCl_3$) δ = 4.79 (s, 1H), 4.59 (ddd, J = 7.2, 5.9, 3.3 Hz, 1H), 4.23 – 4.17 (m, 2H), 4.15 – 4.09 (m, 1H), 3.65 (dd, J = 7.8, 5.9 Hz, 1H), 3.11 (dd, J = 11.2, 7.2 Hz, 1H), 2.85 (dd, J = 11.2, 3.3 Hz, 1H), 1.46 (s, 9H), 1.30 (s, 3H), 1.28 (s, 3H), 1.05 – 0.92 (m, 2H), 0.04 (s, 9H).
^{13}C NMR (151 MHz, $CDCl_3$) δ = 177.6, 81.5, 79.3, 63.4, 60.2, 49.8, 46.3, 34.9, 28.4, 22.5, 22.0, 17.3, -1.4.
Due to insufficient measuring time, no quaternary carbons are visible in ^{13}C NMR.
HR-MS: ESI+: m/z calculated for $C_{18}H_{35}O_5NSSiNa$ [M+Na$^+$]: 428.1903, found: 428.1897.

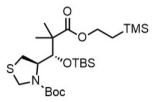

tert-Butyl (_R_)-4-((_S_)-2,2,7,7,10,10,11,11-octamethyl-6-oxo-5,9-dioxa-2,10-disiladodecan-8-yl)thiazolidine-3-carboxylate (42)[29]

tert-Butyldimethylsilyl trifluormethansulfonate (0.28 mL, 1.2 mmol, 1.2 equiv.) and dry lutidine (0.17 mL, 1.5 mmol, 1.5 equiv.) were added to a stirred solution of **39** (0.40 g, 1.0 mmol) in dry dichloromethane (5 mL) at 0 °C. After 15 min, the mixture was diluted with dichloromethane (40 mL) and aqueous saturated $NaHCO_3$ solution (20 mL). The mixture was extracted with dichloromethane (3 x 40 mL), and the combined organic layers were dried over sodium sulfate and concentrated under reduced pressure. The residue was purified by flash chromatography (petrol ether : ethyl acetate, 8 : 1) to yield the product **42** (0.38 g, 0.32 mmol, 64%) as colorless viscous liquid.

^{1}H NMR (400 MHz, $CDCl_3$) δ = 4.95 – 4.68 (m, 1H), 4.67 – 4.36 (m, 1H), 4.18 (m, 2H), 4.14 – 4.04 (m, 2H), 3.15 – 2.72 (m, 2H), 1.48 (s, 9H), 1.23 (d, 6H), 1.02 – 0.95 (m, 2H), 0.90 (s, 9H), 0.14 – 0.06 (m, 6H), 0.05 (s, 9H).
^{13}C NMR (176 MHz, $CDCl_3$) δ = 177.0, 62.4, 61.6, 50.2, 33.8, 33.5, 28.6, 26.2, 25.9, 25.8, 20.4, -1.3, -4.4.
Due to insufficient measuring time, no quaternary carbons are visible in ^{13}C NMR.
HR-MS: ESI+: m/z calculated for $C_{24}H_{49}NO_5SSi_2$ [M+Na$^+$]: 542.2768, found: 542.2762

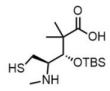

(_3S_,_4R_)-3-hydroxy-5-mercapto-2,2-dimethyl-4-(methylamino)pentanoic acid (44)[34,35]

Trifluoroacetic acid (4.0 mL, 53 mmol, 18 equiv.) was added to a stirred solution of **42** (0.17 g, 0.32 mmol) in dichloromethane (3 mL) at 0 °C. After 5 h, the solvents were removed at high vacuum and the residue **43** was used directly in the next step.

Sodium pieces (0.18 g, 7.8 mmol, 24 equiv., pre-washed with methanol) were added alternately with compound **43** (dissolved in dry tetrahydrofuran, 2.5 mL) to liquid ammonia (4 mL) at –50 °C. Upon the addition of sodium, the solution turned dark blue. Addition of **43** in dry tetrahydofuran discharged the blue color, which necessitated the further addition of sodium pieces. This alternating addition was continued until all of **43** had been introduced. After the final addition, the mixture was maintained for 5 min with a persistent dark blue color. Solid ammonium chloride was then added, and the mixture was allowed to warm to room temperature, during which the ammonia was evaporated through a toluene-filled bubbler. The remaining solvent was removed under high vacuum, and the crude residue was used directly in the subsequent step without further purification.

References

(1) Cañedo, L. M.; de la Fuente, J. A.; Gesto, C.; Ferreiro, M. J.; Jiménez, C.; Riguera, R. *Tetrahedron Lett.* **1999**, *40*, 6841–6844.

(2) Acebal, C.; Cañedo, L. M.; Puentes, J. L. F.; Baz, J. P.; Romero, F.; Calle, F. D. L.; Grávalos, M. D. G.; Rodriguez, P. *J. Antibiot.* **1999**, *52*, 983–987.

(3) Diettrich, J.; Kage, H.; Nett, M. *Beilstein J. Org. Chem.* **2019**, *15*, 1298–1303.

(4) Hider, R. C.; Kong, X. *Nat. Prod. Rep.* **2010**, *27*, 637.

(5) Chaaban, T.; Mohsen, Y.; Ezzeddine, Z.; Ghssein, G. *Biology* **2023**, *12*, 598.

(6) Caldwell, K. A.; Tucci, M. L.; Armagost, J.; Hodges, T. W.; Chen, J.; Memon, S. B.; Blalock, J. E.; DeLeon, S. M.; Findlay, R. H.; Ruan, Q.; Webber, P. J.; Standaert, D. G.; Olson, J. B.; Caldwell, G. A. *PLoS One* **2009**, *4*, e7227.

(7) Ückert, A.-K.; Rütschlin, S.; Gutbier, S.; Wörz, N. C.; Miah, M. R.; Martins, A. C.; Hauer, I.; Holzer, A.-K.; Meyburg, B.; Mix, A.-K.; Hauck, C.; Aschner, M.; Böttcher, T.; Leist, M. *Environ. Int.* **2023**, *180*, 108229.

(8) Tysnes, O.-B.; Storstein, A. *J. Neural. Trans.* **2017**, *124*, 901–905.

(9) Bloem, B. R.; Okun, M. S.; Klein, C. *The Lancet* **2021**, *397*, 2284–2303.

(10) Dorsey, E. R.; Sherer, T.; Okun, M. S.; Bloem, B. R. *J. Parkinson's Dis.* **2018**, *8*, S3–S8.

(11) Inamdar, A. A.; Hossain, M. M.; Bernstein, A. I.; Miller, G. W.; Richardson, J. R.; Bennett, J. W. *Proc. Natl. Acad. Sci. U.S.A.* **2013**, *110*, 19561–19566.

(12) Caldwell, K. A.; Thies, J. L.; Caldwell, G. A. *Metabolites* **2018**, *8*, 70.

(13) Kaplan, A. R.; Musaev, D. G.; Wuest, W. M. *ACS Infect. Dis.* **2021**, *7*, 544–551.

(14) Jeong, G.-J.; Khan, F.; Tabassum, N.; Jo, D.-M.; Jung, W.-K.; Kim, Y.-M. *Res. Microbiol.* **2024**, *175*, 104211.

(15) Fischbach, M. A.; Lin, H.; Liu, D. R.; Walsh, C. T. *Nat. Chem. Biol.* **2006**, *2*, 132–138.

(16) De Serrano, L. O.; Camper, A. K.; Richards, A. M. *Biometals* **2016**, *29*, 551–571.

(17) Ino, A.; Murabayashi, A. *Tetrahedron Lett.* **2001**, *57*, 9773–9783.

(18) Ino, A.; Hasegawa, Y.; Murabayashi, A. *Tetrahedron Lett.* **1998**, *39*, 3509–3512.

(19) Lou, S.; Fu, G. C. In *Org. Synth.* Kende, A. S., Freeman, J. P., Eds.; Wiley: 2010, pp 330–338.

(20) Tan, F.; Shi, B.; Li, J.; Wu, W.; Zhang, J. *Molecules* **2015**, *20*, 20118–20130.

(21) ElSohly, M. A.; Adawadkar, P. D.; Benigni, D. A.; Watson, E. S.; Little, T. L. *J. Med. Chem.* **1986**, *29*, 606–611.

(22) Ino, A.; Murabayashi, A. *Tetrahedron Lett.* **1999**, *55*, 10271–10282.

(23) Yu, M.; Price, J. R.; Jensen, P.; Lovitt, C. J.; Shelper, T.; Duffy, S.; Windus, L. C.; Avery, V. M.; Rutledge, P. J.; Todd, M. H. *Inorg. Chem.* **2011**, *50*, 12823–12835.

(24) Smith, M. B.; March, J., *March's Advanced Organic Chemistry: Reactions, Mechanisms, and Structure*, 1st ed.; Wiley: 2006.

(25) Shapiro, J. A.; Morrison, K. R.; Chodisetty, S. S.; Musaev, D. G.; Wuest, W. M. *Org. Lett.* **2018**, *20*, 4123–4127.

(26) Khalid, M.; Mohammed, S.; Kalo, A. *Orient. J. Chem* **2020**, *36*, 206–219.

(27) Ratner, S.; Clarke, H. T. *J. Am. Chem. Soc.* **1937**, *59*, 200–206.

(28) Duthaler, R. O.; Wyss, B. *Eur. J. Org. Chem* **2011**, *2011*, 4667–4680.

(29) Ino, A.; Hasegawa, Y.; Murabayashi, A. *Tetrahedron Lett.* **1999**, *55*, 10283–10294.

(30) Kranich, R.; Busemann, A. S.; Bock, D.; Schroeter-Maas, S.; Beyer, D.; Heinemann, B.; Meyer, M.; Schierhorn, K.; Zahlten, R.; Wolff, G.; Aydt, E. M. *J. Med. Chem.* **2007**, *50*, 1101–1115.

(31) Fukuyama, T.; Xu, L. *Tetrahedron Lett.* **2004**, *45*, 347–350.

(32) Axelrod, A.; Eliasen, A. M.; Chin, M. R.; Zlotkowski, K.; Siegel, D. *Angew. Chem. Int. Ed.* **2013**, *52*, 3421–3424.

(33) Wang, Z.; Wu, J.; Lamine, W.; Li, B.; Sotiropoulos, J.-M.; Chrostowska, A.; Miqueu, K.; Liu, S.-Y. *Angew. Chem. Int. Ed.* **2021**, *60*, 21231–21236.

(34) Blondeau, P.; Berse, C.; Gravel, D. *Canadian Journal of Chemistry* **2011**, *45*, 49–52.

(35) Zeng, X.; Yin, B.; Hu, Z.; Liao, C.; Liu, J.; Li, S.; Li, Z.; Nicklaus, M. C.; Zhou, G.; Jiang, S. *Org. Lett.* **2010**, *12*, 1368–1371.

(36) Önen-Bayram, F. E.; Buran, K.; Durmaz, I.; Berk, B.; Cetin-Atalay, R. *Med. Chem. Commun.* **2015**, *6*, 90–93.

(37) Mahdy, A. R. E.; Elboray, E. E.; Fandy, R. F.; Abbas-Temirek, H. H.; Aly, M. F. *Arkivoc* **2017**, *2016*, 105–121.

(38) Almahli, H.; Jimenez, N. C.; Moloney, M. G. *Synlett* **2019**, *30*, 1237–1240.

Appendix

Analysis for 22

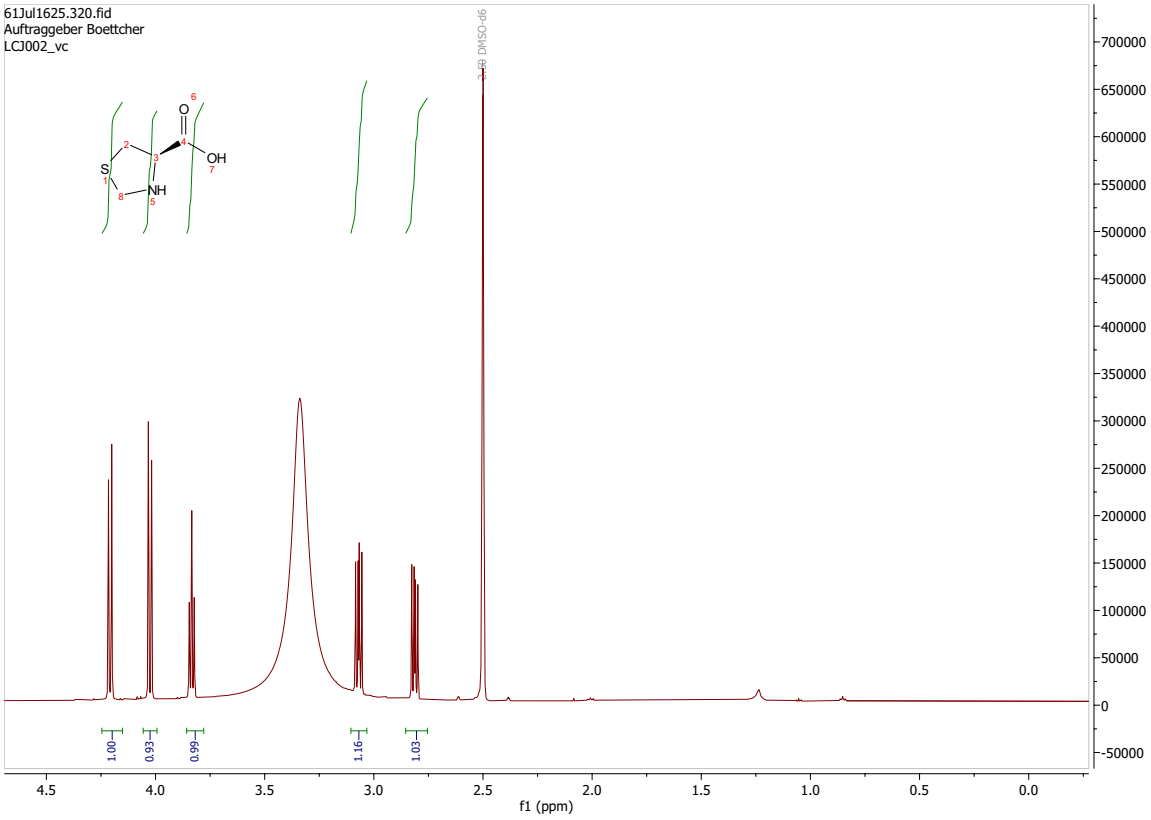

Figure 30: ^{1}H NMR

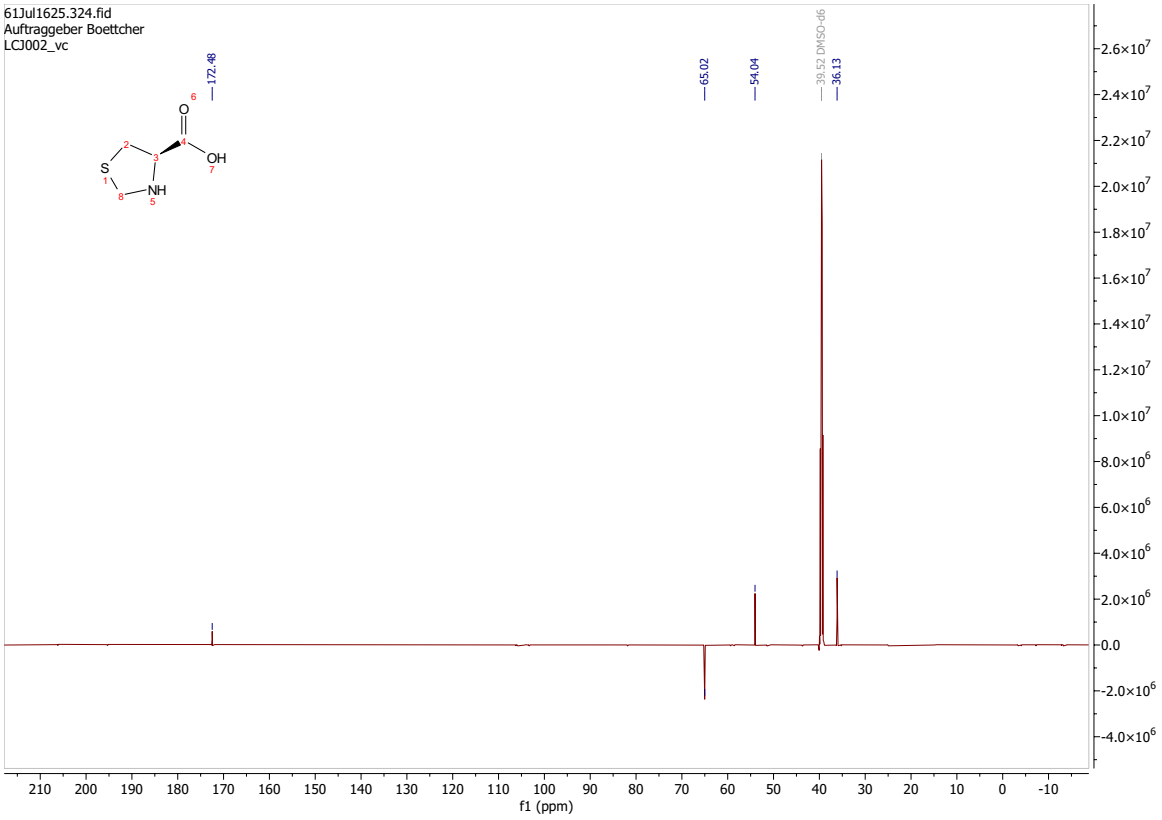

Figure 31: ^{13}C NMR

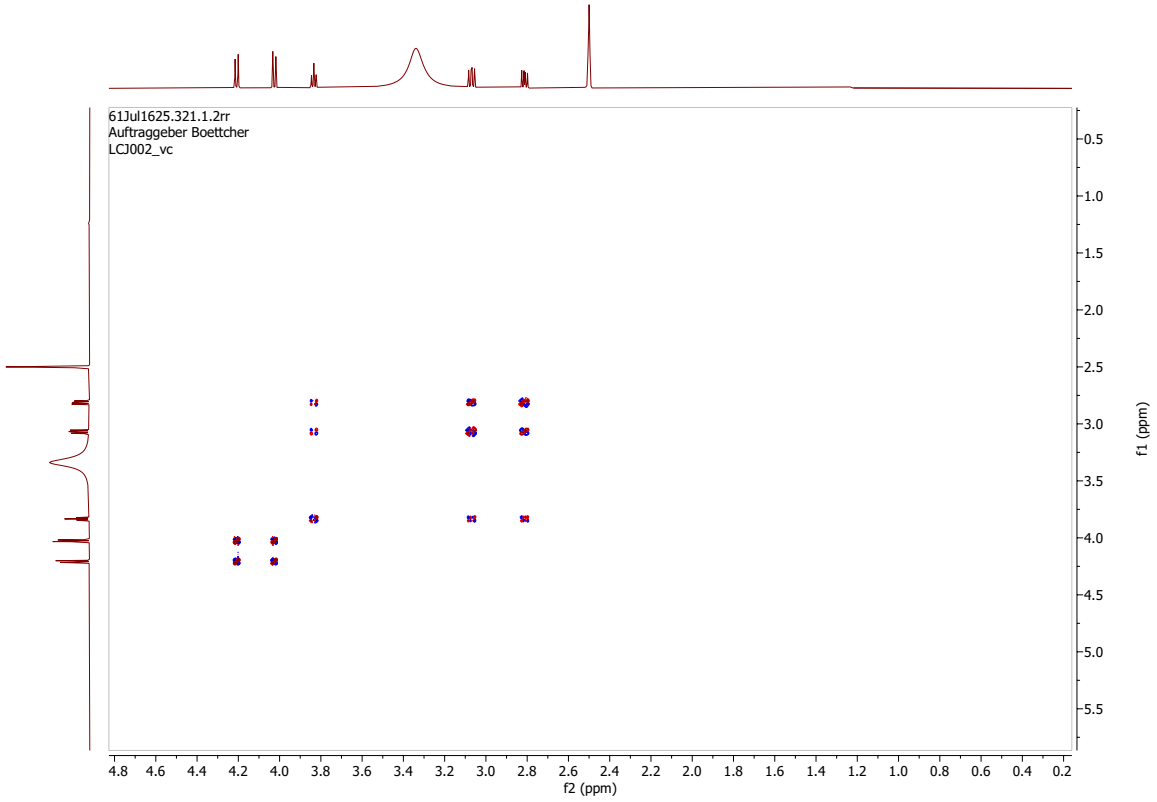

Figure 32: COSY NMR

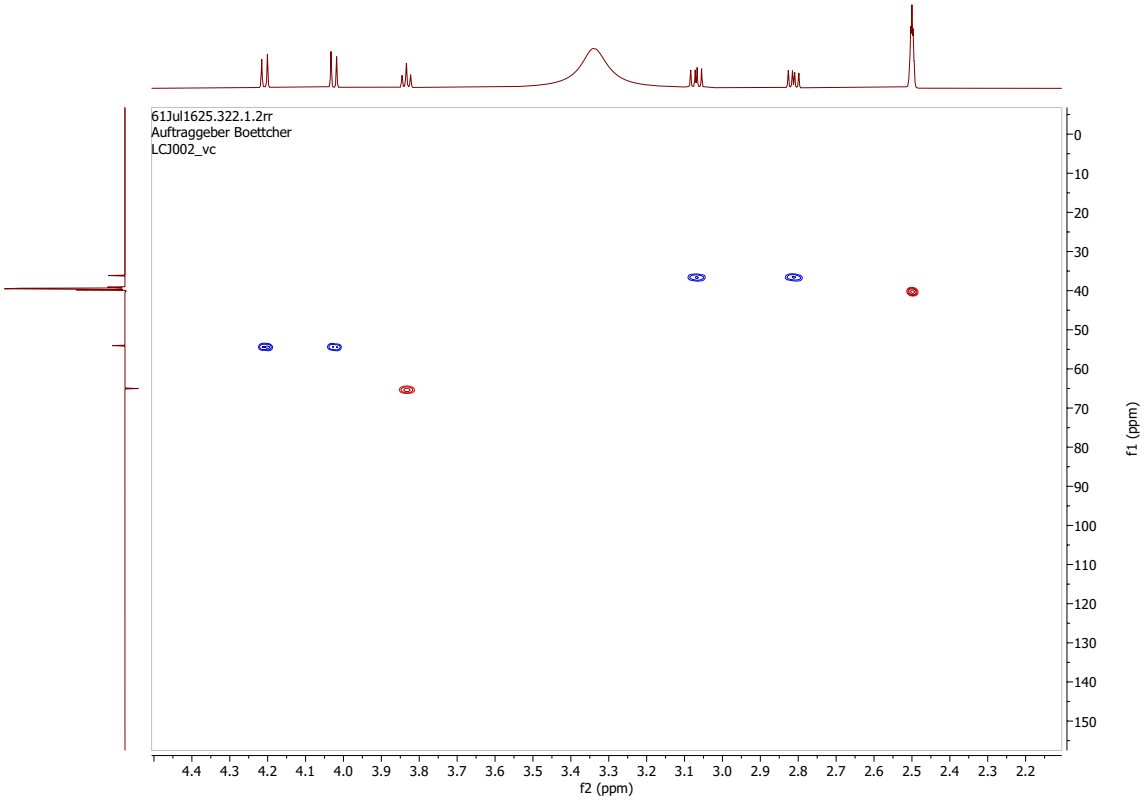

Figure 33: HSQC NMR

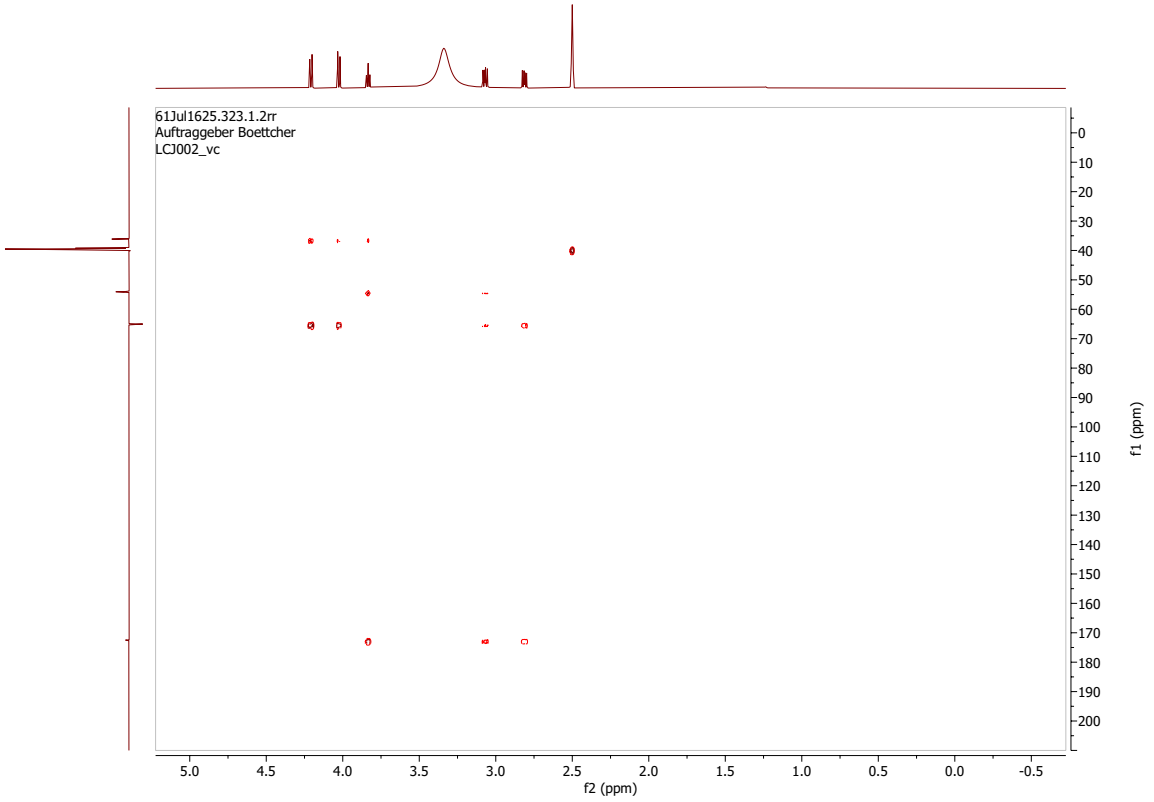

Figure 34: HMBC NMR

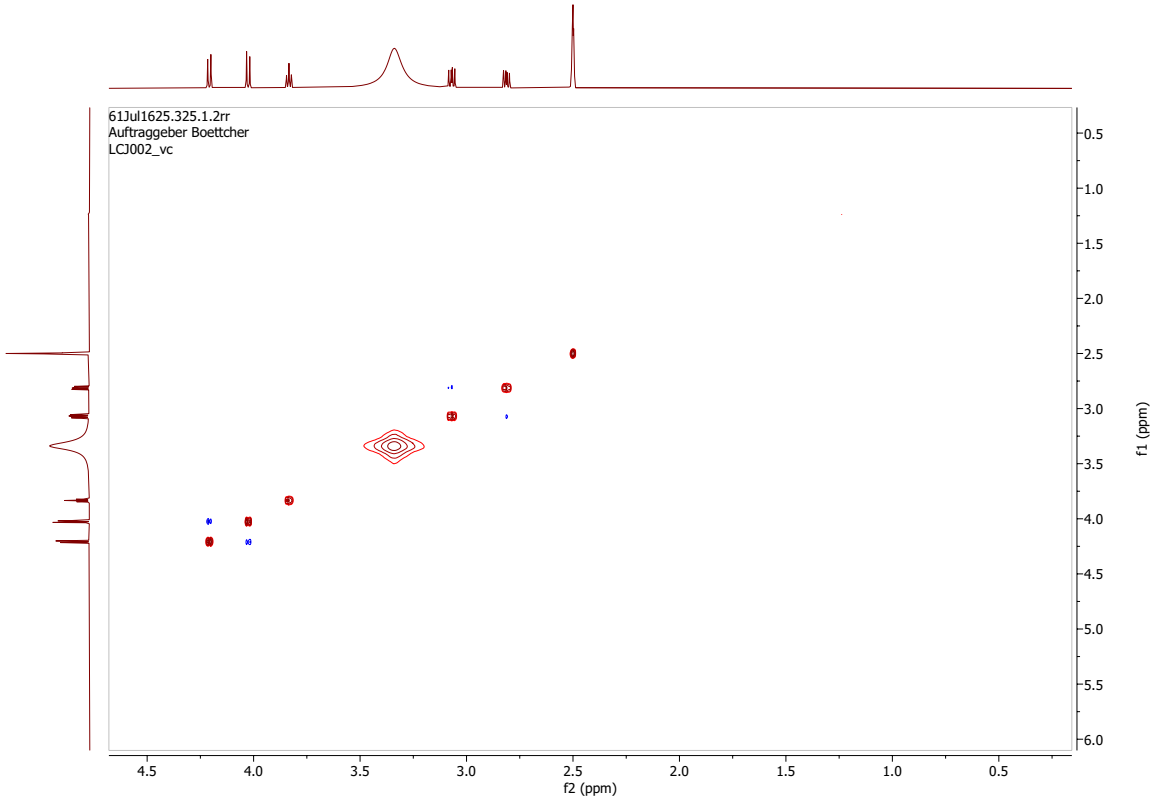

Figure 35: NOESY NMR

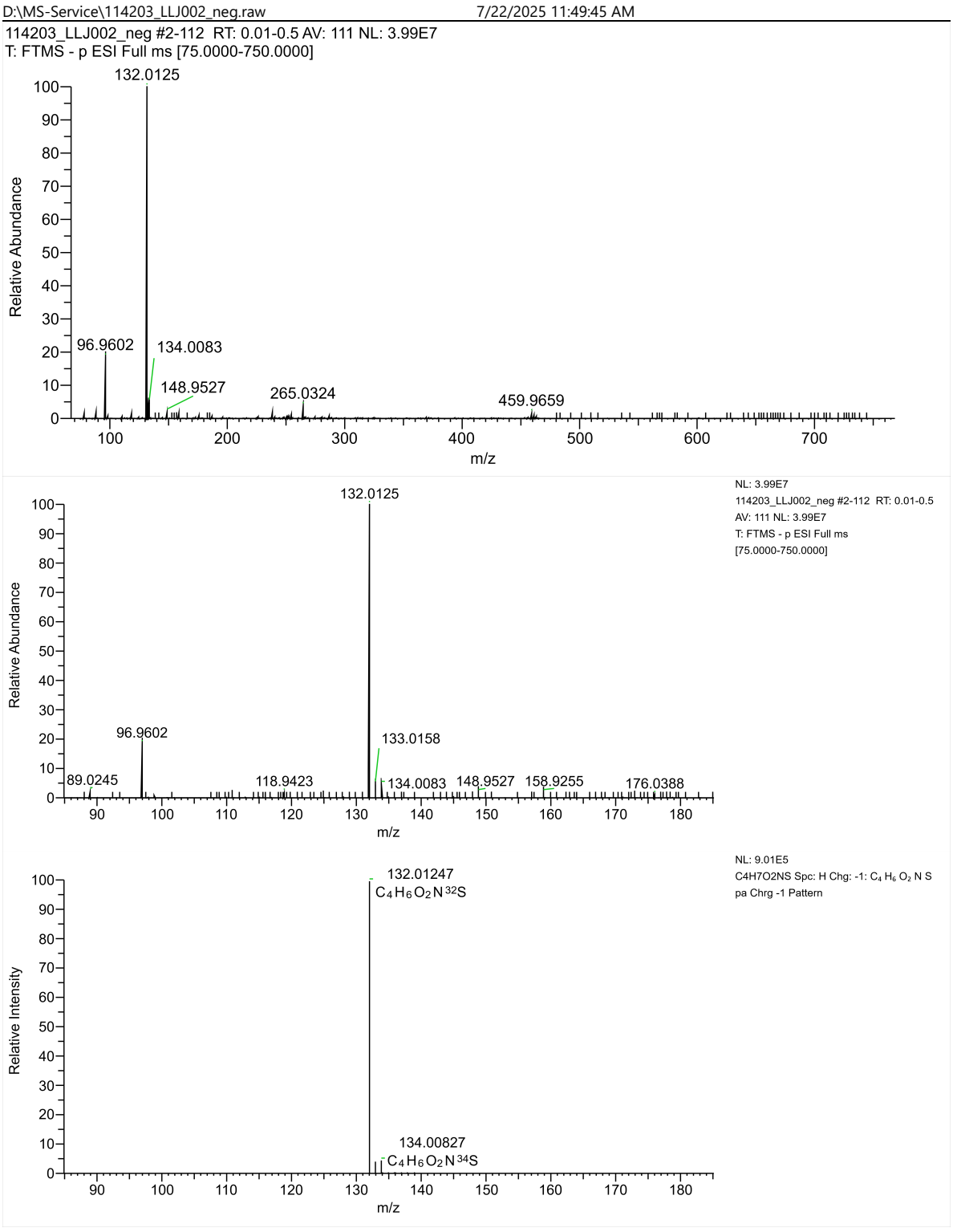

Figure 36: HRMS

Analysis for 23

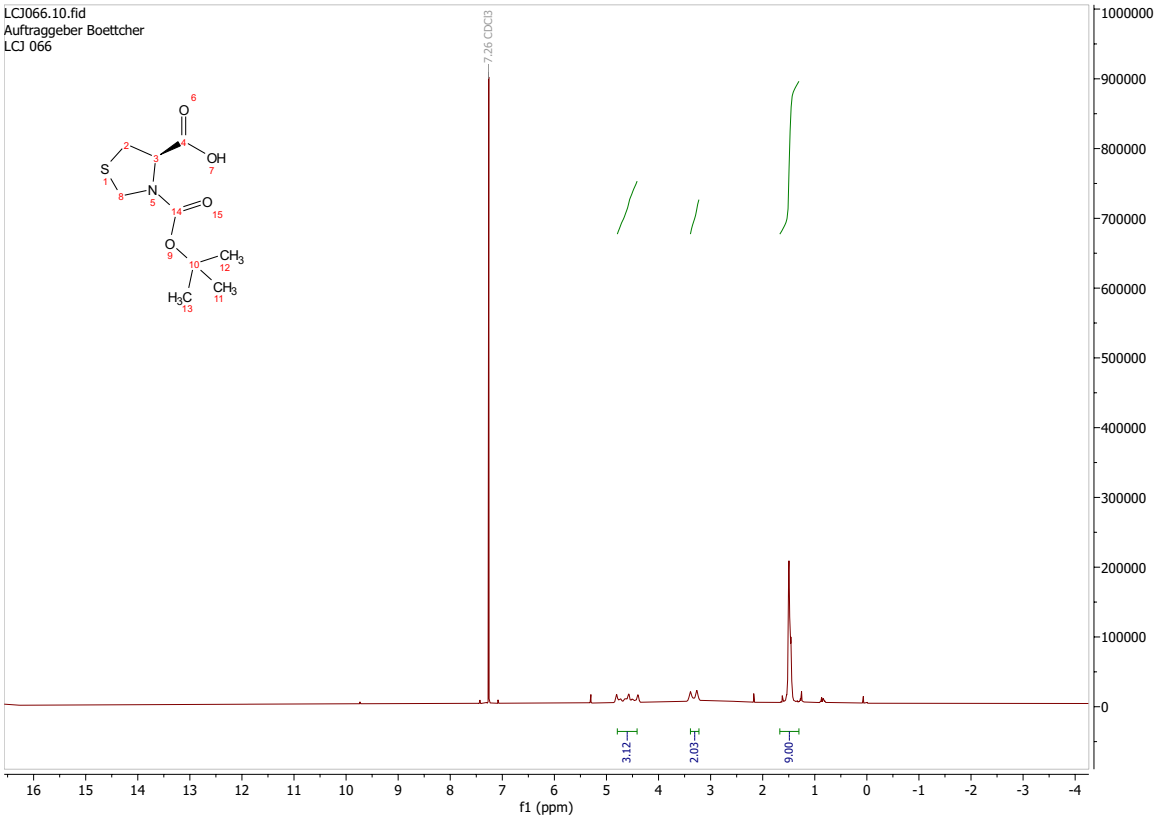

Figure 37: ^{1}H NMR

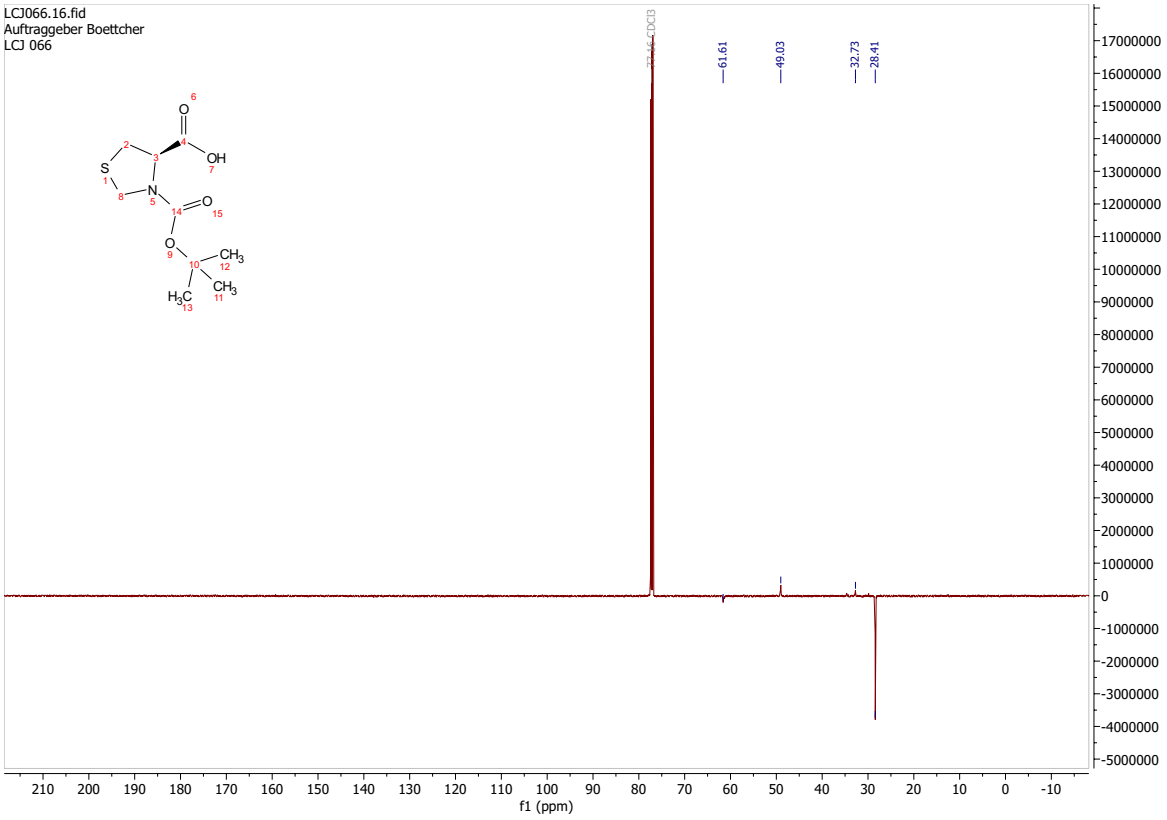

Figure 38: ^{13}C NMR

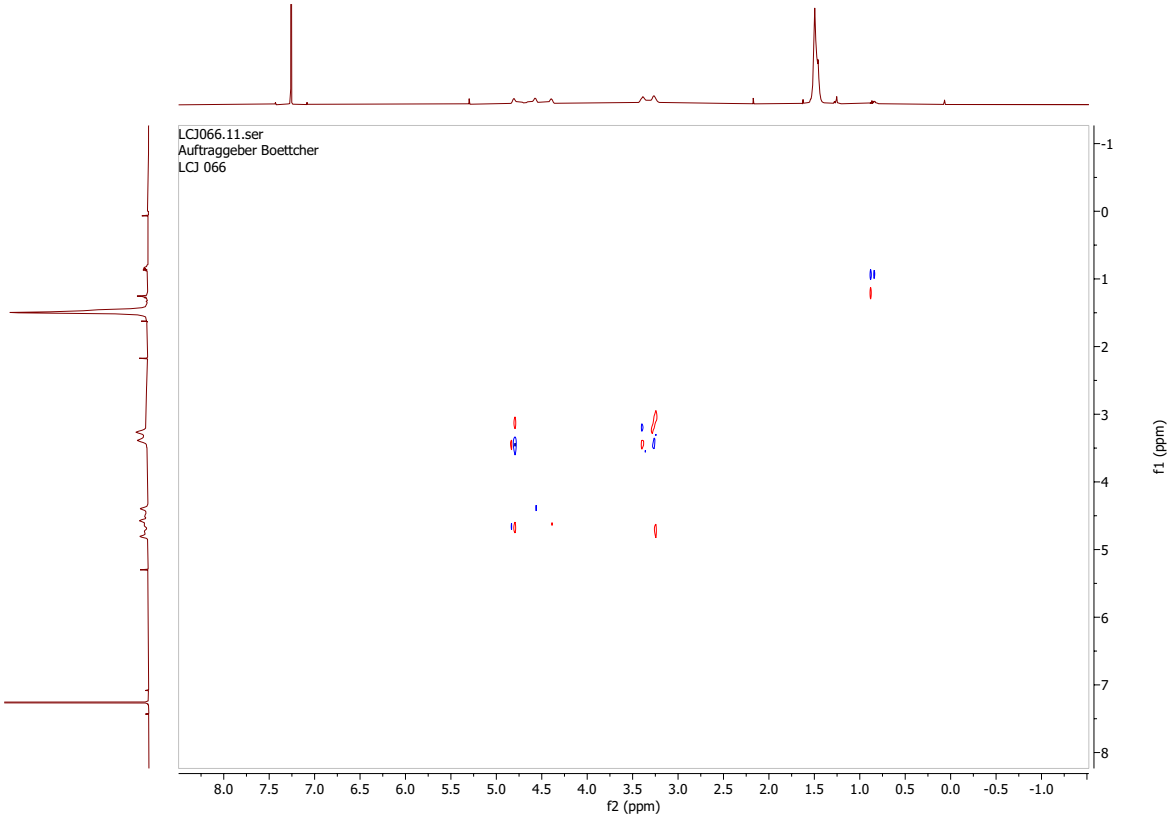

Figure 39: COSY NMR

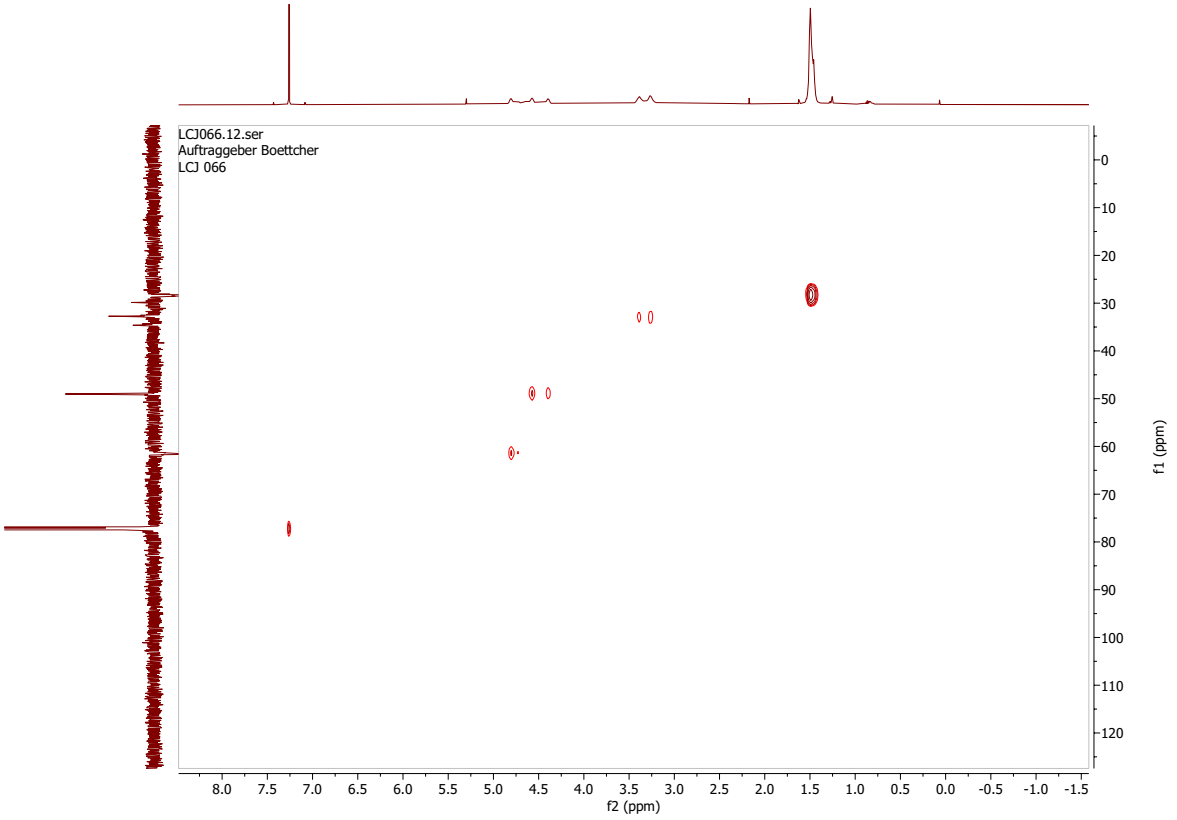

Figure 40: HSQC NMR

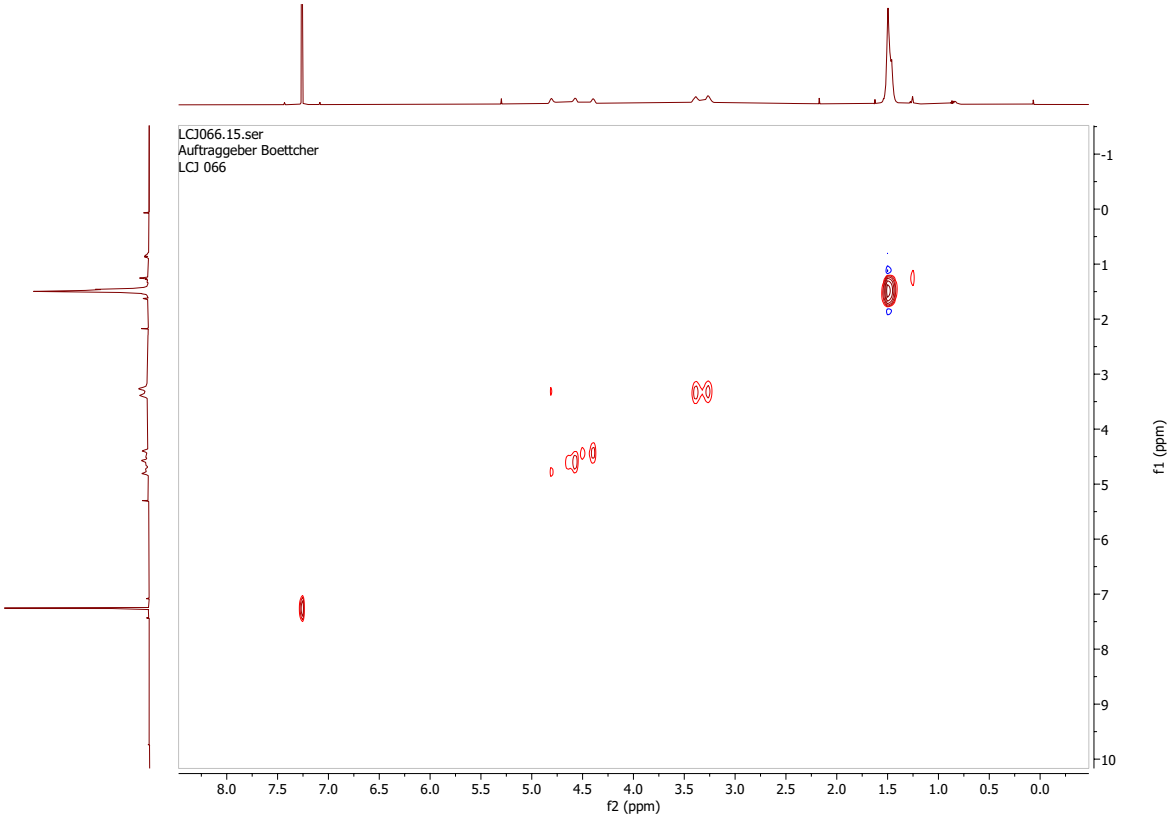

Figure 41: TOCSY NMR

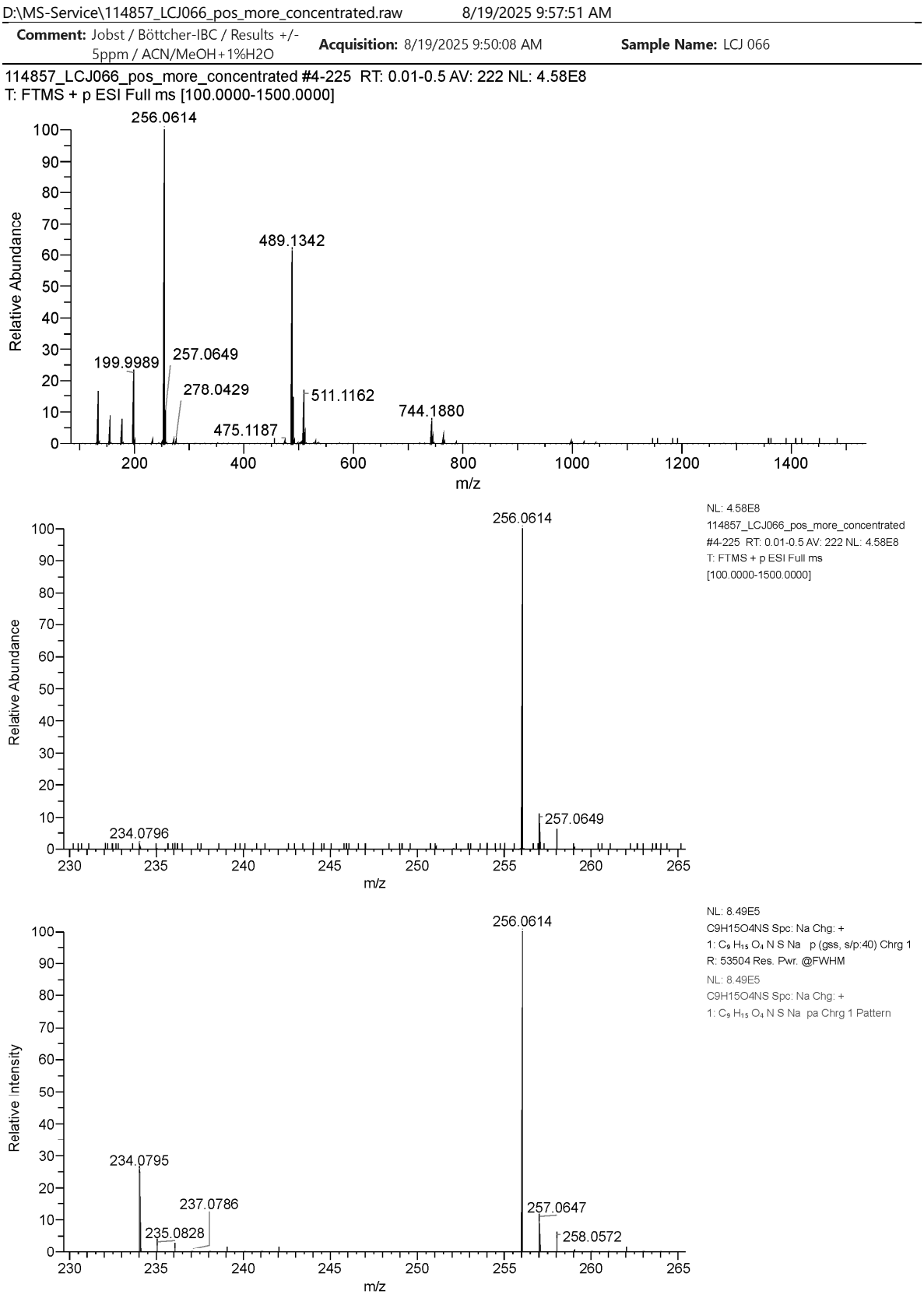

Figure 42: HRMS

Analysis for 24

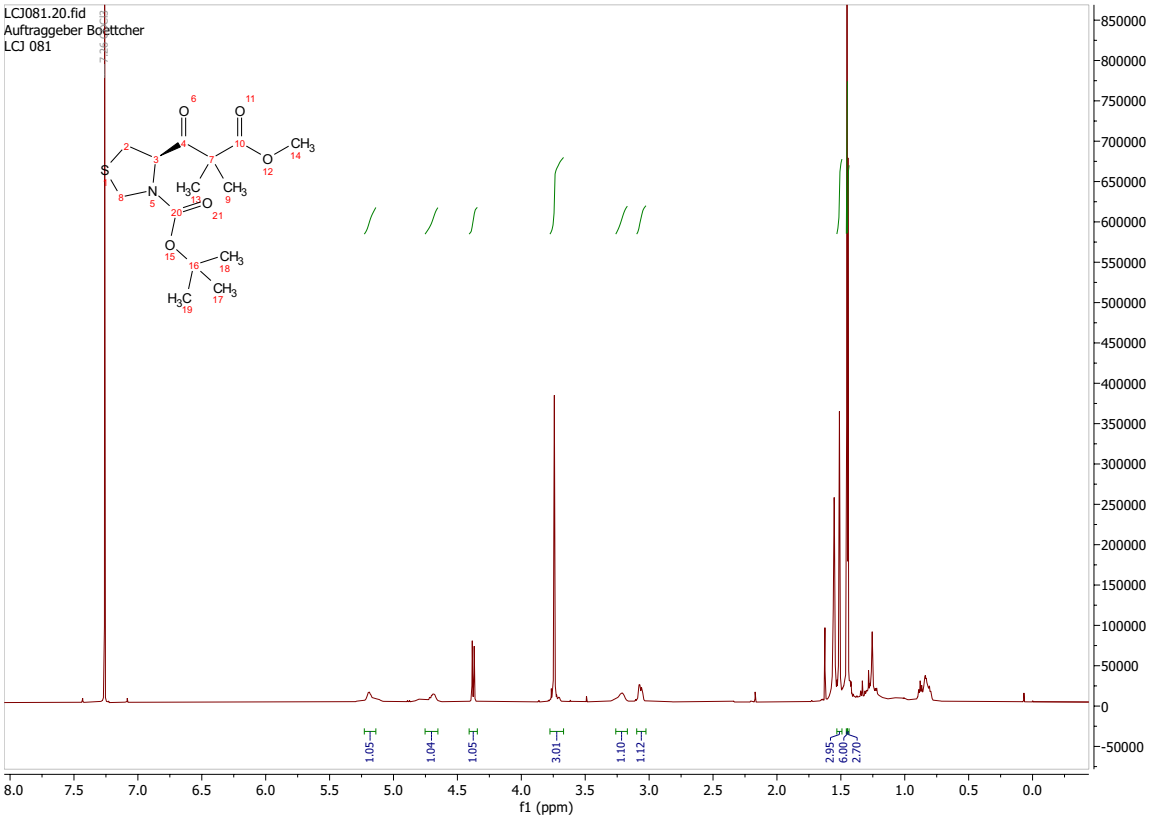

Figure 43: ^{1}H NMR

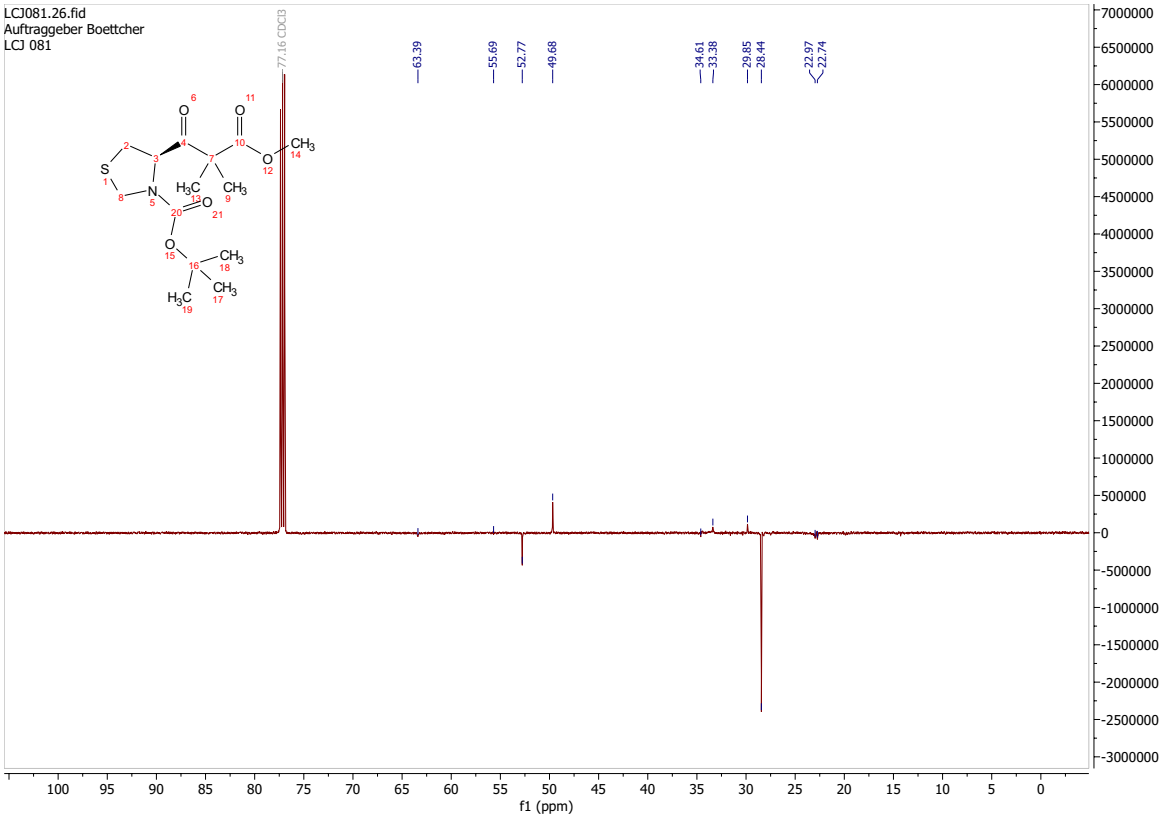

Figure 44: ^{13}C NMR

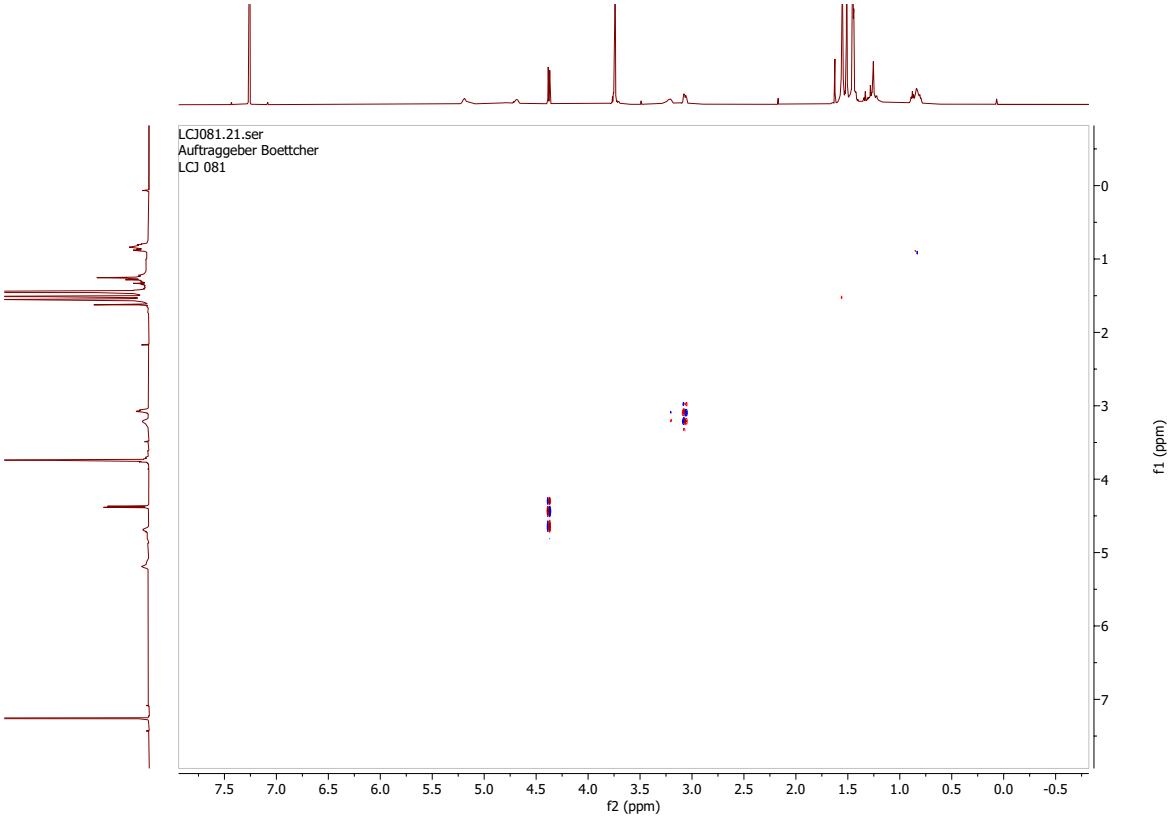

Figure 45: COSY NMR

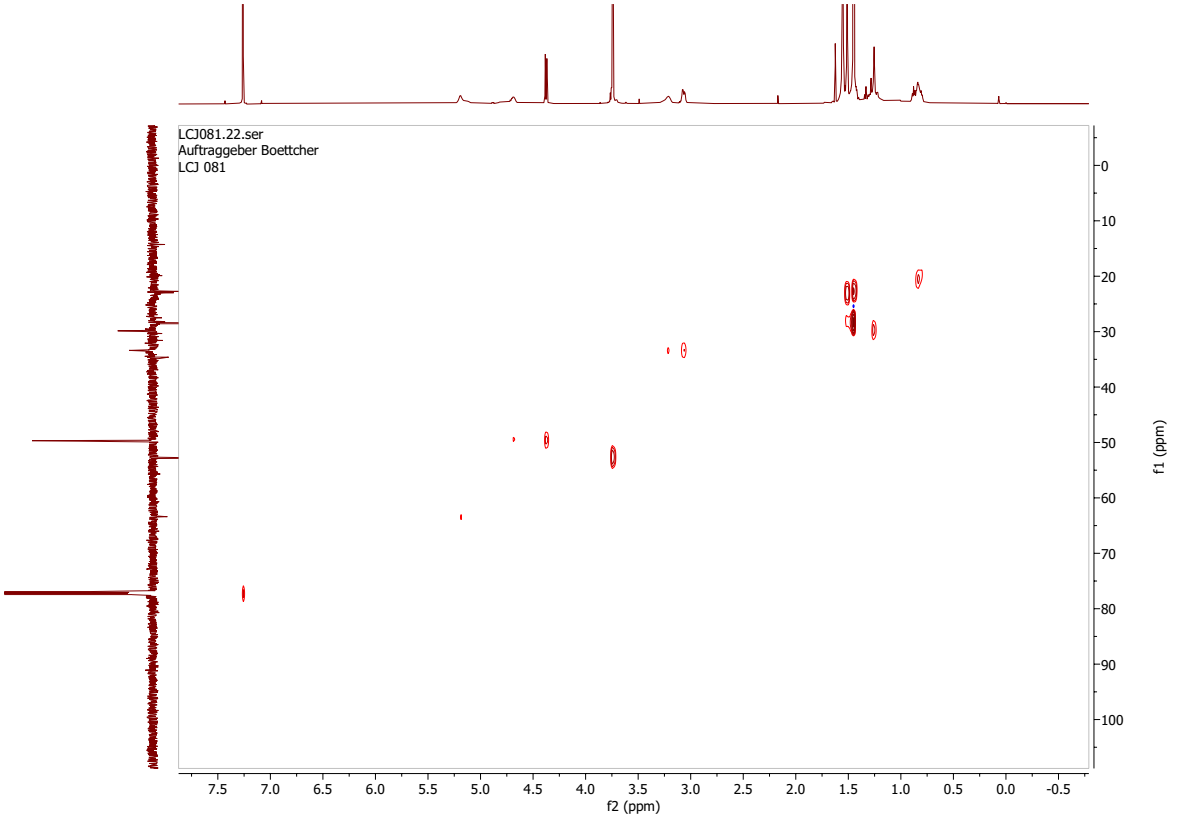

Figure 46: HSQC NMR

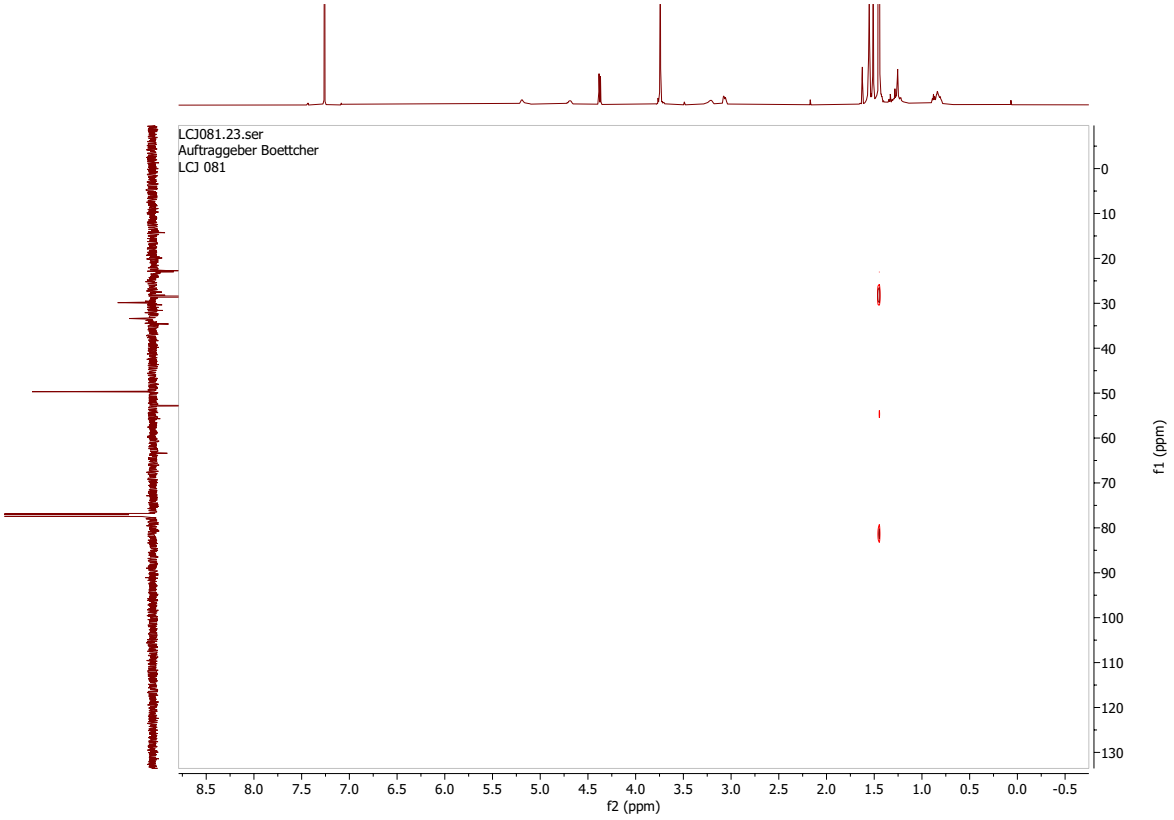

Figure 47: HMBC NMR

D:\MS-Service\114858_LCJ081_pos.raw 8/19/2025 10:06:32 AM

Comment: Jobst / Böttcher-IBC / Results +/- 5ppm / ACN/MeOH+1%H2O **Acquisition:** 8/19/2025 10:02:32 AM **Sample Name:** LCJ 081

114858_LCJ081_pos #3-224 RT: 0.01-0.5 AV: 222 NL: 1.85E8
T: FTMS + p ESI Full ms [100.0000-1500.0000]

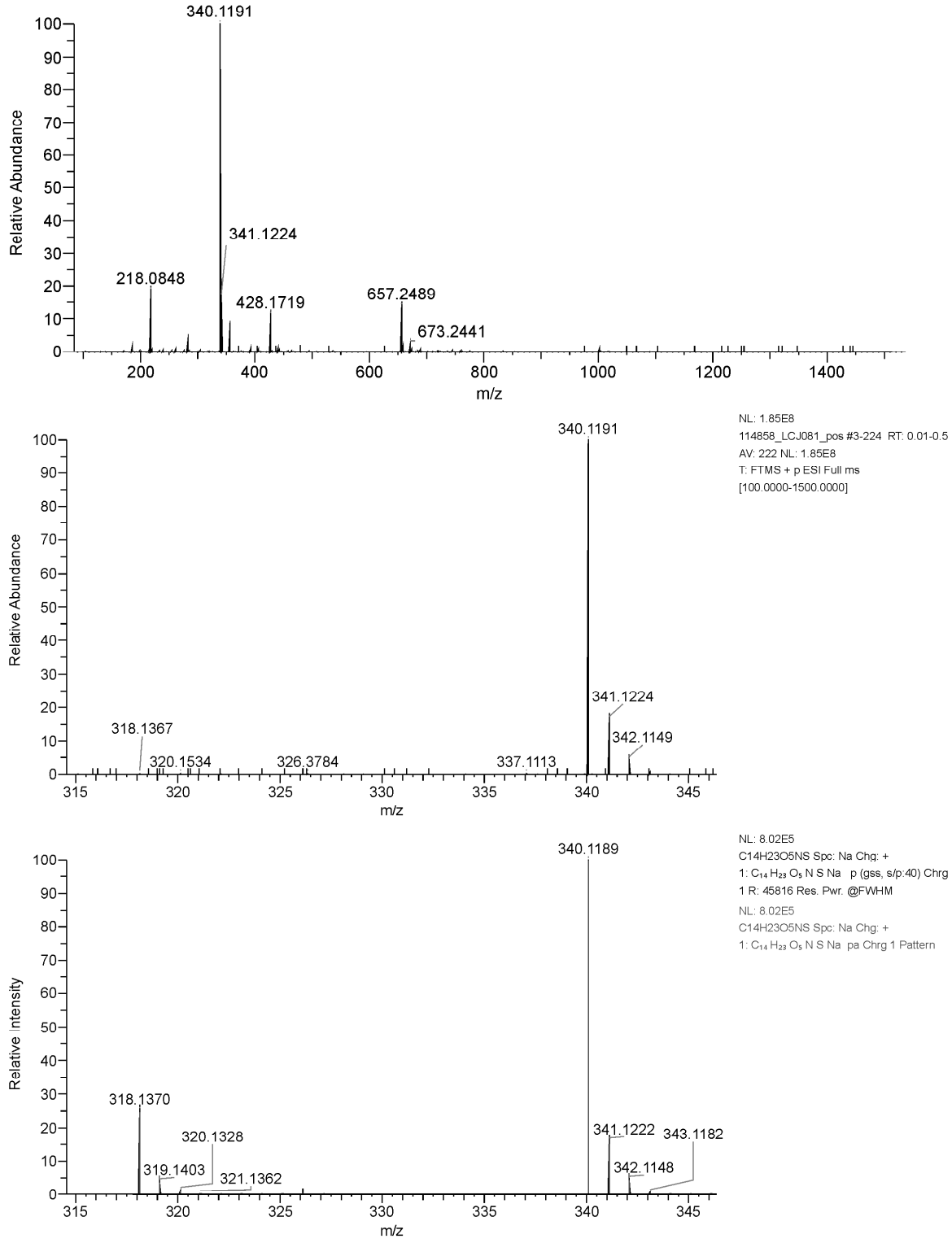

Figure 48: HRMS

Analysis for 26

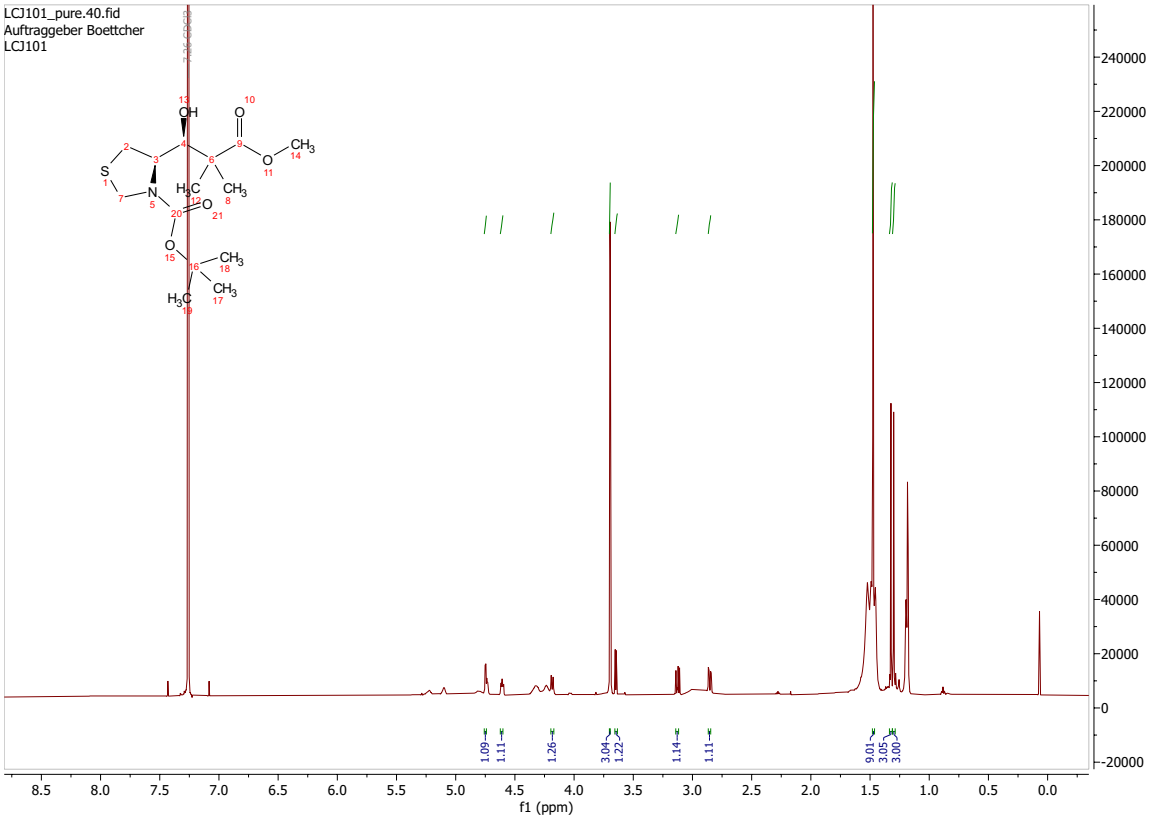

Figure 49: ^{1}H NMR

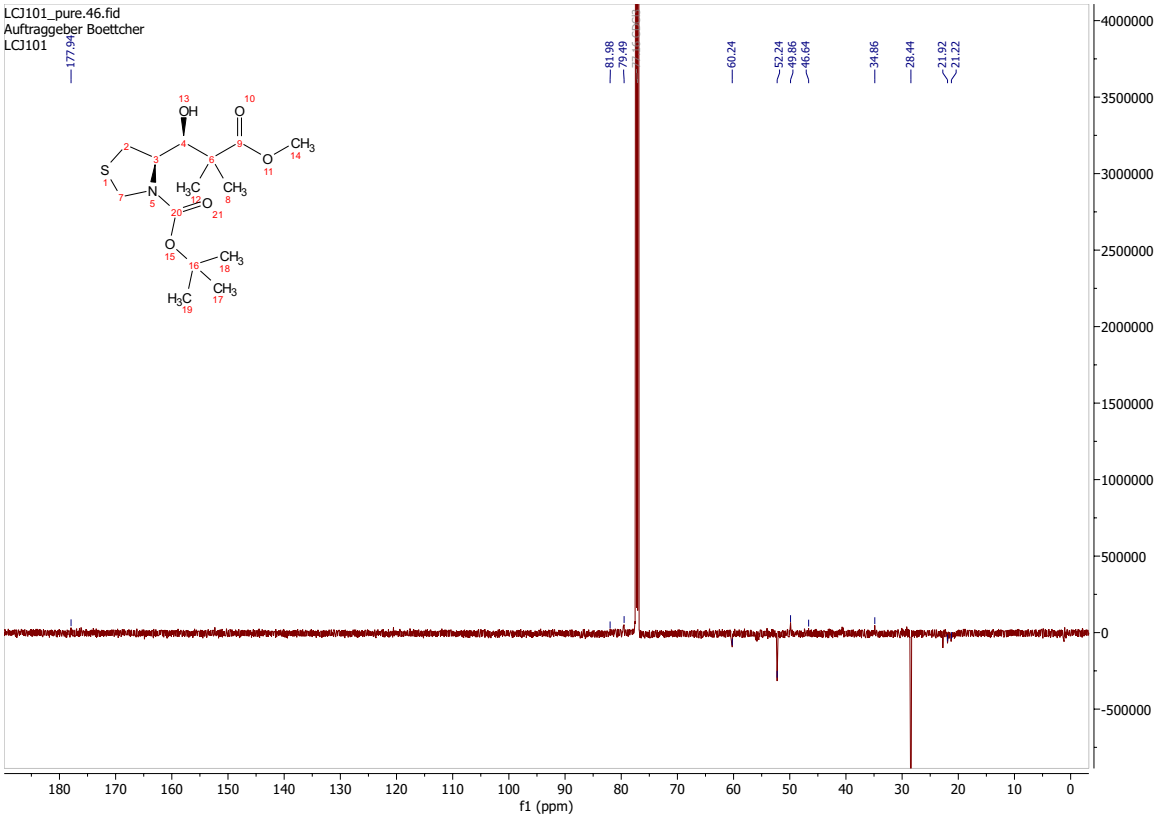

Figure 50: ^{13}C NMR

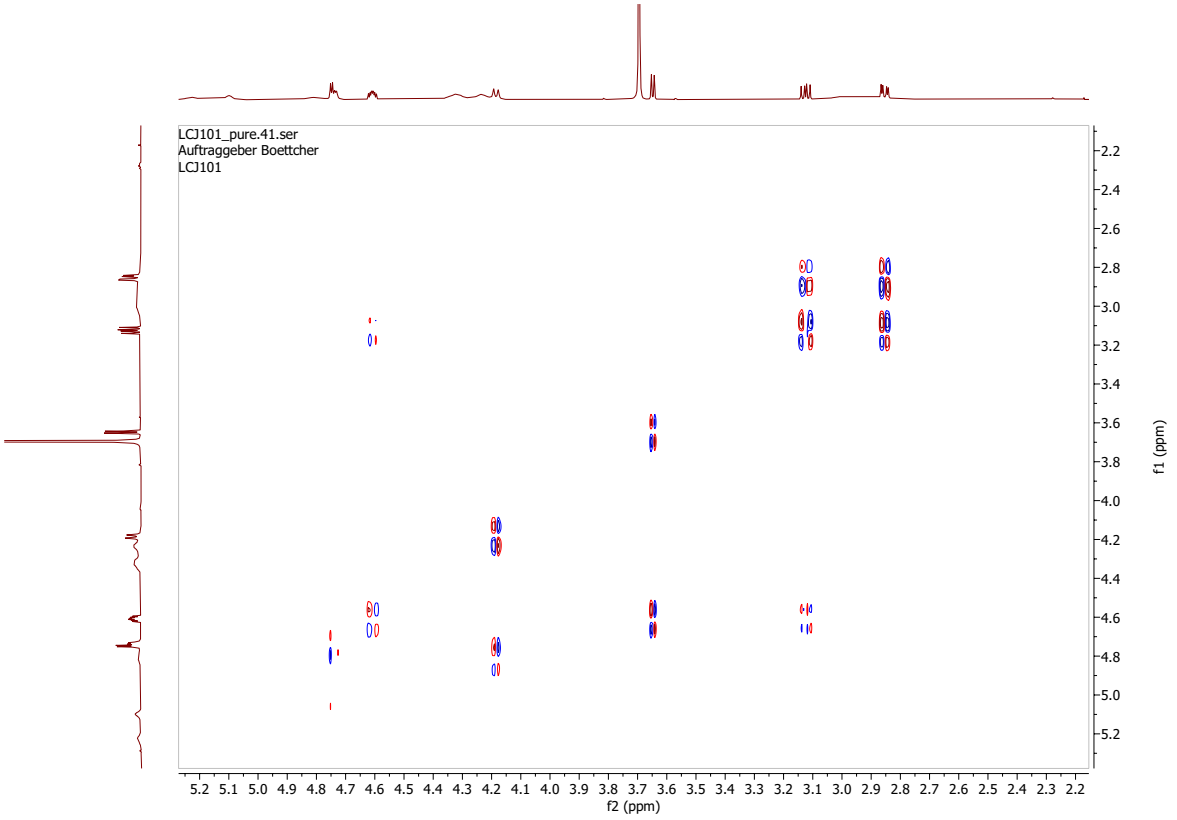

Figure 51: COSY NMR

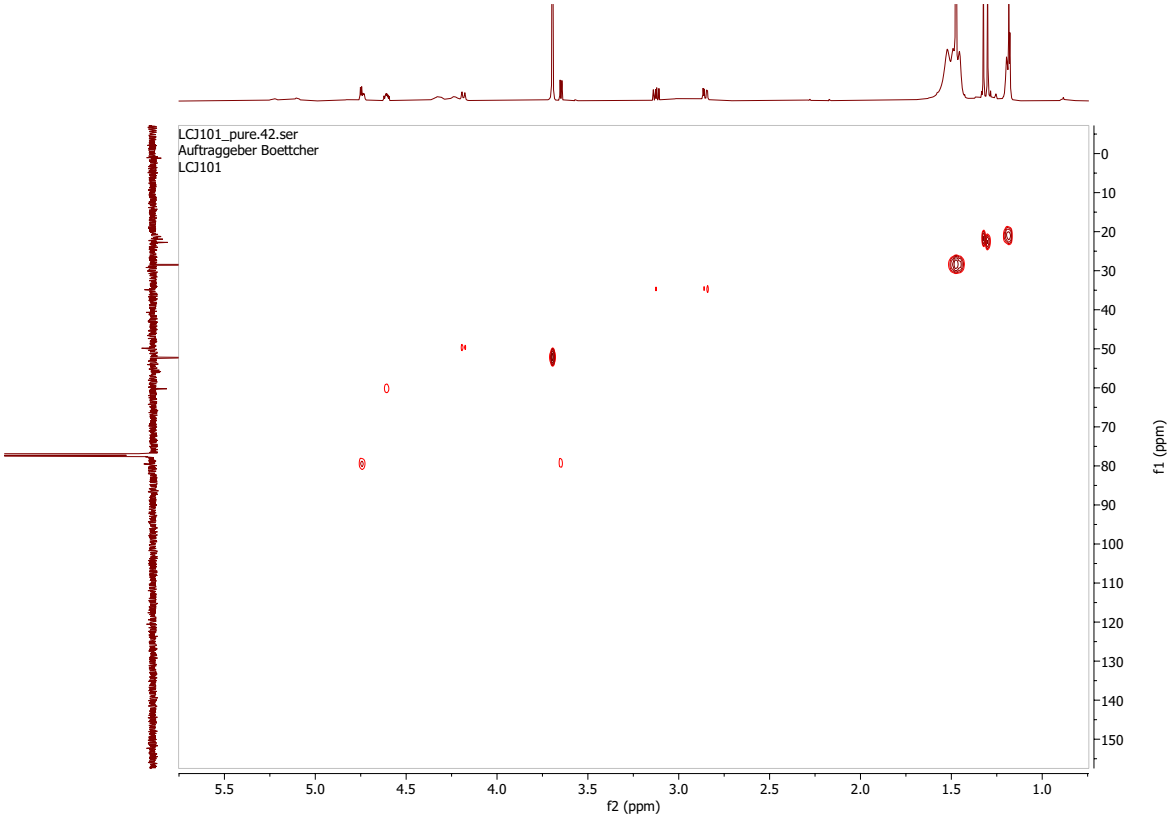

Figure 52: HSQC NMR

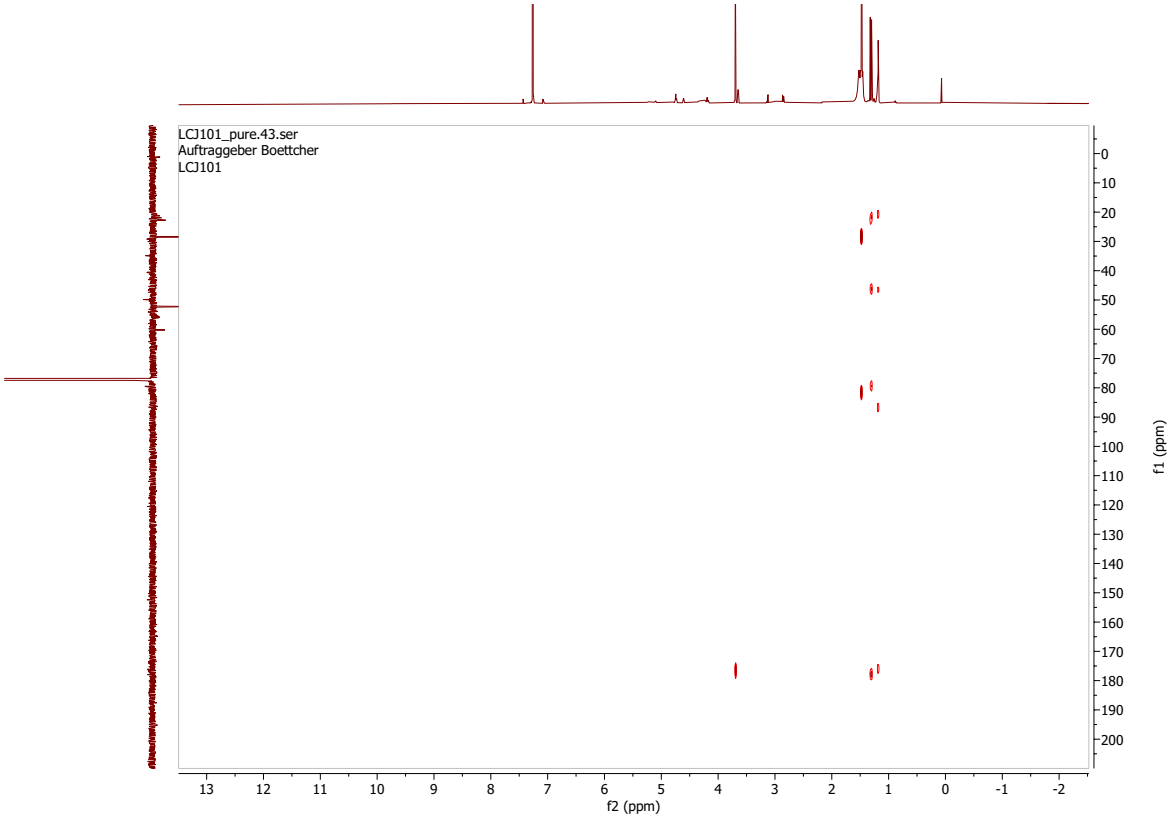

Figure 53: HMBC NMR

Generic Display Report

Analysis Info

Analysis Name	D:\Data\MS_MessService\114780_LCJ101_amazon.d	Acquisition Date	8/12/2025 4:25:11 PM
Method	MSC-Service_direct-injection.m	Operator	MSC
Sample Name	114780_LCJ101_amazon	Instrument	amaZon speed ETD
Comment	Jobst / Böttcher / IBC ACN / MeOH + 1% H2O		

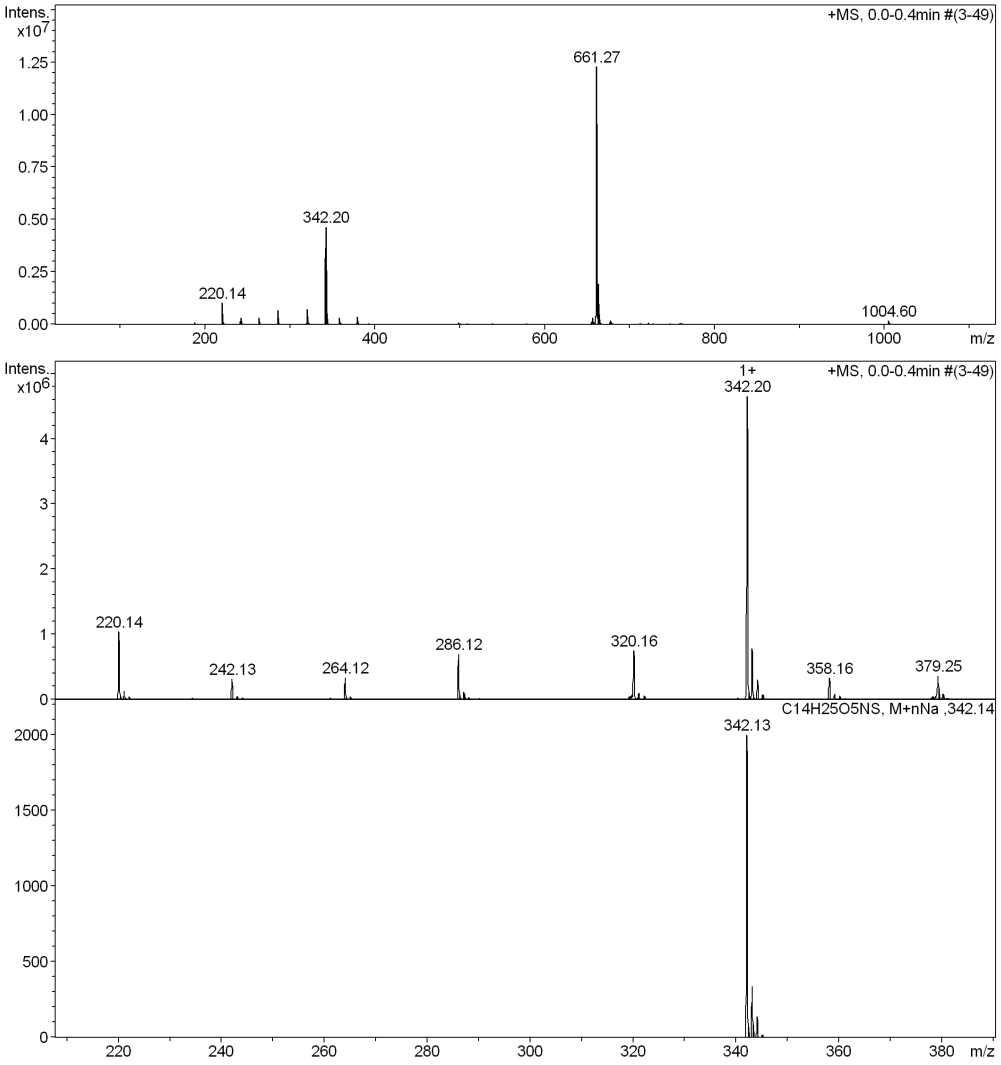

Bruker Compass DataAnalysis 4.0 printed: 8/12/2025 4:29:38 PM Page 1 of 1

Figure 54: HRMS

Analysis for 27

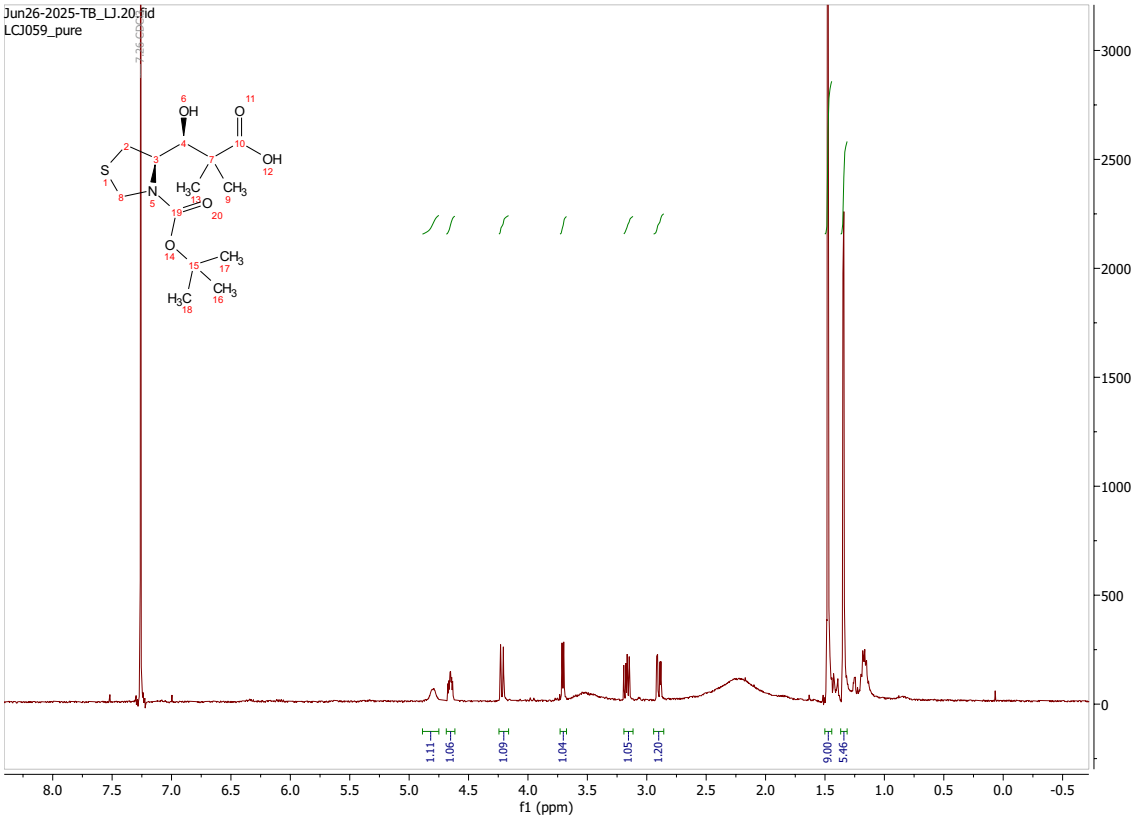

Figure 55: ^{1}H NMR

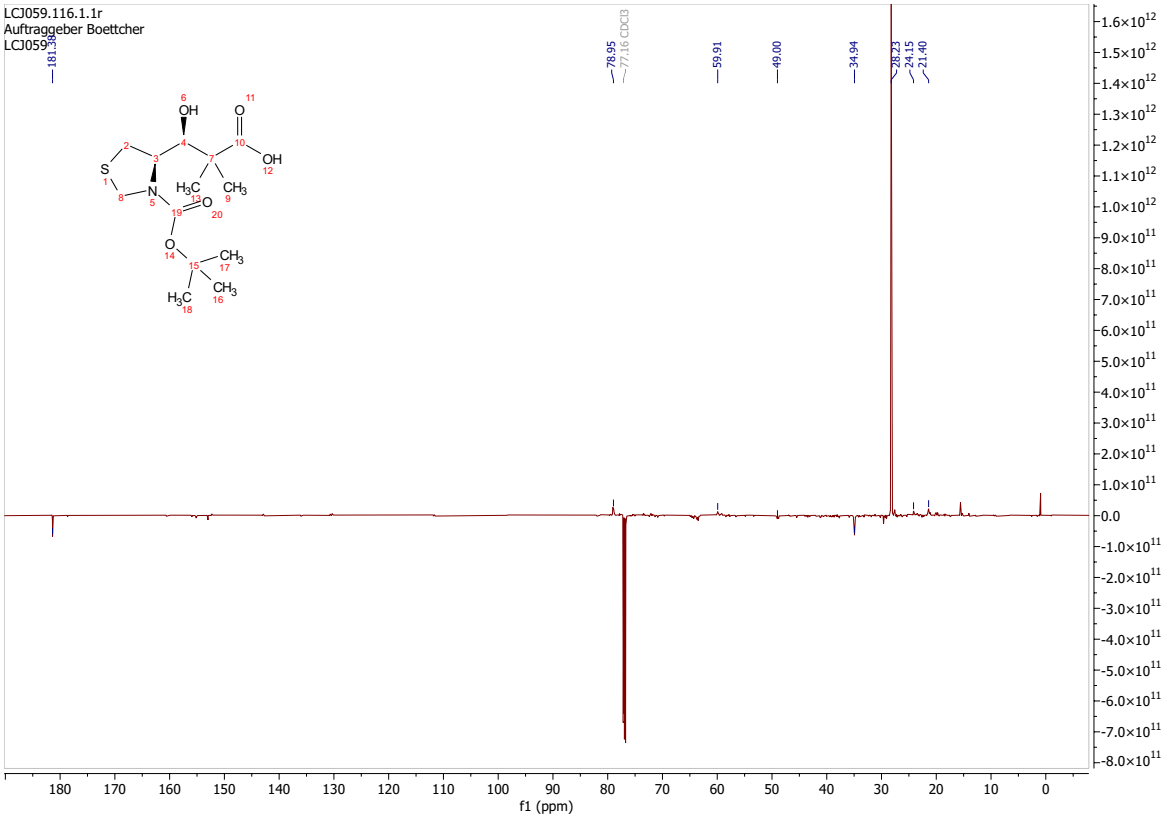

Figure 56: ^{13}C NMR

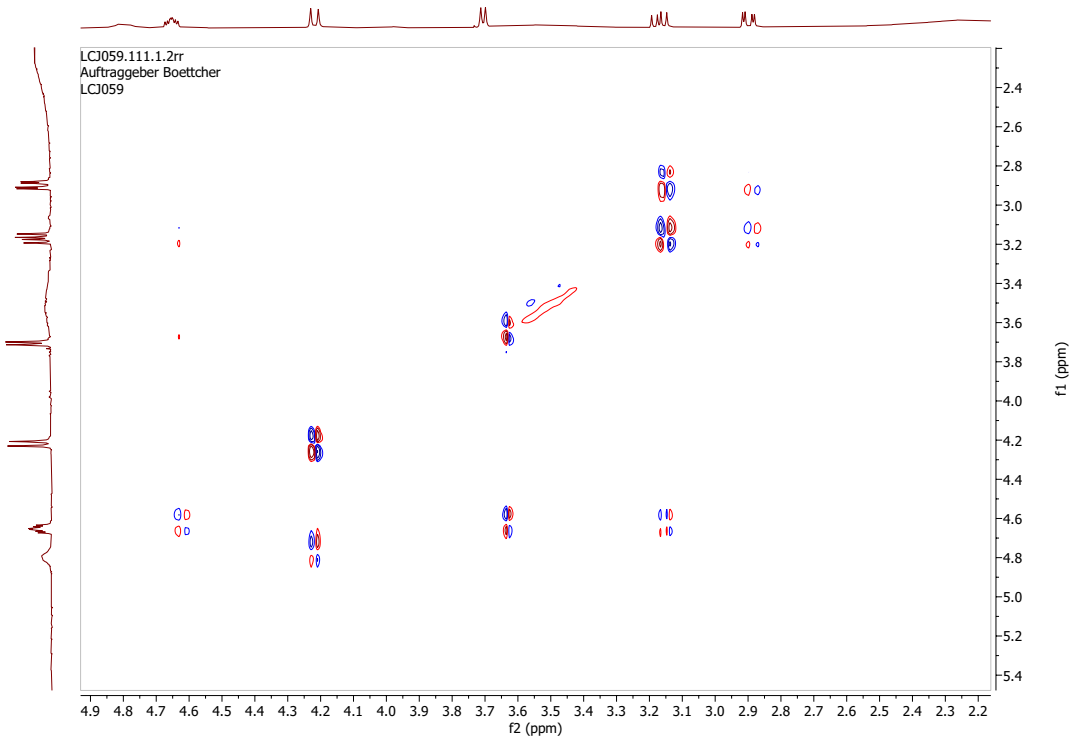

Figure 57: COSY NMR

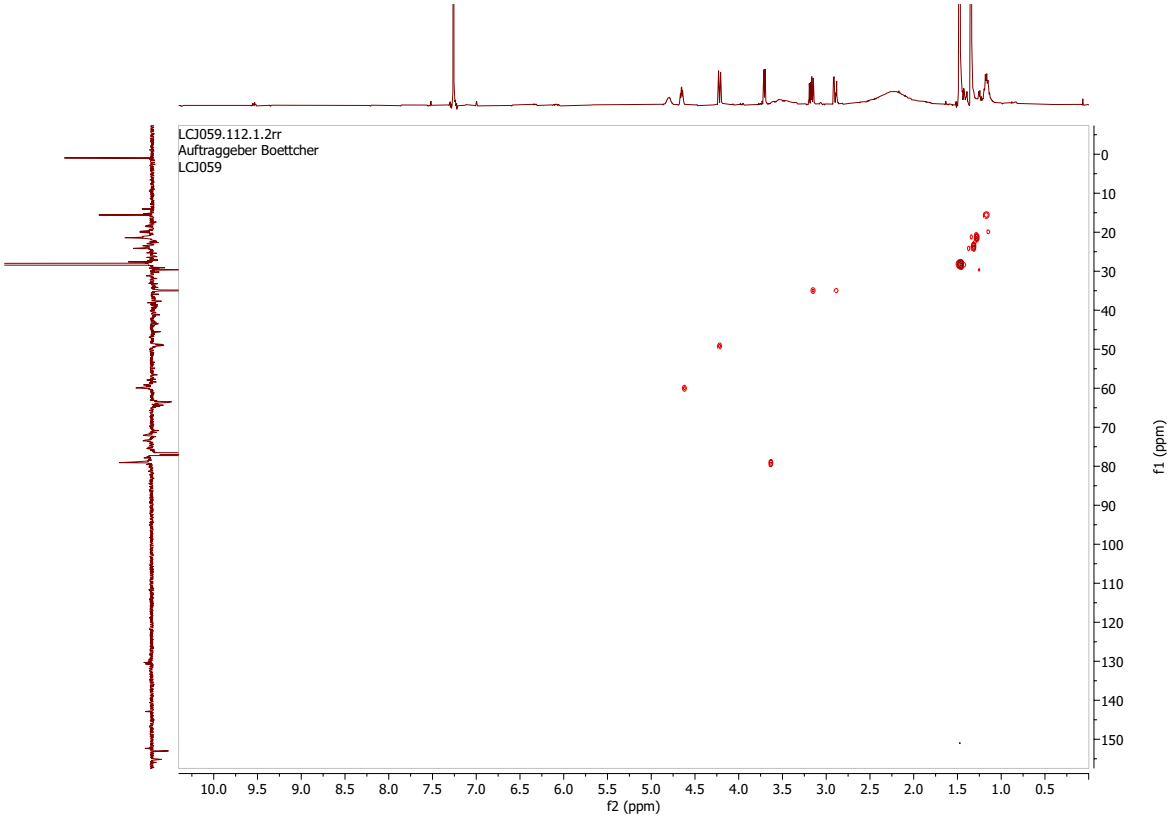

Figure 58: HSQC NMR

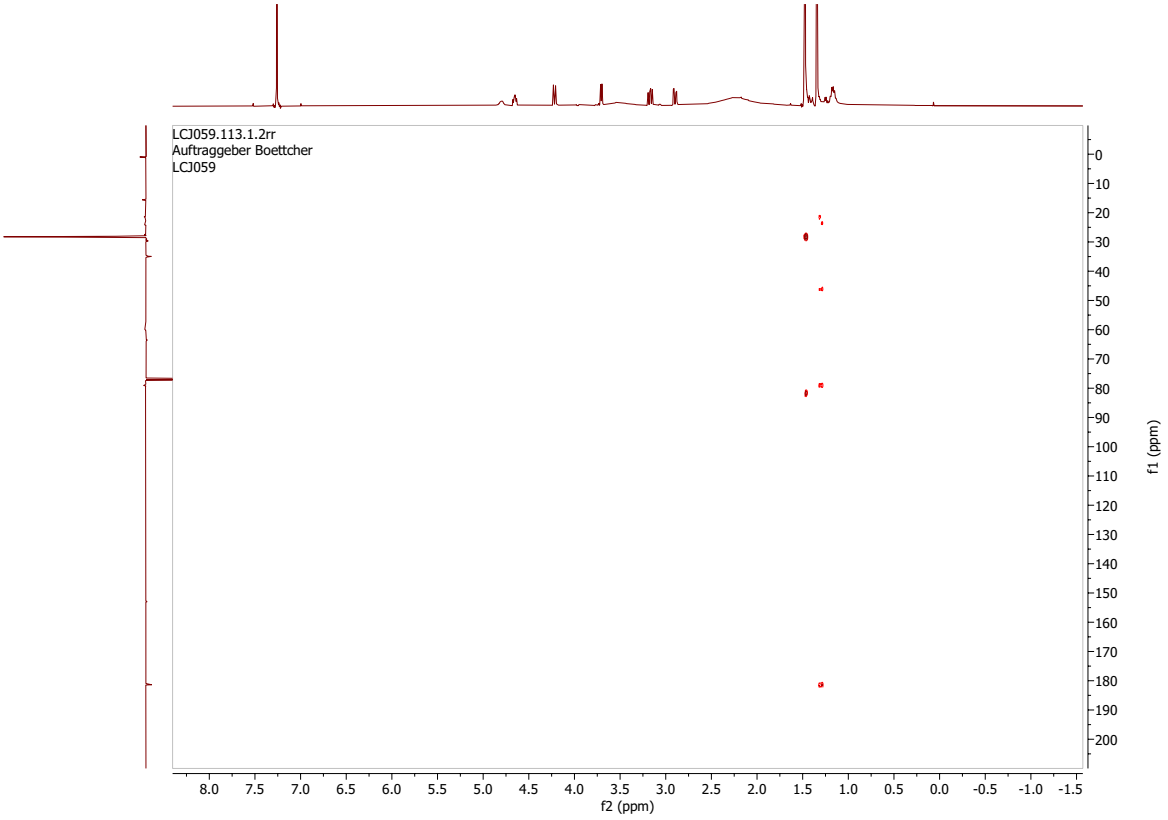

Figure 59: HMBC NMR

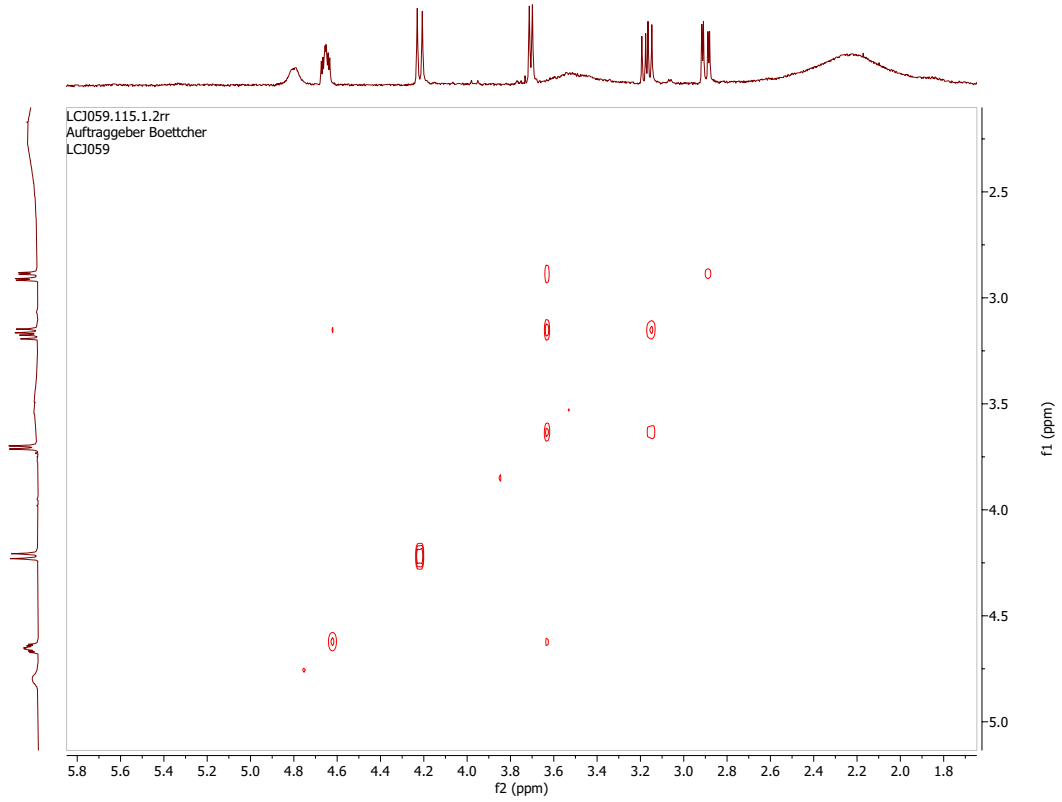

Figure 60: TOCSY NMR

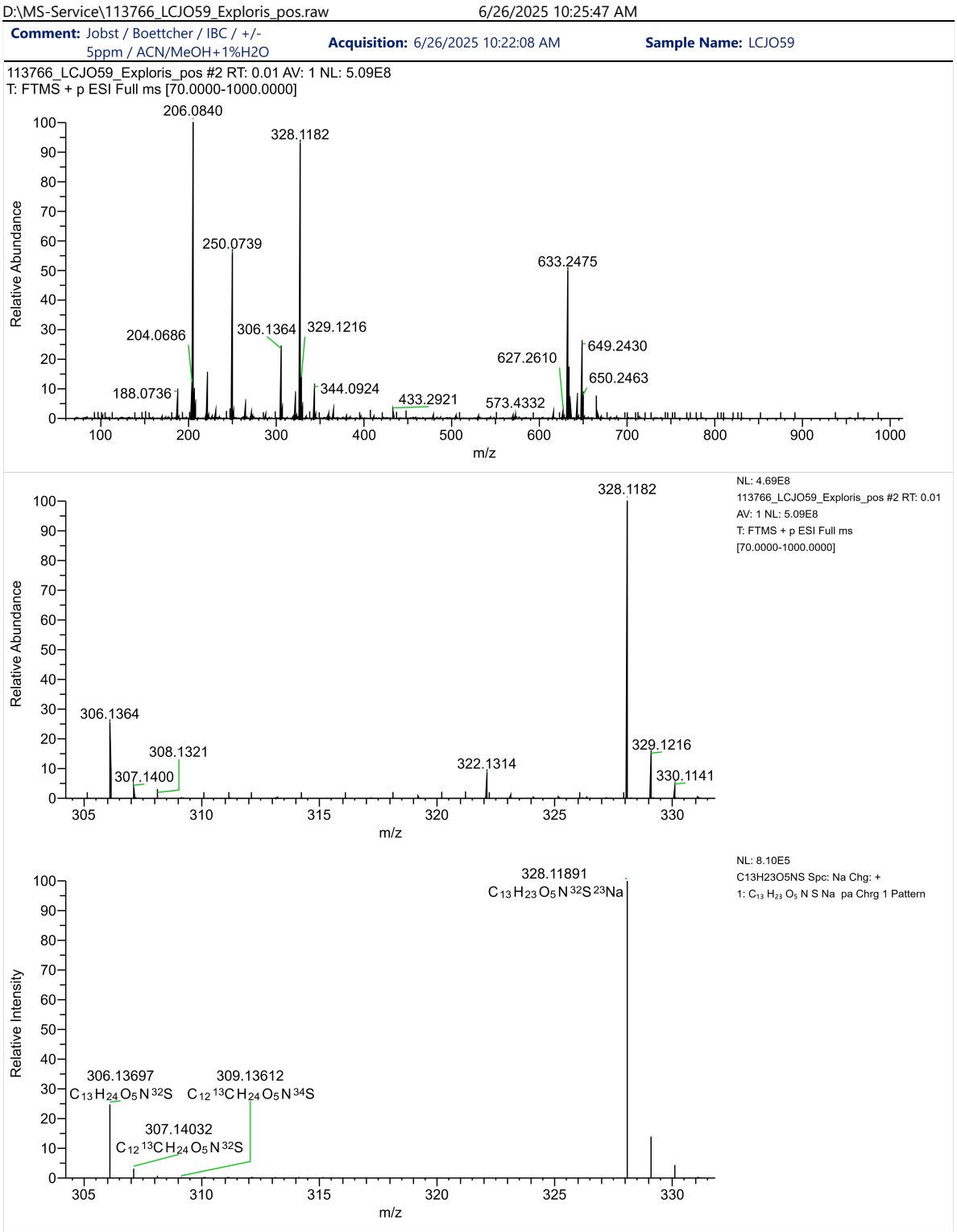

Figure 61: HRMS

Analysis for 30

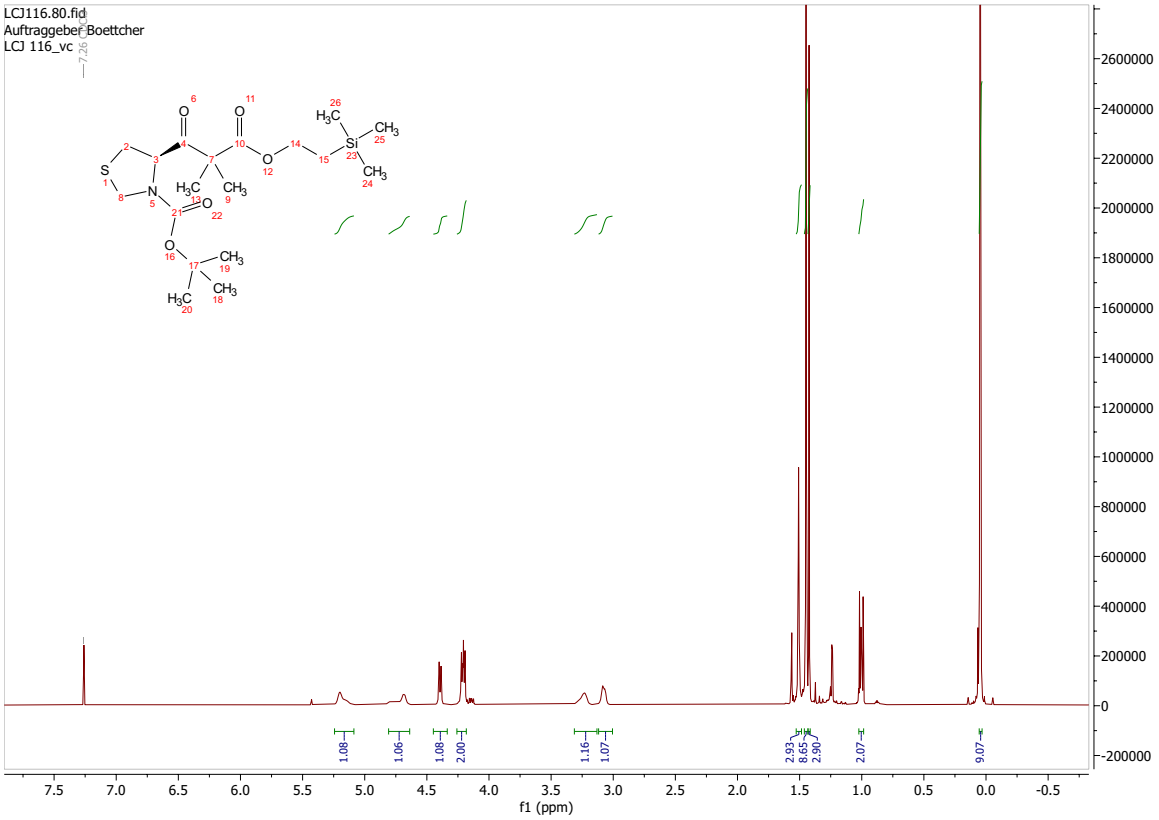

Figure 62: ^{1}H NMR

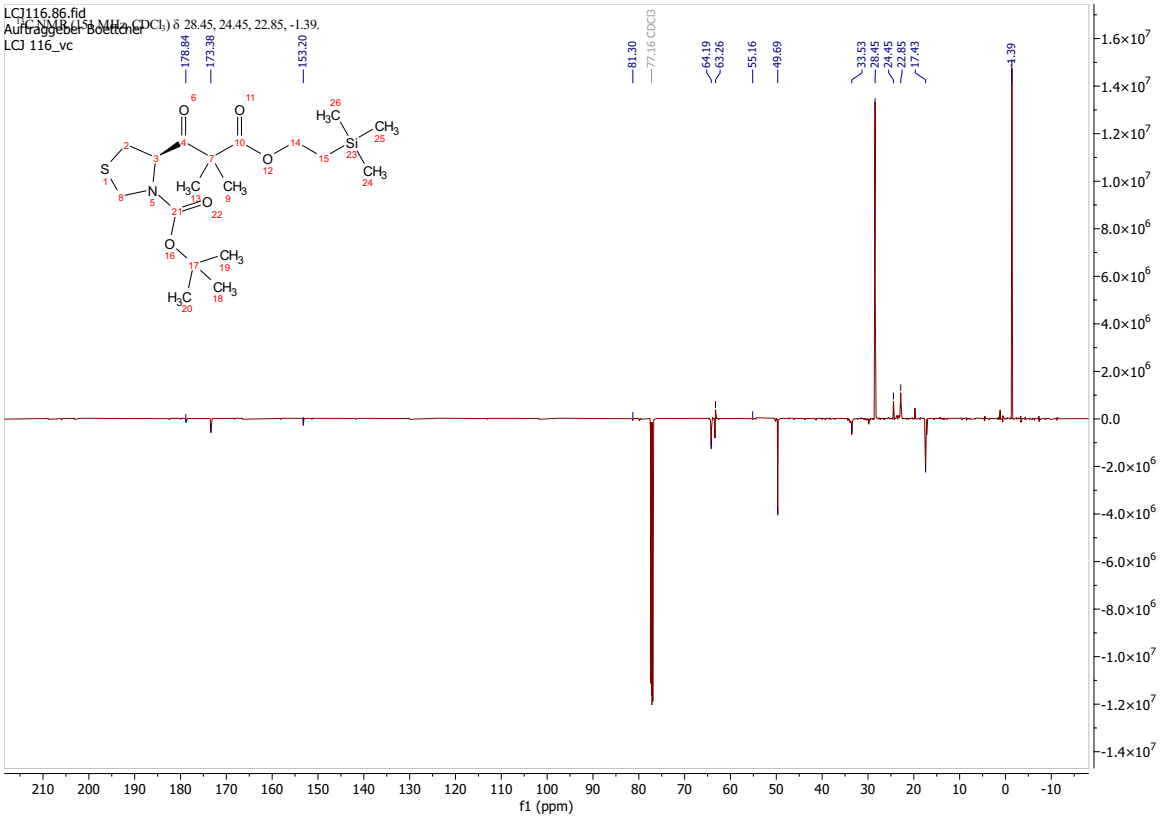

Figure 63: ^{13}C NMR

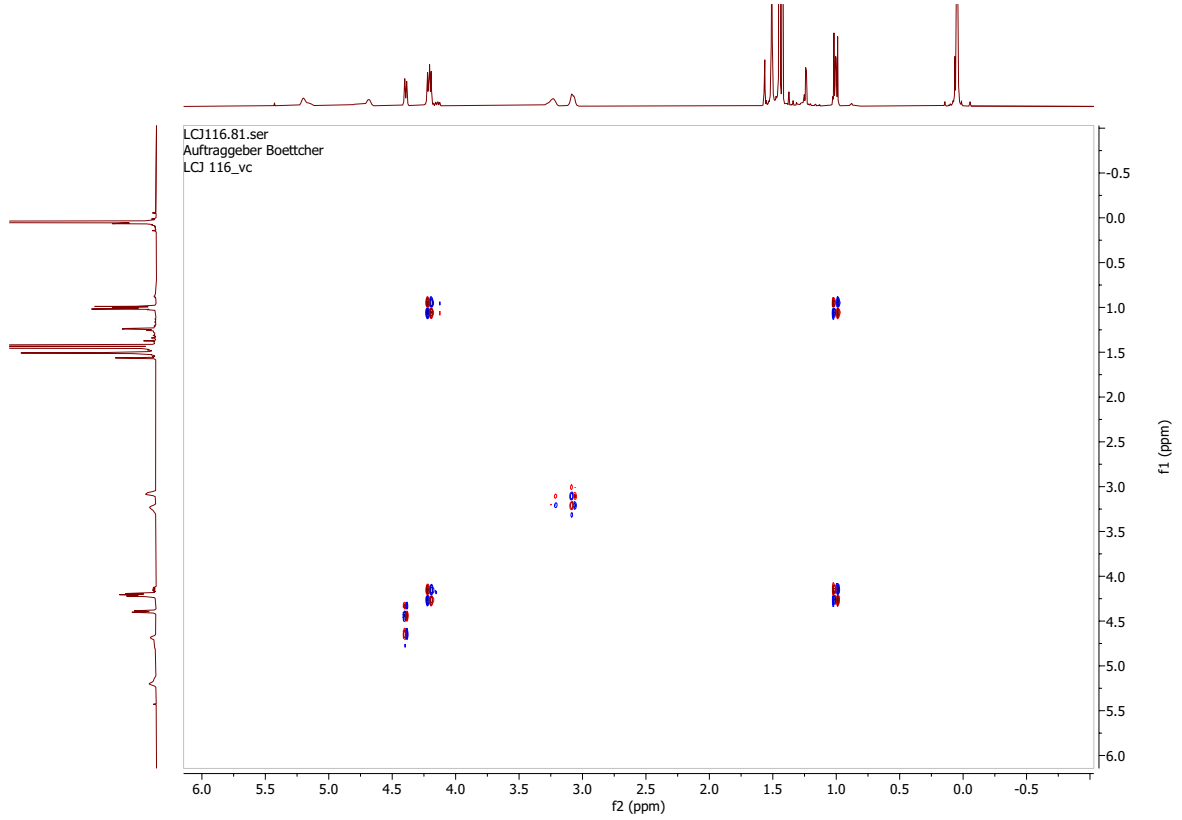

Figure 64: COSY NMR

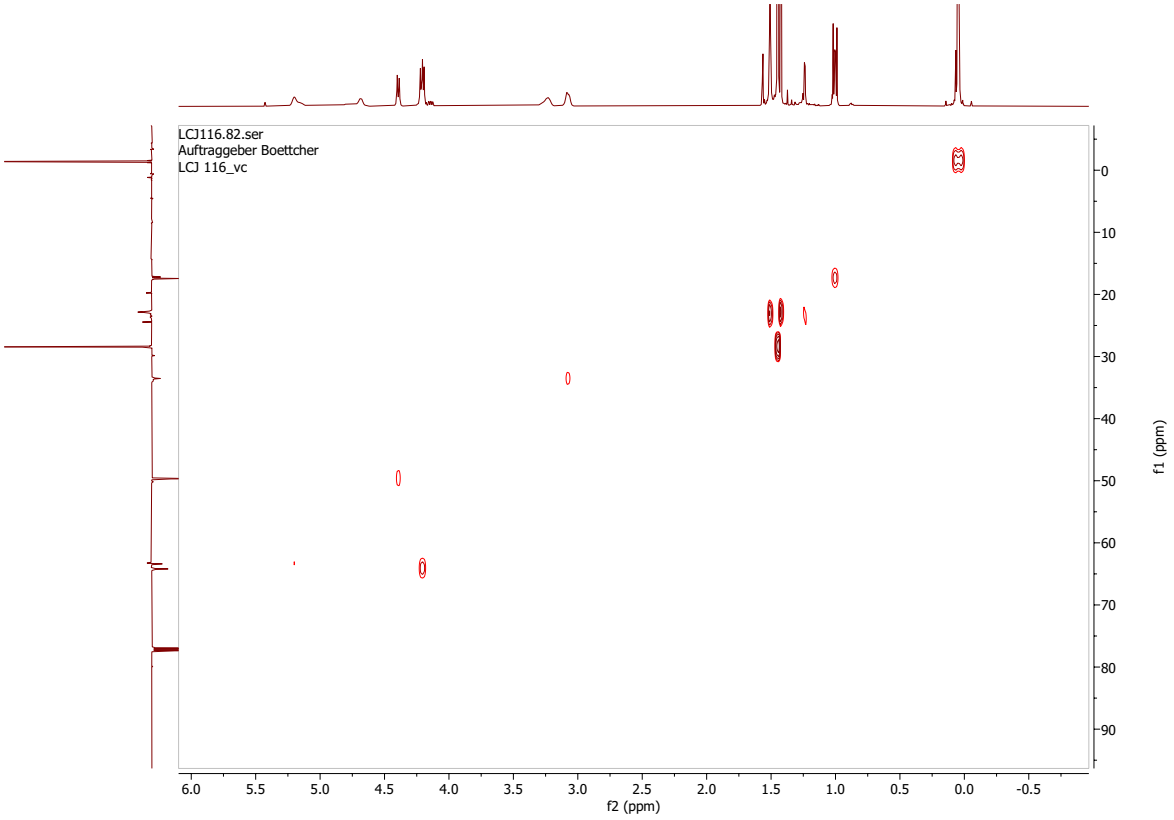

Figure 65: HSQC NMR

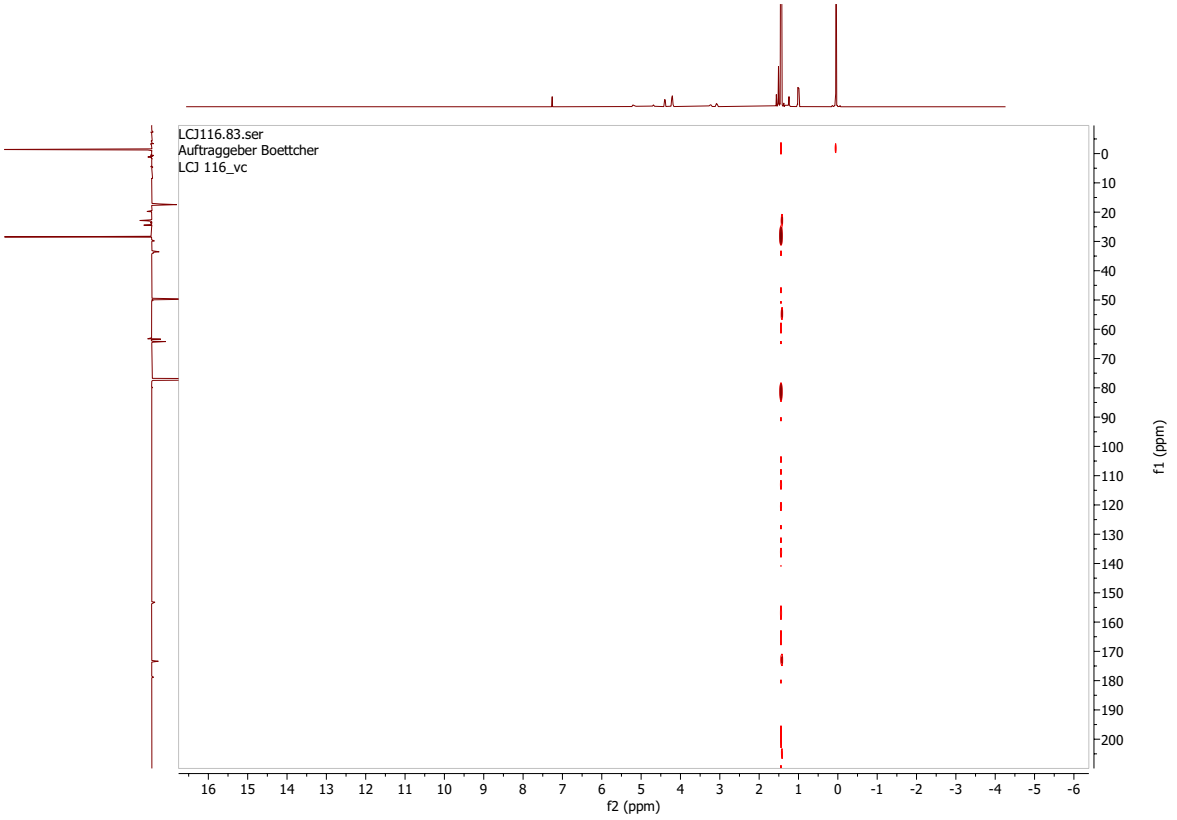

Figure 66: HMBC NMR

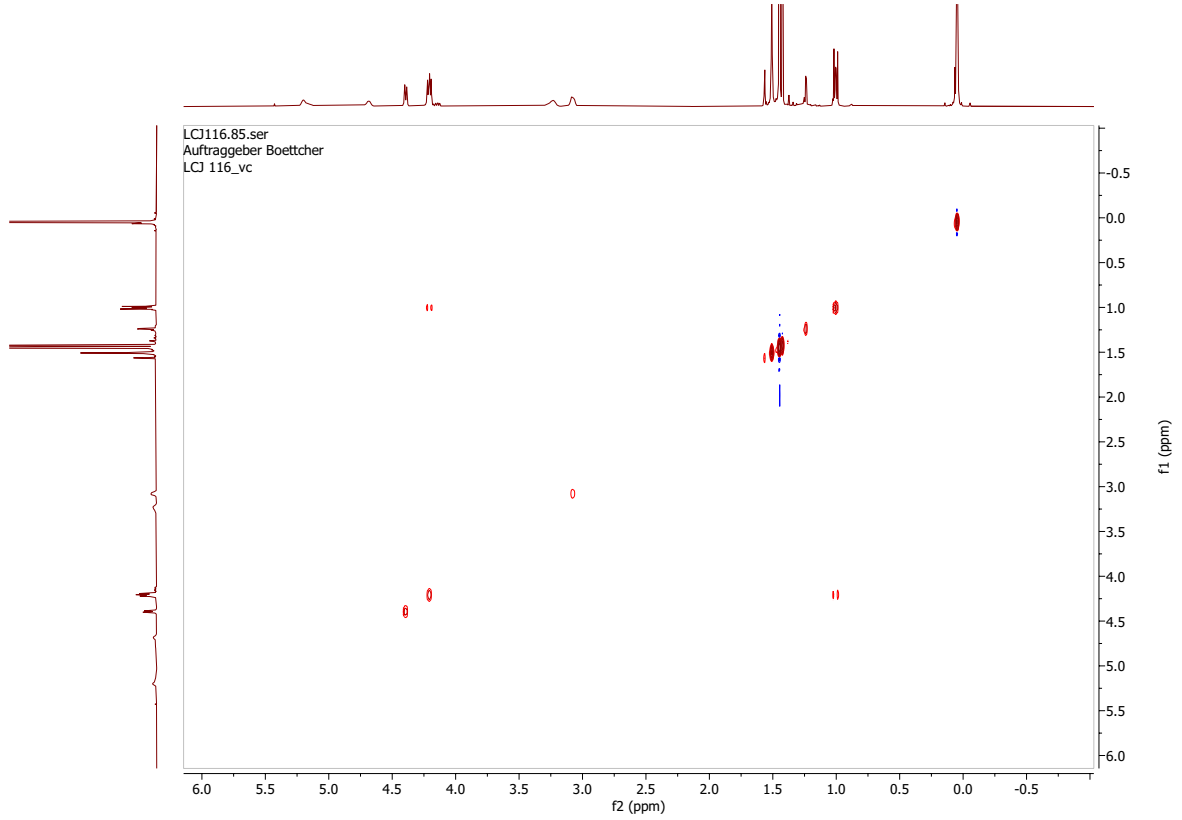

Figure 67: TOCSY NMR

Generic Display Report

Analysis Info

Analysis Name	D:\Data\MSC service\115425000001.d	Acquisition Date	9/22/2025 11:47:56 AM
Method	ESI_DI_standard_2023.m	Operator	Demo User
Sample Name	LCJ116v.c.	Instrument	timsTOF fleX
Comment	Jobst / Boettcher - IBC Ergebnis: +/- 5 ppm ACN / MeOH + 1% H2O		

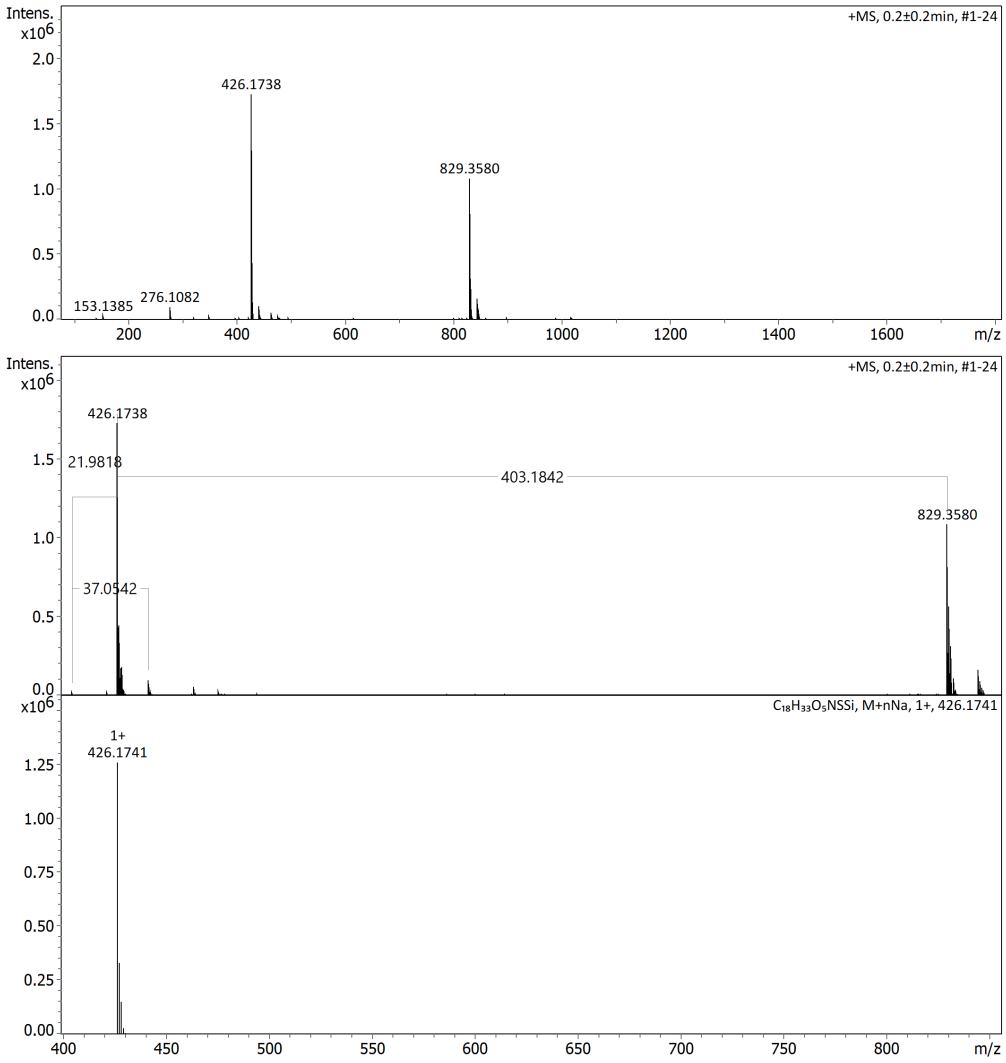

Bruker Compass DataAnalysis 5.3 printed: 9/22/2025 11:52:27 AM by: demo Page 1 of 1

Figure 68: HRMS

Analysis for 31

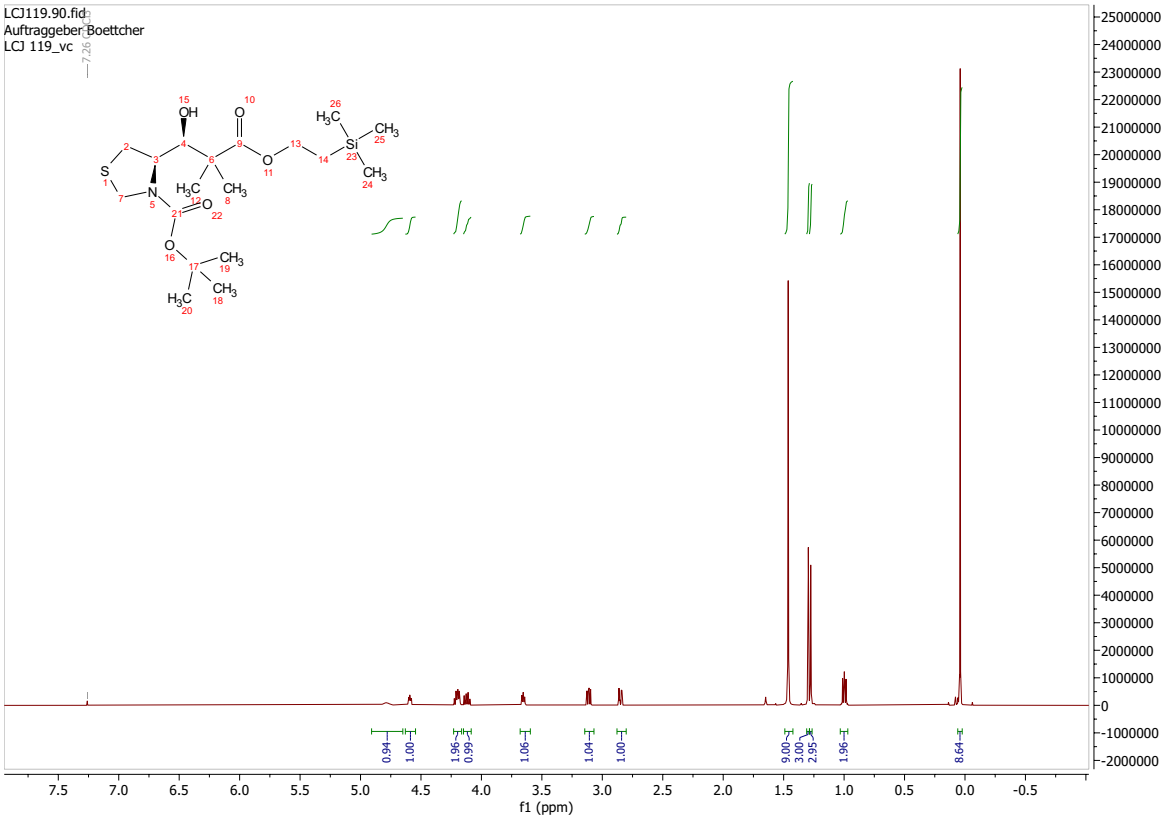

Figure 69: ^{1}H NMR

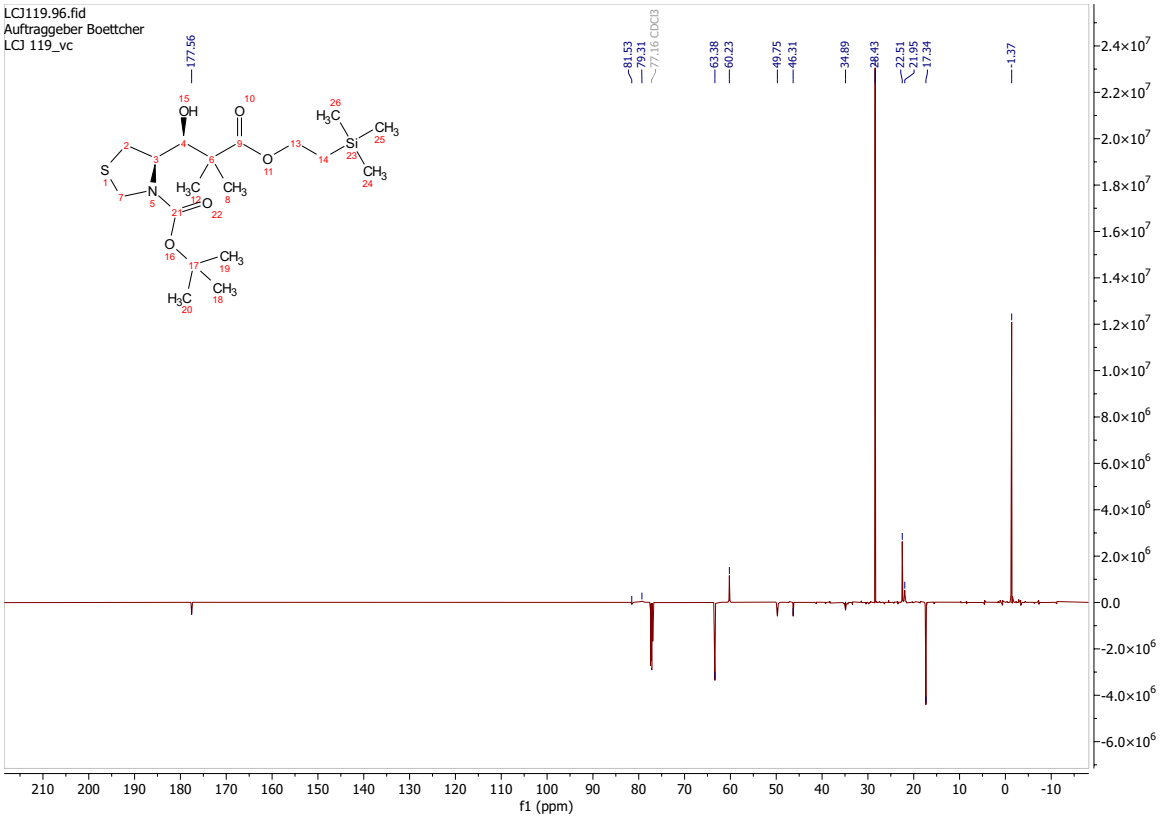

Figure 70: ^{13}C NMR

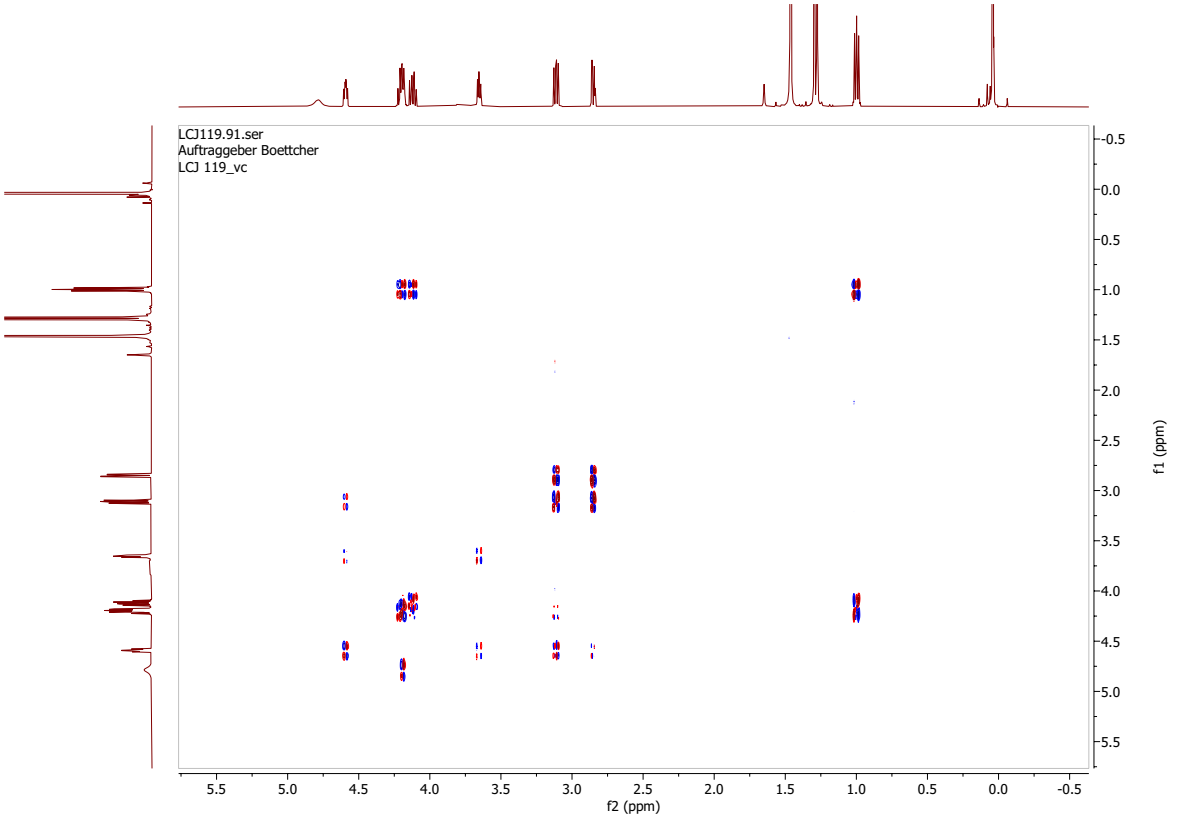

Figure 71: COSY NMR

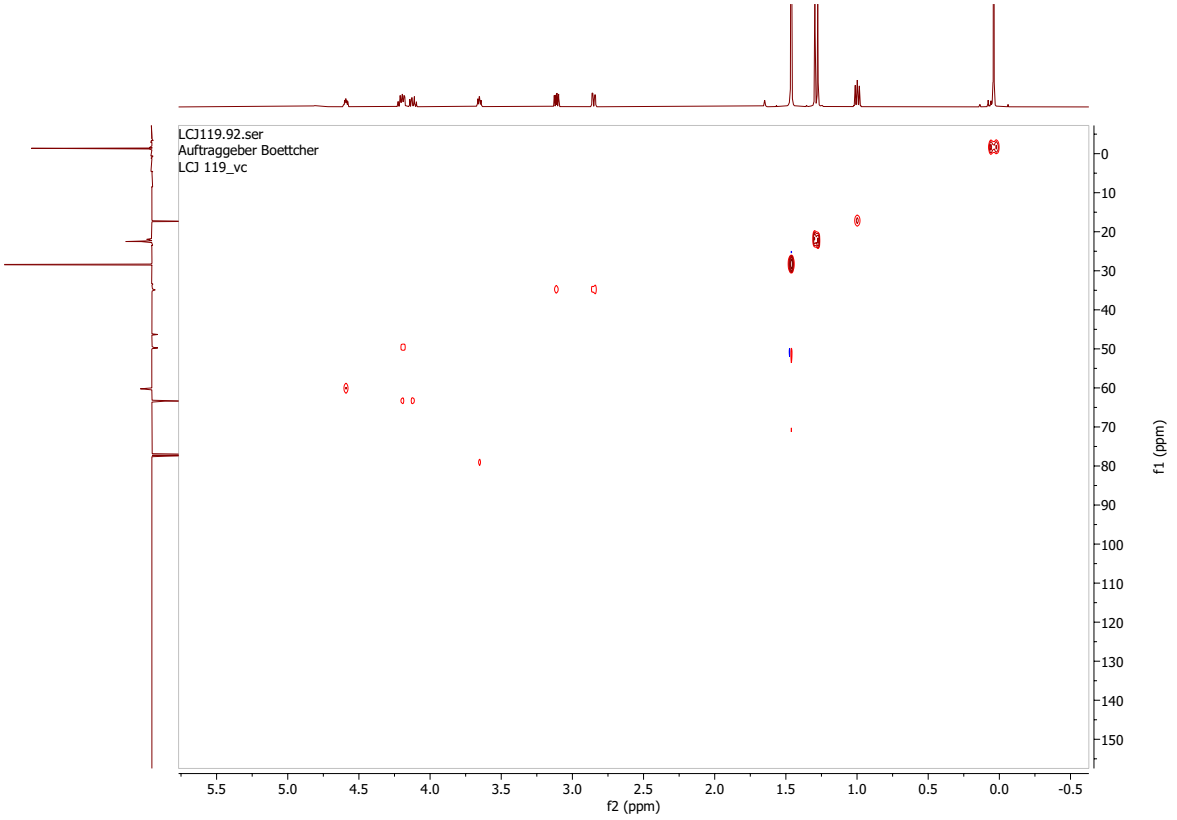

Figure 72: HSQC NMR

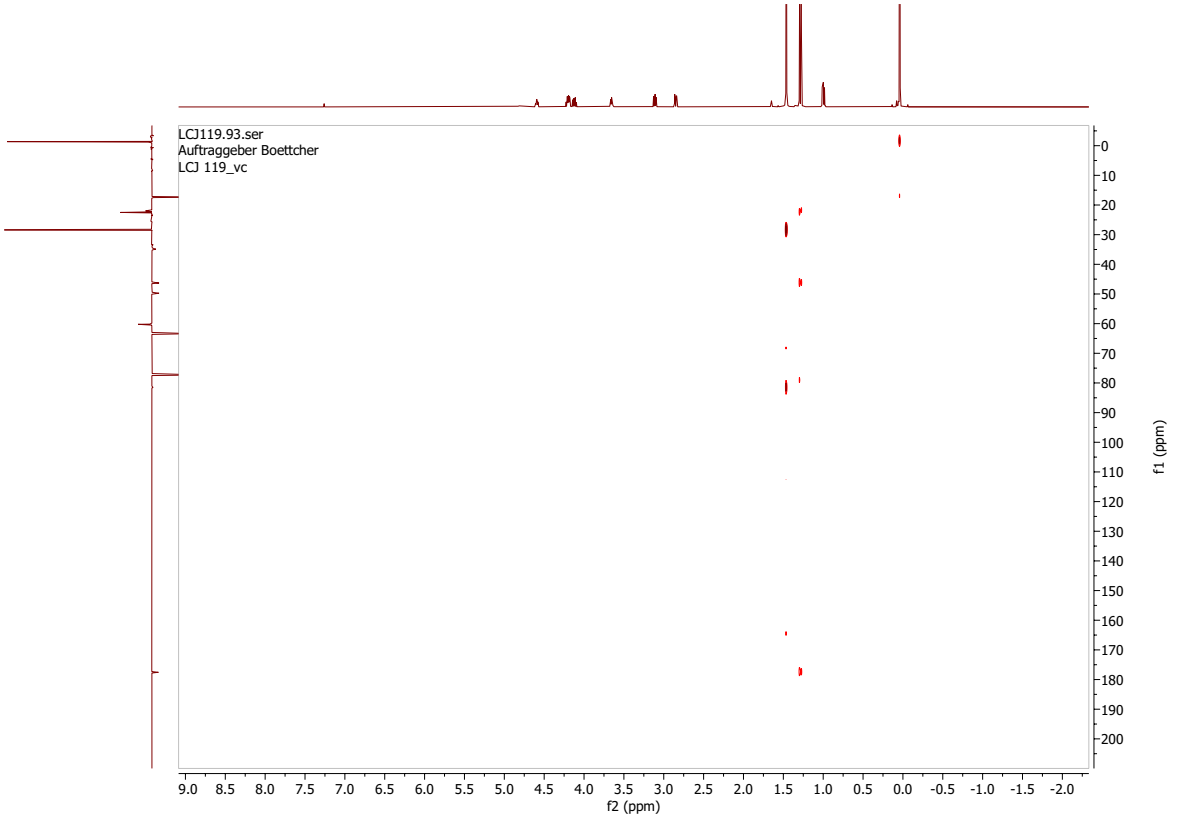

Figure 73: HMBC NMR

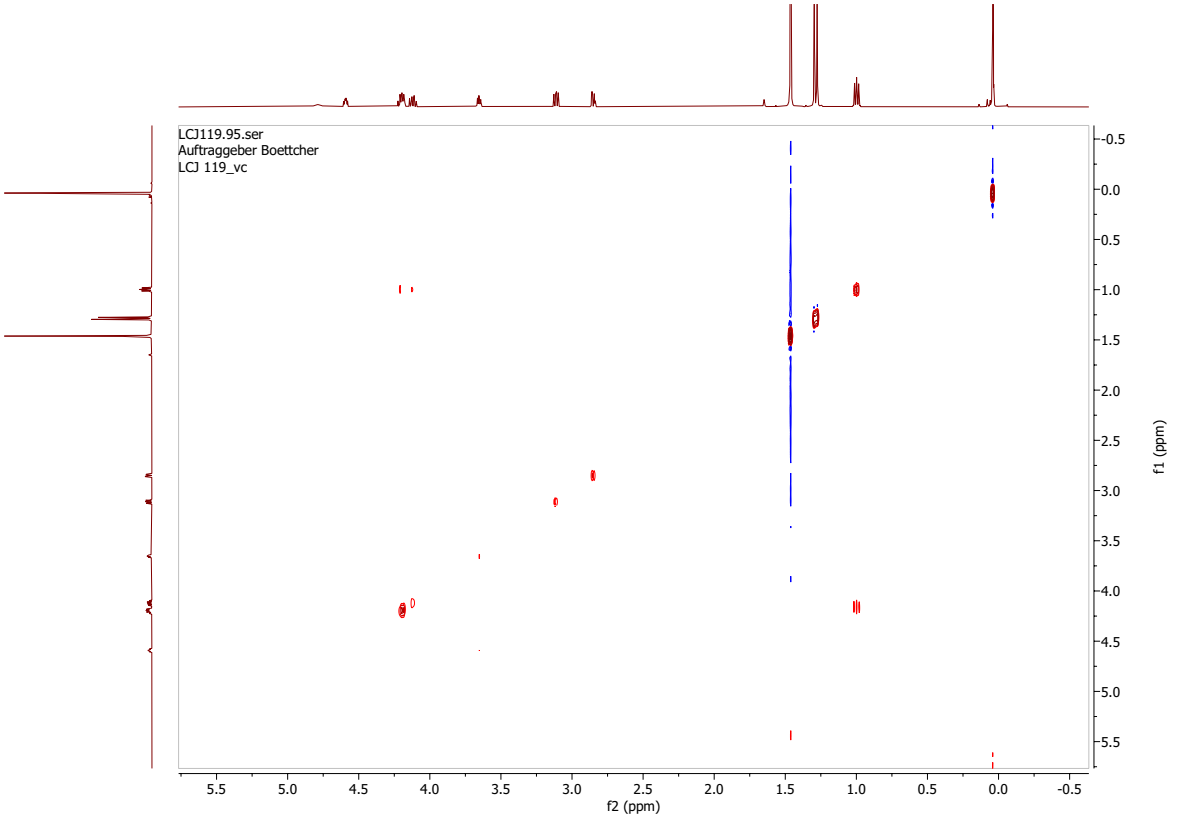

Figure 74: TOCSY NMR

Generic Display Report

Analysis Info

Analysis Name	D:\Data\MSC service\115426000001.d	Acquisition Date	9/22/2025 11:57:32 AM
Method	ESI_DI_standard_2023.m	Operator	Demo User
Sample Name	LCJ119v.c.	Instrument	timsTOF fleX
Comment	Jobst / Boettcher - IBC Ergebnis: +/- 5 ppm ACN / MeOH + 1% H2O		

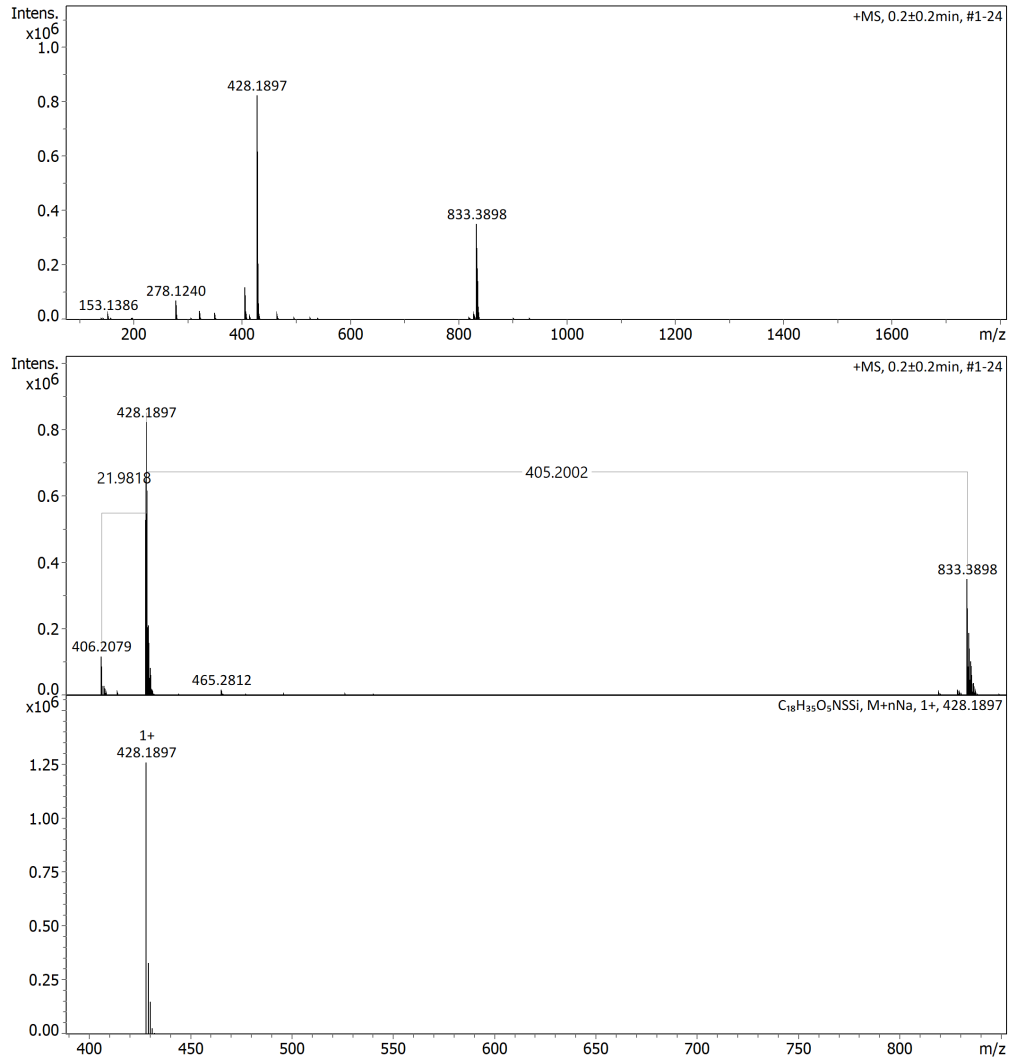

Bruker Compass DataAnalysis 5.3 printed: 9/22/2025 12:00:58 PM by: demo Page 1 of 1

Figure 75: HRMS

Analysis for 33

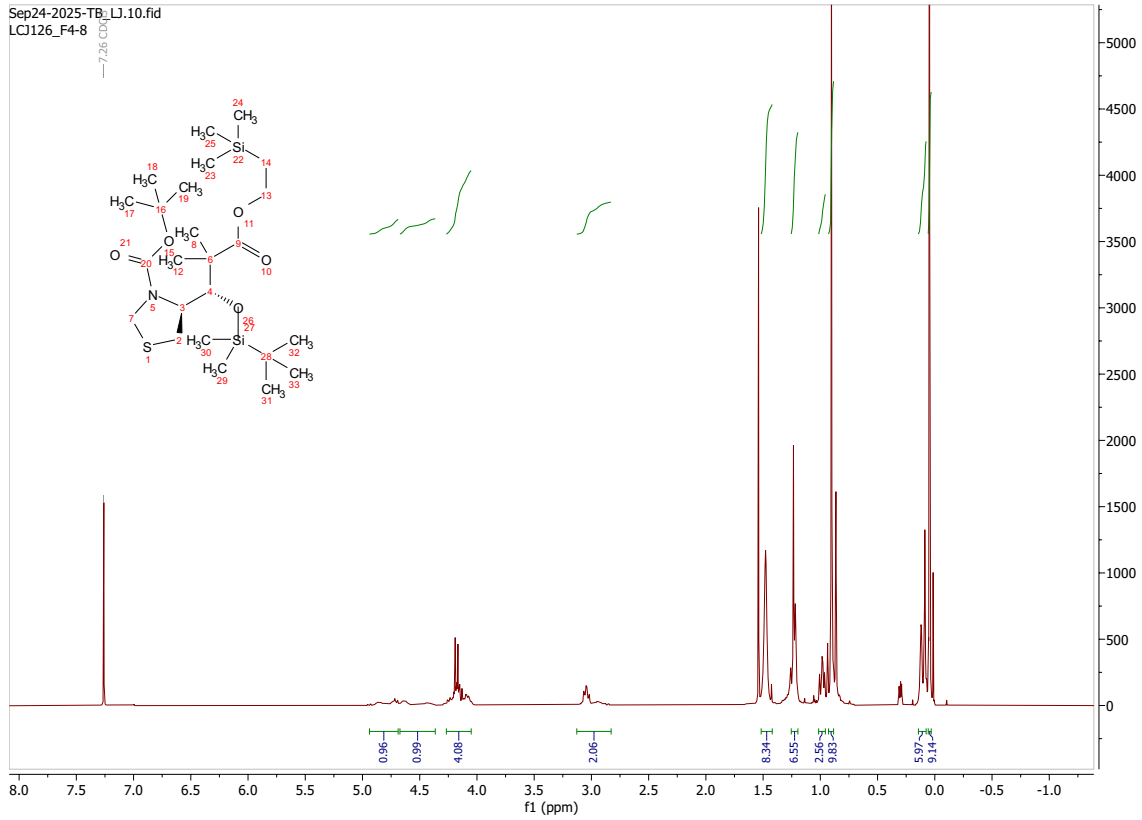

Figure 76: ^{1}H NMR

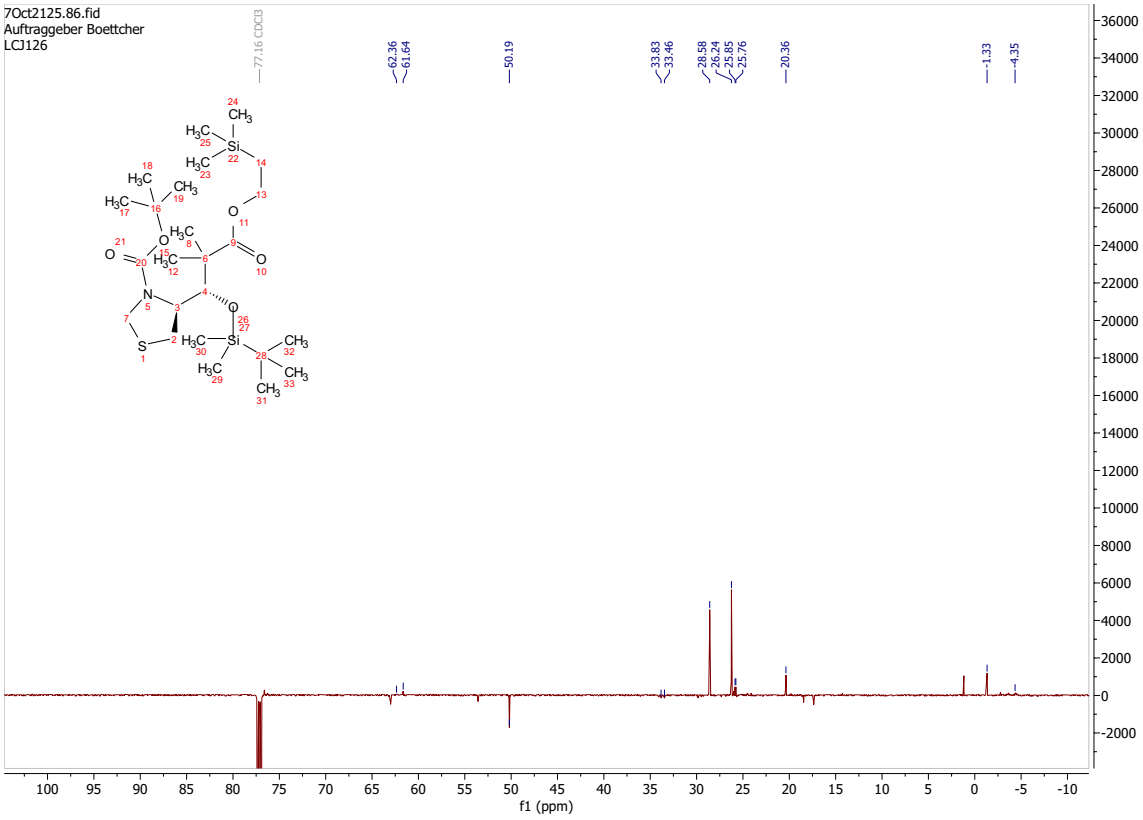

Figure 77: ^{13}C NMR

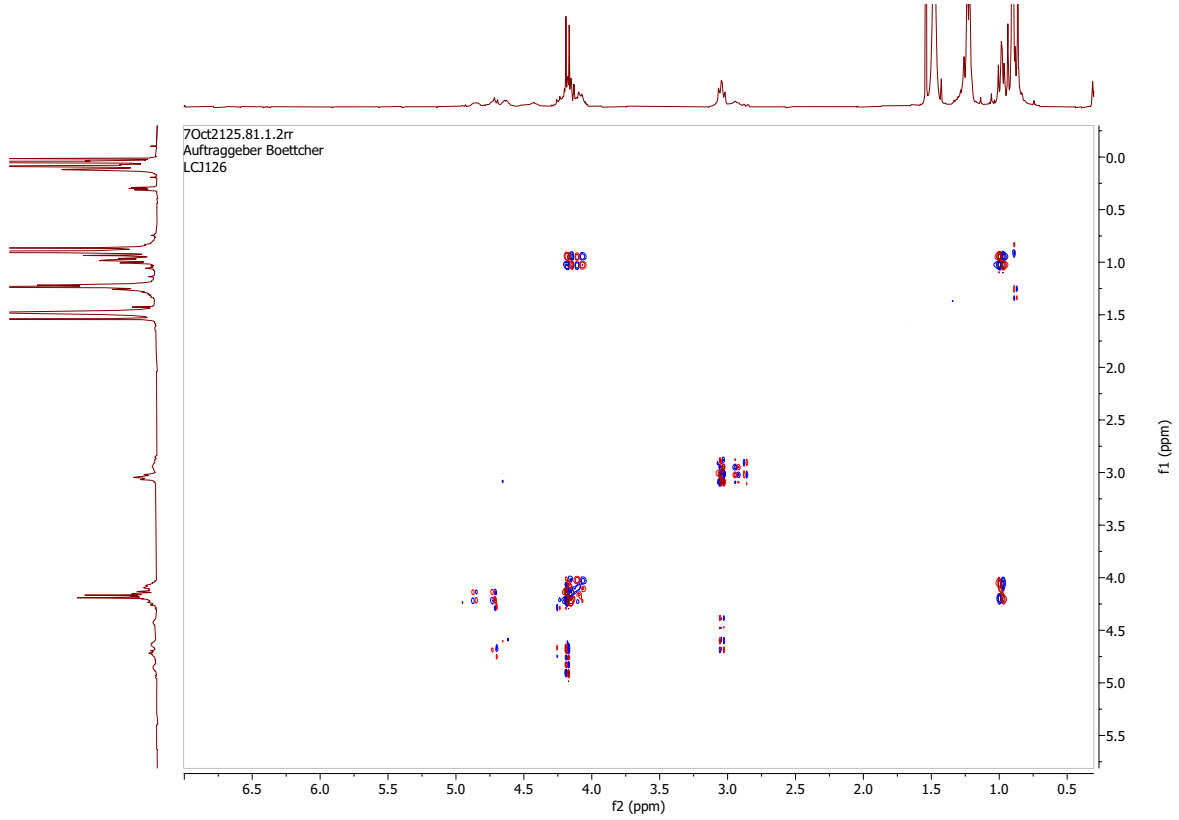

Figure 78: COSY NMR

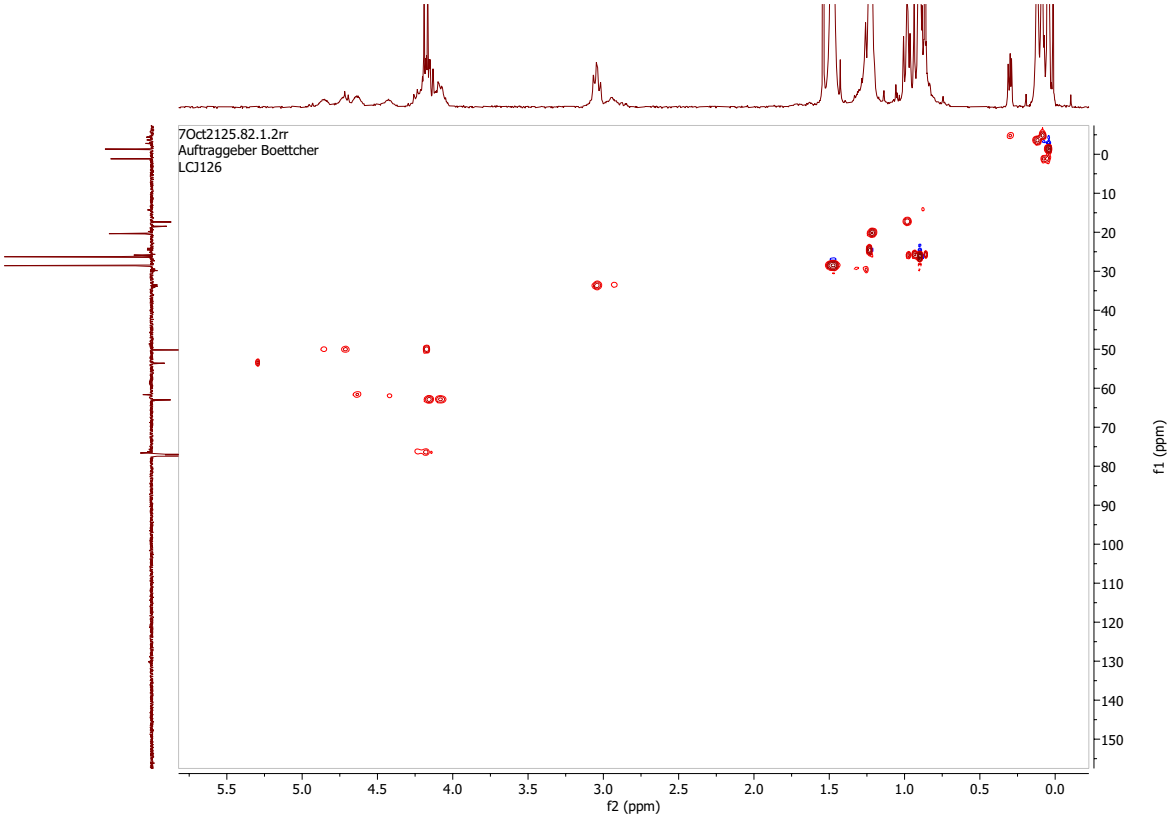

Figure 79: HSQC NMR

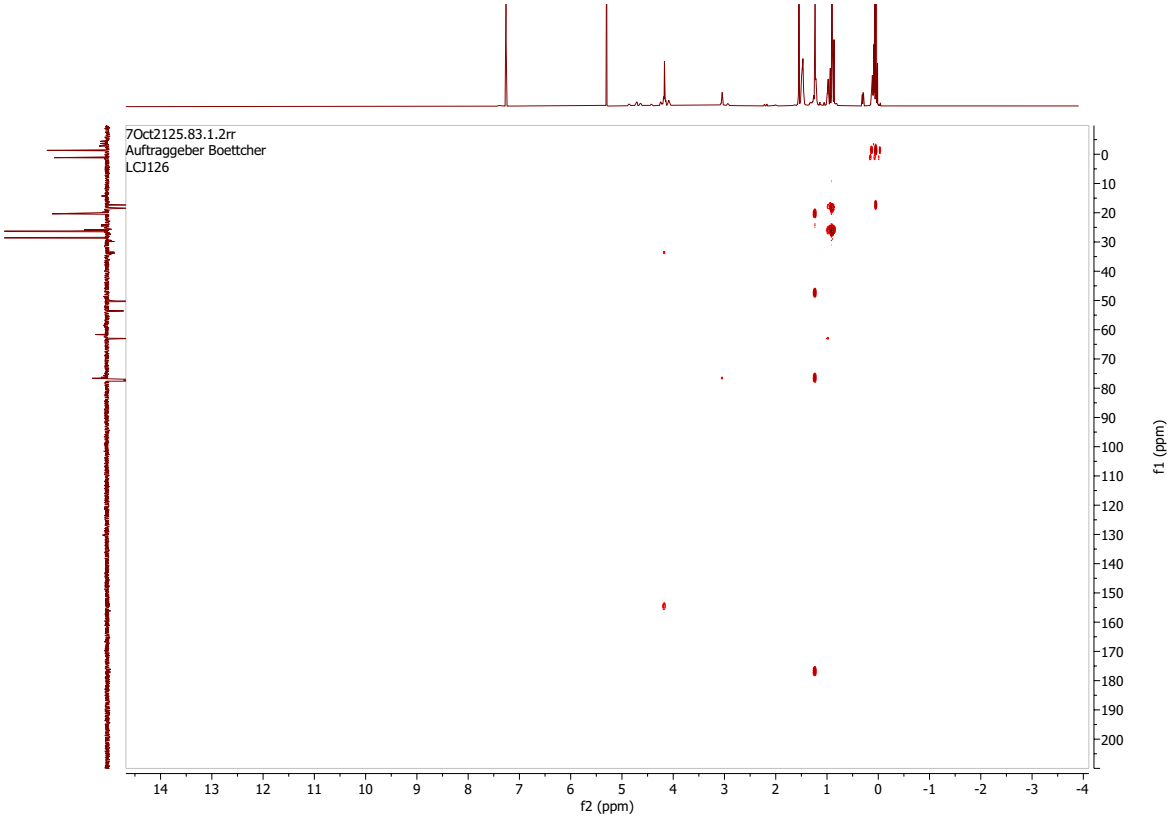

Figure 80: HMBC NMR

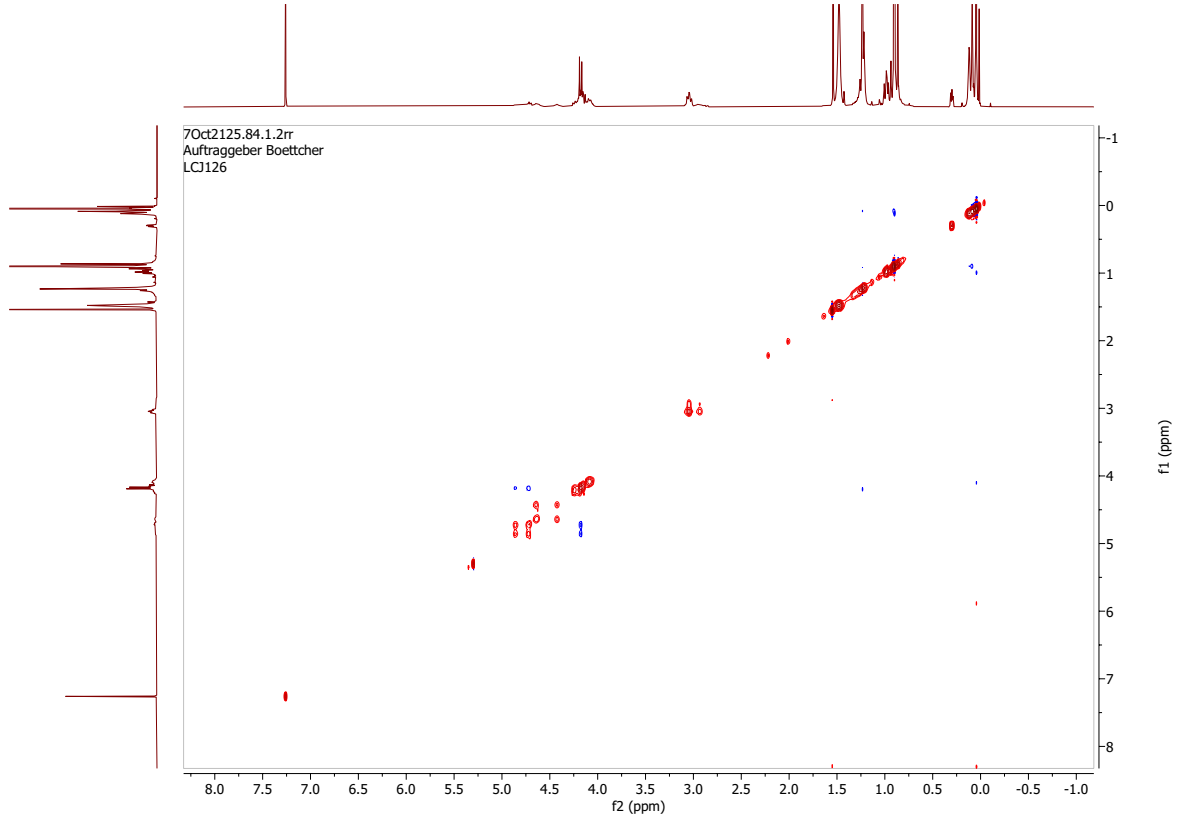

Figure 81: NOESY NMR

File Name: D:\MS-Service\116199_LCJ126_pos
Comment: Jobst / Boettcher-IBC / Result +/- 5ppm / ACN/MeOH+1%H2O
Acquisition: 10/16/25 16:35:58

Sample name: LCJ126

Device model: Orbitrap Exploris MB11205C

116199_LCJ126_pos #1-114 RT: 0.01-0.51 AV: 114 NL: 4.67E7
T: FTMS + p ESI Full ms [125.0000-1500.0000]

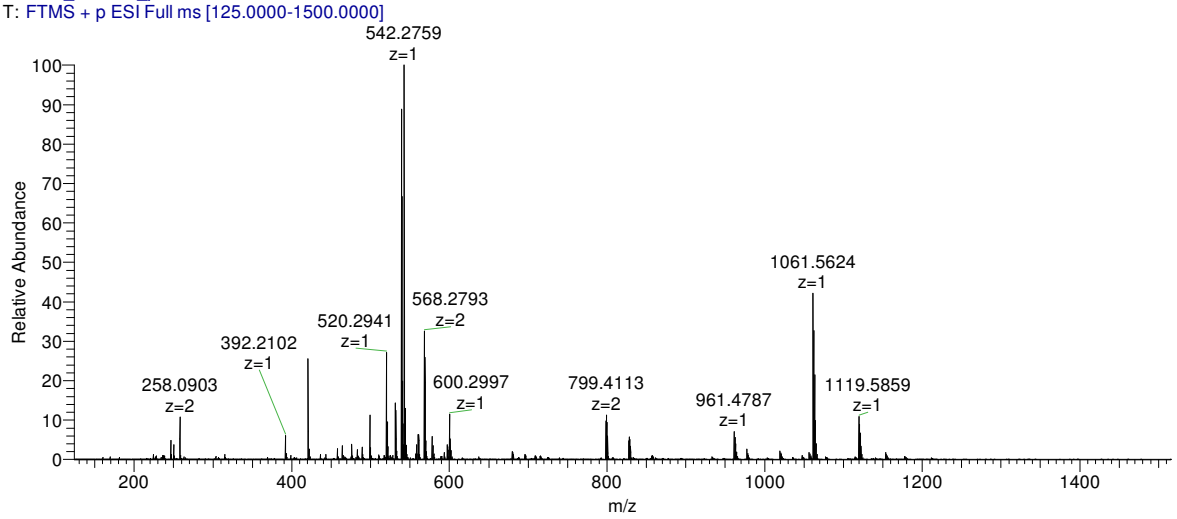

116199_LCJ126_pos #2-114 RT: 0.01-0.51 AV: 113 NL: 4.66E7
T: FTMS + p ESI Full ms [125.0000-1500.0000]

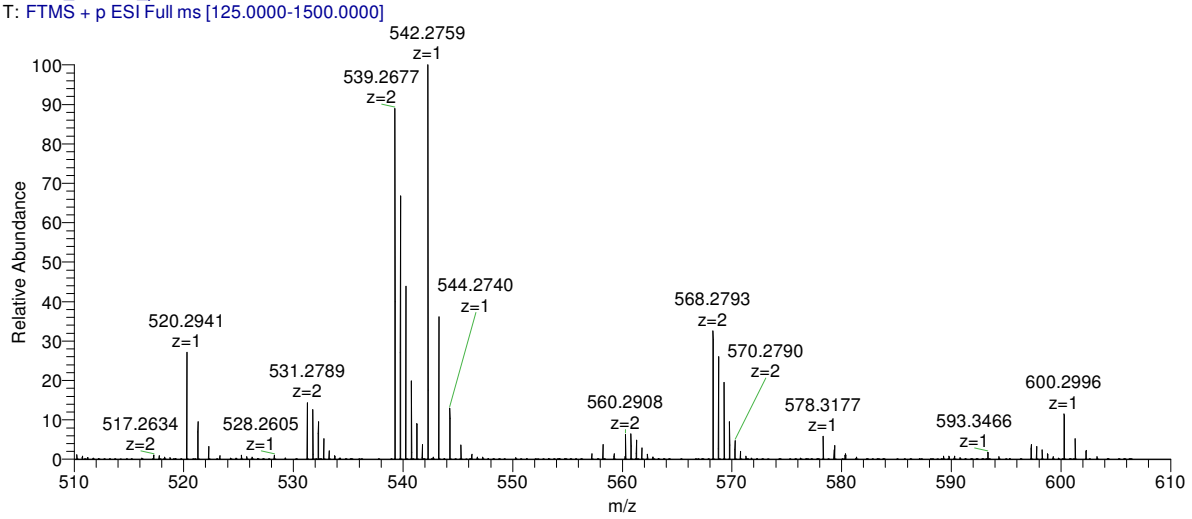

C24H49O5NSSi2 +Na: C24 H49 O5 N1 S1 Si2 Na1 p(gss, s...

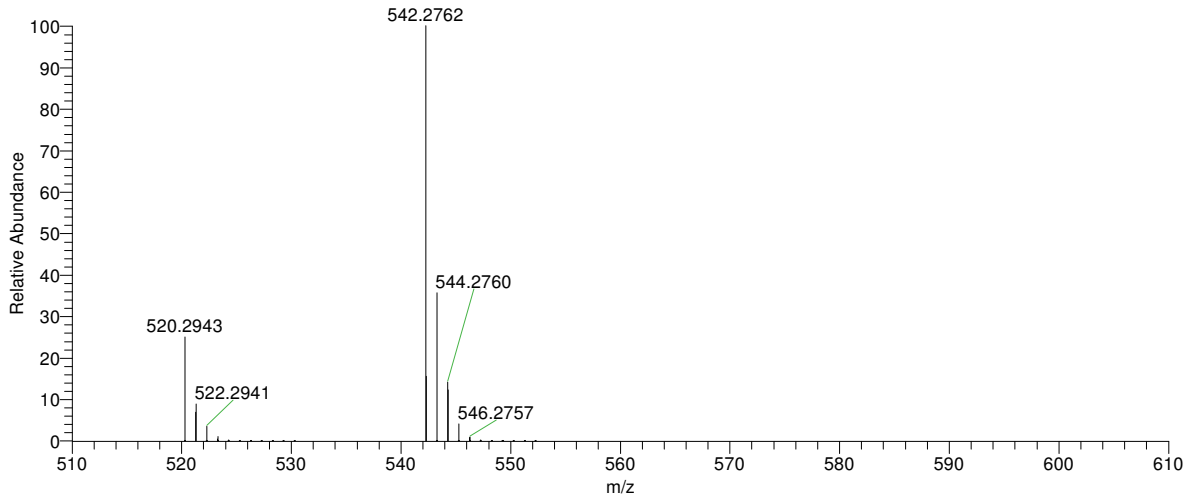

Figure 82: HRMS